

CHIRAL AND RACEMIC CALIX[6]ARENES AND THEIR SELF-
ASSEMBLY

Presented to the Graduate Council of
Texas State University-San Marcos
in Partial Fulfillment
of the Requirements

for the Degree

Master of SCIENCE

by

Monty Hayes, B.S.

San Marcos, Texas

December 2008

CHIRAL AND RACEMIC CALIX[6]ARENES AND THEIR SELF-
ASSEMBLY

Committee Members Approved:

Michael Blanda, Chair

Walter Rudzinski

Chang Ji

Approved:

Michael J. Willoughby

Dean of the Graduate College

ACKNOWLEDGEMENTS

Many thanks go to Dr. Michael Blanda, Dr. Walter Rudzinski, Dr. Chang Ji, Dr. Anne Hayes, Dr. Vincent Lynch, Norman Reitzel, John Gateley, Taylor Barker and the Department of Chemistry at Texas State University-San Marcos.

This manuscript was submitted on December 8, 2008.

TABLE OF CONTENTS

	Page
ACKNOWLEDGMENTS	iii
LIST OF FIGURES	v
CHAPTER	
I INTRODUCTION	1
II RESULTS AND DISCUSSION	15
III CONCLUSIONS AND FUTURE WORK	50
IV EXPERIMENTAL	53
SUPPLEMENTAL MATERIAL	72
REFERENCES	122

LIST OF FIGURES

FIGURE	Page
1 The calixarene building block.....	1
2 Phenoxide anions of the calix[6]arene bind to the rubidium cation	2
3 Kinetic profile of the methylation of 1a,1b	3
4 Inherently chiral 1,3-[4-methoxy]xylylenyl bridged calix[6]arene 3	4
5 Transannular distal diagonal bridging pattern	5
6 Crystal structure of compound 4 (arrow points to single H ₂ O molecule)	5
7 Activation/deactivation cycle	8
8 Compound 5 monomer and dimer.....	8
9 Head-to-head carboxylate-ammonium heteroditropic dimer.....	9
10 Homo/hetero dimeric species from analogues of 8	11
11 schematic showing chiral induction phenomenon through chiral R group (green).....	11
12 Crystal structure of 9	13
13 1,4-alkylation and subsequent bridging	16
14 Synthetic resolution of racemates	17
15 a. 10 ¹ H-NMR at 22°C	18
b. 10 ¹ H-NMR at 50°C	18
16 10 FT-IR.....	19
17 a. 10 ¹ H-COSY spectrum in the methylene region	20

b. 10 ¹ H-NMR in the methylene region	21
18 a. 11 ¹³ C-DEPT	22
b. 11 ¹³ C-HETCOR.....	23
c. 11 ¹ H-NMR in the methylene region	23
19 16 FT-IR (nujol).....	25
19 a. 17 ESI-MS (PIM).....	26
b. McLafferty rearrangement of N-BOC group	27
21 FT-IR overlay of di-acid 19 (purple), anhydride 20 (green), and background (red). (KBr pellets).....	28
22 a. (left) Unrefined crystal structure of single enantiomer of 19 with solvent molecules omitted for clarity (P2 ₁ /c space group, $\alpha=\beta=\gamma=90^\circ$, $V=11282.7 \text{ \AA}^3$, $Z=8$, R-factor=21.13 %). (right) 9 with hydrogen atoms and solvent omitted for clarity.	29
b. The unit cell geometry of 19 shows 2 open-ended dimers. The dimer on the right contains two identical enantiomers while the dimer on the left contains two identical enantiomers of the opposite chirality [S--S R--R]. (a=14.725 red, b=17.378 green, c=44.092 blue).	30
c. 19 -P viewed orthogonally to helical axis	31
d. 19 -P viewed parallel to helical axis	31
e. Staggered P and M helicites as extrapolated from single unit cell geometry (solvent molecules included). Also shown is a crude representation of one possible helical stacking arrangement from the same perspective.	32
23 Ibuprofen-(S)-phenylglycinol phase diagram with characteristics of ideal eutectic behavior-high $\Delta T_{A,B}$ values between pure diastereomers, steep slope of eutectic point and substantial shift from $x_A=0.5$	35
24 ROESY spectrum with t-butyl to aromatic NOEs	36
25 ROESY spectrum in methylene-aromatic region	37
26 COSY spectrum in the methylene region	38
27 Solid-state structure in methylene(syn) region with NOE interactions and bond distances labeled	39
28 COSY spectrum in the aromatic region	40
29 Syn/anti system	41
30 Phenolic proton with adjacent inner cavity methylene protons labeled	42

31	Syn/anti portion of the molecule.....	43
32	¹ H-NMR in the aromatic region.....	44
33	ROESY t-bu-aromatic labeled.....	45
34	Variable temperature ¹ H-NMR in aromatic region 23°C (top left), 33°C (top right), 43°C (bottom left), 53°C (bottom right)	46
35	Variable temperature ¹ H-NMR in methylene region 23°C (top), 33°C (bottom)	48
	(continued) 43°C (top), 53°C (bottom)	49
36	Diastereomer 21 _{s,s}	52

CHAPTER I

INTRODUCTION

A calixarene is a type of $[1_n]$ metacyclophane. The most popular of these macrocycles consist of phenol or resorcinol subunits. The name “calixarene” is derived from an ancient greek vase, the *calyx krater*, owing to a similar geometry when all subunits are pointed in the same direction (cone conformation). Gutsche and coworkers have pioneered the phenolic $n=4, 6, 8$ series (figure 1). The R groups comprise the “upper rim” of the molecule and the OH groups the “lower rim,” as the free hydroxy groups tend to form a hydrogen-bonding network that will form the tip of the cone.

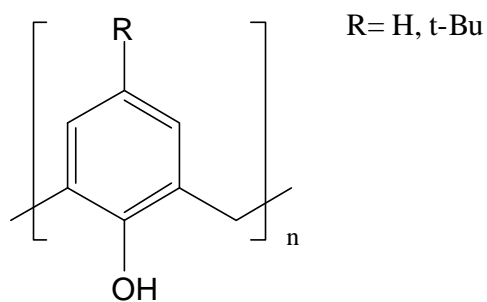


Figure 1. The calixarene building block

The calix[4]arenes have been extensively studied, however, the calix[6]arenes are popular due to the larger cavity, which can accommodate larger guest molecules. Calix[6]arenes mimic enzymatic systems particularly well due to their concave binding site. The t-bu-calixarene can be synthesized on a large scale by reacting t-bu-phenol with paraformaldehyde in a base-induced condensation reaction forming the macrocycle. The size of the macrocycle is contingent on the base, where the cation serves as a template around which the calixarene will form (figure 2).¹ Use of RbOH allows formation of the t-bu-calix[6]arene in 85% yield.

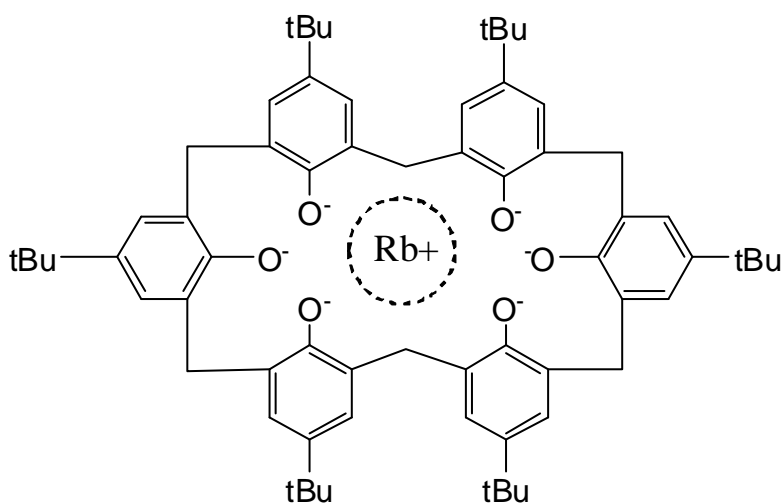


Figure 2. Phenoxide anions of the calix[6]arene bind to the rubidium cation

Chirality in calixarenes was explored as far back as 1979, where a chiral moiety (camphorsulfonyl ester) was attached to a calix[4]arene.² Chirality can also involve a regioselective asymmetric substitution pattern or a conformationally immobile species. This is known as *inherent chirality*. Conformational immobility can be attained by placing bulky O-substituents on the lower rim, preventing rotation through the annulus or

by attaching one or more intramolecular spanners to the molecule. In t-bu-calix[4]arenes, the t-butyl upper rim through annulus pathway has been disregarded generally and qualitative O-substituent size limit guidelines for a lower rim through annulus pathway have been established by observing conformational changes through variable temperature NMR experiments.

The situation becomes complicated in the calix[6]arene series as the t-butyl upper rim through annulus pathway has been observed^{3,4,5} and lower rim O-substituents large enough to curtail their respective annular rotation are relatively unexplored. Space-filling models along with variable temperature NMR suggest that benzyloxy groups undergo annular rotation while p-cyano-benzyloxy groups do not.⁶ Even bridged calix[6]arenes will exhibit conformational inversion as demonstrated by the 1,4-bridged-2,3,5,6-ether conformers **2a** and **2b** in which the bridging unit threads itself through the annulus forming a “self-anchored rotaxane.”⁷ (Figure 3) Equilibrium favors the cone conformation **1a** due to the larger hydrogen-bonding network among the free hydroxyl groups. The methylation product is **2b** exclusively, as electrostatic repulsion prevents **2a** from forming.

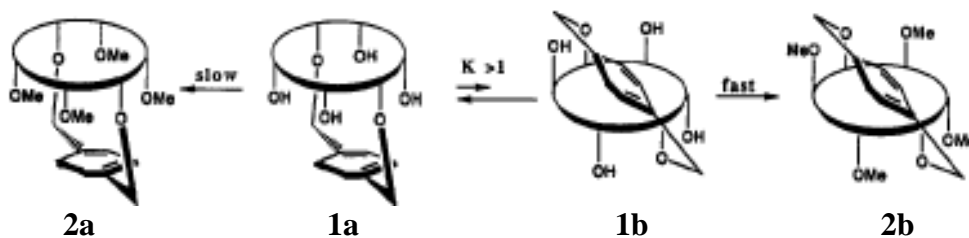


Figure 3. Kinetic profile of the methylation of **1a,1b**

The first inherently chiral calix[4]arene resolved through a chiral HPLC column had an AABC substitution pattern in the cone/partial cone conformation.⁸ A chiral (-)-menthoxyacetate auxiliary (*) was attached to the free phenolic residue to form a AABC* diastereomer with subsequent separation using a conventional HPLC column.⁹ Reports of inherently chiral hexamers are sparse. Shinkai and coworkers, in effort to establish a conformationally immobile calix[6]arene analogue, synthesized a racemic mixture of 1,3-xyleneyl bridged compound **3** (figure 4) and separated the enantiomers through a chiral HPLC column.¹⁰

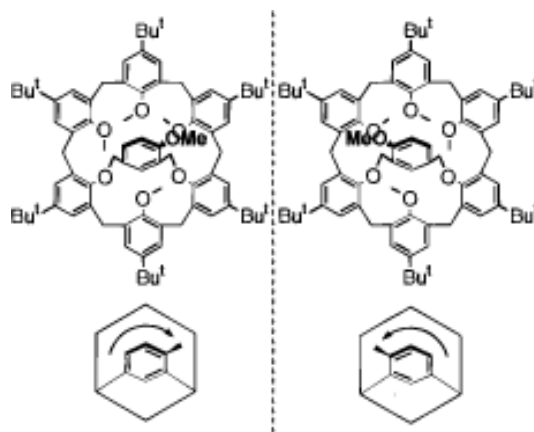


Figure 4. Inherently chiral 1,3-[4-methoxy]xylylenyl bridged calix[6]arene **3**

A reciprocal circular dichroism (CD) plot confirmed the chirality. The separate enantiomers were then subjected to heating (up to 100°C, the degradation limit) in various solvents and durations. Chiral HPLC showed *no racemization*, thus, no ring inversion occurs. This method circumvents the possibility of undetected ring inversion on the NMR time-scale.

The ABCABC substitution pattern will be a recurrent theme throughout this thesis. Such a pattern bearing a 2,5 (BB) bridging unit oriented orthogonal to the oligomer plane will result in an inherently chiral molecule (figure 5). A first of such calix[6]arenes using a 1,4-tolueneoxy-2,5-diester bridging pattern was made by Gutsche and coworkers, but no attempt at resolution was made.¹¹ More recently, the Lunig group synthesized a 1,4-tolueneoxy-2,5-phenanthroline bridged compound **4**. Attempts were made at resolving the racemic mixture through fractional crystallization but to no avail. An attempt to react the two remaining phenolic residues with chiral auxiliaries failed, which can be explained by the crystal structure (figure 6), which shows the two residues

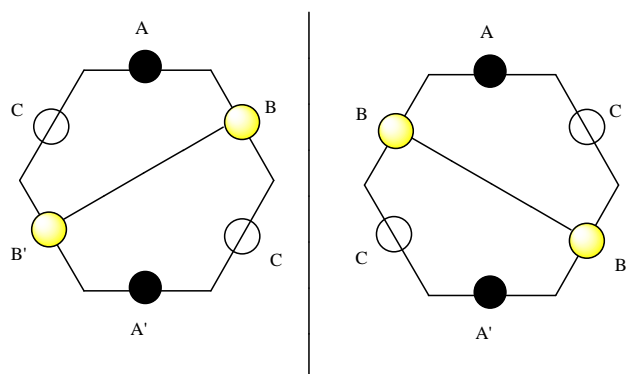


Figure 5. Transannular distal diagonal bridging pattern

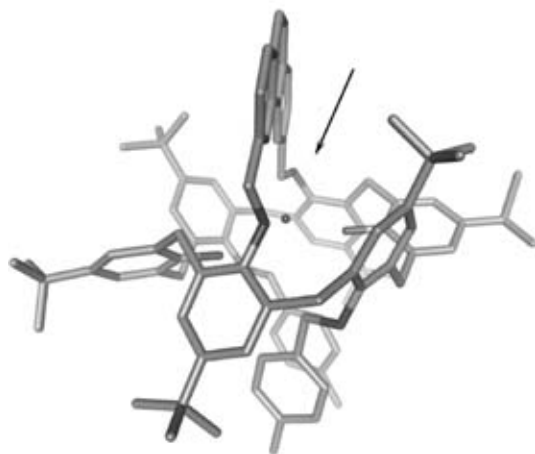


Figure 6. Crystal structure of compound **4** (arrow points to single H₂O molecule)

hydrogen-bound to a single H₂O molecule inside the cavity, rendering them inaccessible to Williamson-type alkylation. An alternate approach where a 2,5-bridged compound was monosubstituted with (+)camphorsulfonyl chloride resulting in the 1/6-(+)camphorsulfonyl-2,5-bridged diastereomers, which were separated via tedious chromatography on a cyclotron (90% ee, 3% total yield).¹²

An inherently chiral calix[5]arene was made having a 1-acetate-2,4-tetraethyleneoxy bridged substitution pattern.¹³ The acetate group was hydrolyzed with Me₄N⁺OH⁻ to form the carboxylic acid which was then reacted with (R)-BINOL chiral auxiliary on a mmol scale to form the diastereomers. Both diastereomers showed ¹³C methylene carbon signals ~30 ppm which indicates the molecule adopts a cone conformation through the ‘de-Mendoza’ rule. Subtle differences in NMR signals between the two diastereomers can be taken into consideration when devising a chromatographic separation. Ultimately, the diastereomers were separated by silica gel

chromatography and the auxiliaries cleaved with $\text{Me}_4\text{N}^+\text{OH}^-$. CD spectroscopy values of $[\alpha]=+4.8$ and -4.9 were found for each enantiomer.

Metal-ion mediated catalysis is another application for calixarenes. One example is a cone t-Bu-calix[4]arene with a single tetraethyleneoxy bridge in the 1,3 position. When in the presence of barium ion, the calixarene serves as a transacylation catalyst, converting p-NO₂-phenyl acetate to methyl acetate.¹⁴ Figure 7 depicts the mechanism where the calixarene becomes acylated through one of the free phenoxide anions along with extrusion of phenol. The activated transacylation catalyst harbors a reactive carbonyl due to close proximity of the lewis acid Ba^{2+} , which is bound to the crown ether bridge. This allows the normally sluggish background methanolysis a rate enhancement of approximately one order of magnitude larger.

Calixarenes are suitable monomers for self-assembly. An example of a hydrogen-bonded dimer species is the upper rim 1,3,5-alt urea substituted calix[6]arene **5** (figure 8) with $\text{C}_{3\text{V}}$ symmetry.¹⁵ In the presence of small guest molecules the urea-containing monomers dimerize, forming cylindrical cavities. N-substituted urea groups do not hydrogen bond efficiently and the system remains monomeric. 1,3,5-O-methoxy t-bu-calix[6]arenes generally adopt a cone conformation where the methoxy groups are pointed toward the cavity, leaving the remaining urea contacts oriented parallel to the axis of rotation, a favorable orientation for dimerization.

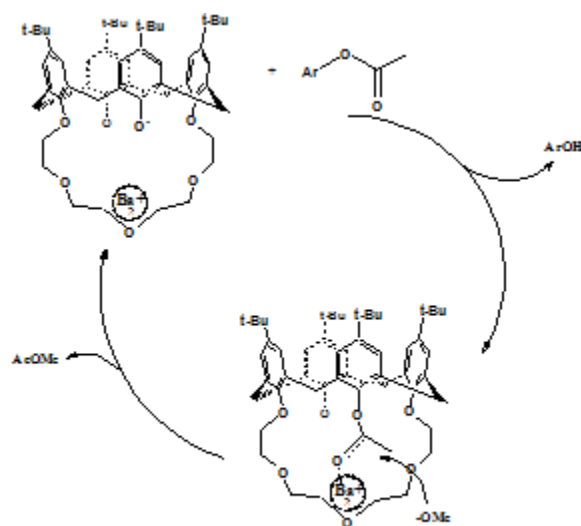


Figure 7. Activation/deactivation cycle

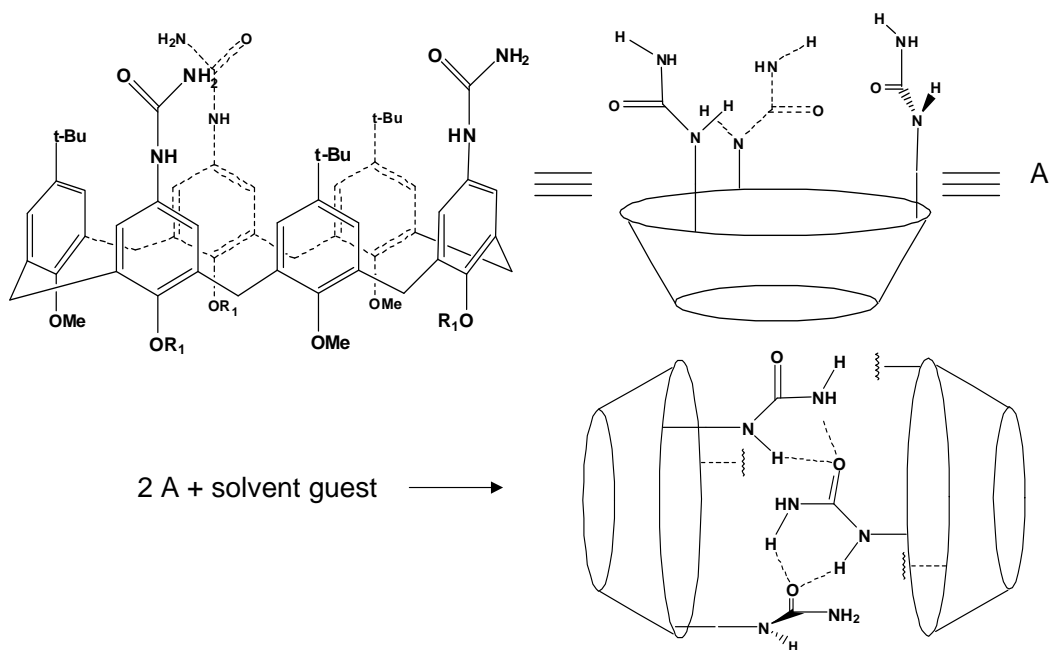


Figure 8. Compound **5** monomer and dimer

Capsular systems using an ionic linkage are also possible. Calix[6]trisamine **6** and calix[6]triacid **7** were assembled successfully as a heteroditropic dimer species (figure 9).¹⁶ When compound **6** and **7** were mixed in equimolar amount in CDCl₃, broadened NMR signals resulted indicating a dynamic heterogeneous aggregation. Upon addition of propylammonium picrate and a small polar guest such as DMF or ethanol, the spectrum sharpened and showed characteristic peaks for a C_{3v} endo complex where the ammonium salt and polar guest occupy the carboxylate and ammonium calixarene monomer cavities, respectively, and maintain an allosterically-induced dimerization. Using an imidazole molecule as the polar guest and a propyl ammonium salt, the quarternary complex was stable over a temperature range of 223-330K, dilution to 70 μM, and in the presence of protic solvents.

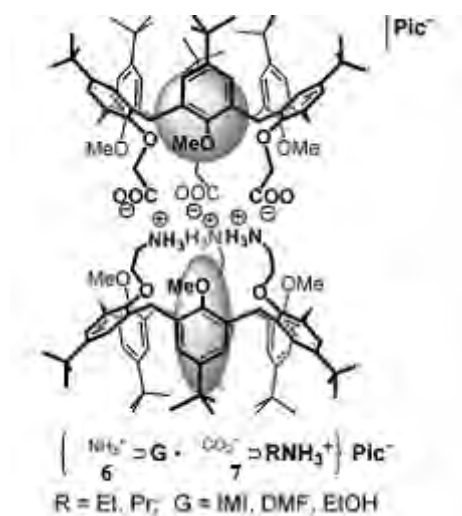


Figure 9. Head-to-head carboxylate-ammonium heteroditropic dimer

Exchange of chiral information between aggregate periphery and interior guest cavity has emerged as one of the intensely researched frontiers of supramolecular chemistry. The capsule formation of pyridine-containing homooxalix[3]aryl esters through Pd^{II}-ligand coordination is an example of chiral guest-induced changes in dimer conformation.¹⁷ The 3-pyridyl contacts are attached to the upper rim of the calix[3]arene and the resulting pyridyl-Pd^{II} dimer complex has a “tail-to-tail” arrangement. The 3-pyridyl substituents form a clockwise or counter-clockwise linkage resulting in rapid equilibrium between dimer enantiomers. The helicity is denoted P or M and the ratio P/M can be controlled upon inclusion of various chiral guest molecules. To preorganize the molecule for dimerization, alkali metal cations (Li⁺ or Na⁺) were extracted onto the lower rim, resulting in a cone conformation with C_{3v} symmetry.

Asymmetric dimeric host assemblies can participate in chiral guest recognition. Calix[4]arene analogues of **8** (figure 10) bearing urea functionalities at the upper rim were studied for asymmetric self-assembly phenomenon. Homodimeric species containing various chiral and achiral guest species showed asymmetric NMR signals indicating a fixed orientation and restricted rotation of the guest within that system.¹⁸ Mixing **8a** and **8b** results in the heterodimer, exclusively. Helical alignment of the urea contacts results in a racemic dimer mixture. Addition of (1*R*)-(-)-myrtenal results in a diastereomeric NMR spectrum, indicating the guest has a fixed north/south orientation on the rotational axis of the host. The next step was to attach a chiral R₂ group to the urea contact of one monomer species in effort to impart chiral information to the host cavity.¹⁹ Chirality was transferred to the cavity, albeit indirectly, through an absolute helicity of the amide linkages, similar to the dimerization of homooxalix[3]aryl ester mentioned

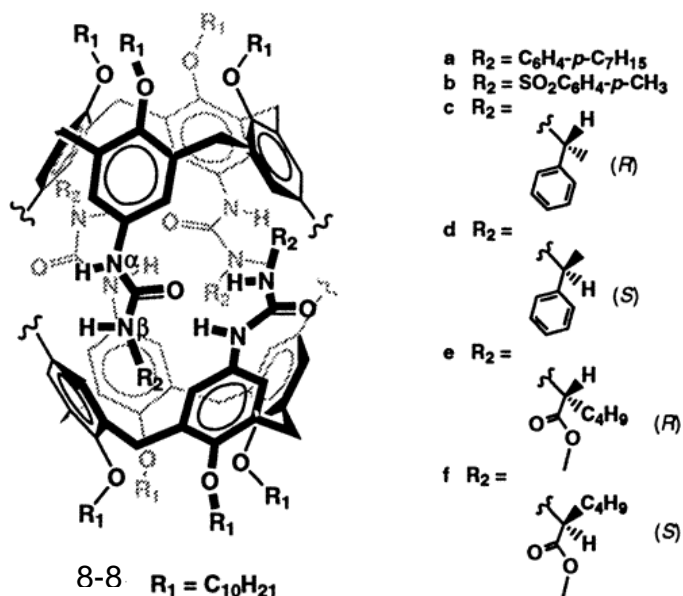


Figure 10. Homo/hetero dimeric species from analogues of **8**

earlier. For that system, the chiral guest rather than a chiral R_2 group on the urea linkage dictated the helicity. The process is depicted in figure 11. Enantioselectivity of racemic guest mixtures was modest (1.3:1 diastereomer ratio). Inherently chiral dimer hosts may contribute a greater chiral induction factor toward enantioselective binding.

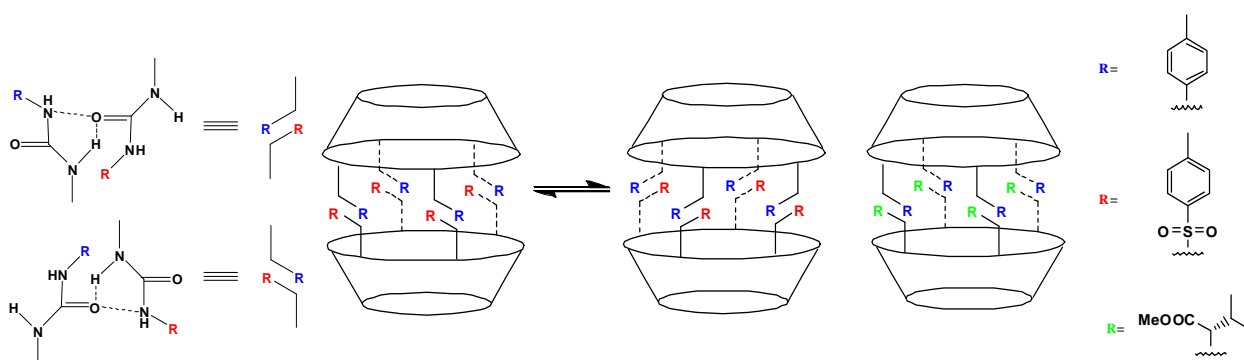


Figure 11. Schematic showing chiral induction phenomenon through chiral R group (green)

Synthetic organic nanotubes are a relatively new type of molecular container inspired by single-walled carbon nanotubes (SWNTs) and biological systems such as ion channels, but possess unique properties.²⁰ Like conventional macrocyclic host molecules, nanotubes contain well-defined cavities which can be used to encapsulate smaller guest species, but they possess the capability of binding and aligning multiple guests in one dimension. The supramolecular (host-guest) chemistry of synthetic nanotubes is an emerging area of interest and potential applications in chemistry and nanotechnology include storage, delivery, catalysts, separation agents and use as templating reaction vessels.²¹ Nanotubes can be self-assembled by manipulating non-covalent interactions (i.e. hydrogen bonding) between simpler, pre-programmed building blocks (tectons) or constructed via covalent syntheses. While covalently attached nanotubes are more structurally robust, those obtained from self-assembly enjoy properties such as error correction and synthetic efficiency. Several types of macrocyclic compounds have been used as tectons in the assembly of organic nanotubes, but calix[n]arenes are particularly attractive building blocks because of their synthetic versatility and tailored architectures.^{22,23} Chirality in the tecton is another key feature since it can be used to control the selective formation of right or left-handed *helical* nanotubes.²⁴ *Inherently* chiral calixarenes have not been commonly used as tectons for this purpose. The reason for this omission is that optically pure inherently chiral calixarenes are difficult to obtain.

Our group developed a strategy where the parent t-bu-calix[6]arene was etherified at the 1,4- position with tolunitrileoxy substituents in high yield.²⁵ A triethyleneoxy bridge was then affixed at the 2,5-position, producing racemic compound **9**. ¹³C-NMR chemical shift values of 29.52, 31.75, and 38.72 ppm for the methylene carbon atoms and

$^1\text{H-NMR}$ chemical shift differences between geminal diastereotopic methylene protons of 1.32, 0.63, and 0.12 ppm are consistent with a syn, syn/anti, anti orientation of the aryl groups. Suitable crystals were obtained and the crystal structure of one enantiomer (figure 12) depicts a solid-state 1,4-alt conformation, which is consistent with the NMR time-scale solution state. $^1\text{H-NMR}$ titration experiments using Pirkle's reagent, a chemical shift reagent, would result in diastereomeric complex formation.

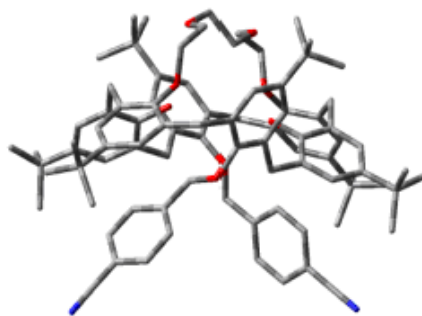


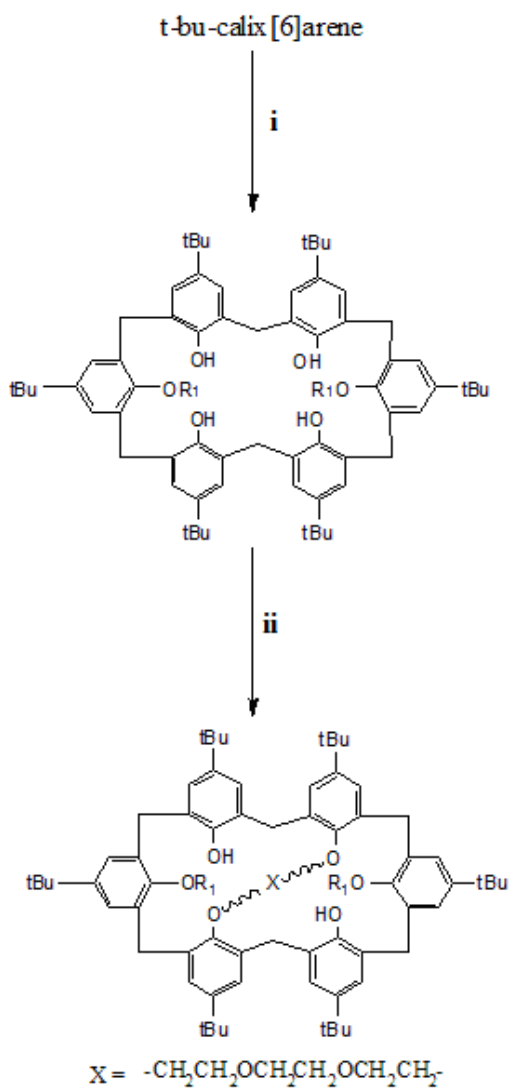
Figure 12. Crystal structure of **9**

Assuming the aforementioned molecule has a sufficient degree of pre-organization, the exposed nitrile moieties would be the logical contact site for aggregation. To allow for aggregation through hydrogen-bonding with retention of the original structural motif, conversion of the nitrile to an appropriate functional group (carboxylic acid, amide, amine, etc.) would be necessary. This thesis describes synthetic methodology and physical studies of self-assembled helical nanotubes derived from inherently chiral calix[6]arene diacid and diamine derivatives in the solid state and in solution. The general goals of the project are to: 1) resolve the racemic mixture of

inherently chiral calix[6]arene building blocks or tectons via formation of diastereomers, 2) determine the effects of concentration, temperature and solvent on the self-assembly of the helical nanotubes in solution by typical spectroscopic techniques such as NMR and CD, 3) investigate the supramolecular (host-guest) chemistry of the racemic and enantiopure helices.

CHAPTER II

RESULTS AND DISCUSSION



Compound	R ₁	I
1,4-di-tolunitrile-t-bu-calix[6]arene	CH ₂ ArCN	KOSi(Me) ₃ , BrCH ₂ ArCN, THF/DMF
1,4-di-pyridine-t-bu-calix[6]arene	CH ₂ C ₅ H ₅ N	BaO/BaOH ₂ , BrCH ₂ C ₅ H ₅ N, DMF
12	CH ₂ COOEt	BaO/BaOH ₂ , BrCH ₂ COOEt, DMF
13	CH ₂ COOH	N/A
14	CH ₂ ArCOOMe	KOSi(Me) ₃ , BrCH ₂ ArCOOMe, THF/DMF

Compound	Starting mat.	R ₁	ii
9	1,4-di-tolunitrile-t-bu-calix[6]arene	CH ₂ ArCN	NaH, TsOXOTs, THF/DMF
10	9	CH ₂ ArCONH ₂	TMAH, THF, Δ
11	1,4-di-pyridine-t-bu-calix[6]arene	CH ₂ C ₅ H ₅ N	NaH, TsOXOTs, THF/DMF
16	9	CH ₂ ArCH ₂ NH ₂	1) LiAlH ₄ , THF 2) 1 N NaOH, H ₂ O
19	14	CH ₂ ArCOOH	NaH, TsOXOTs, THF/DMF
20	19	CH ₂ ArCOOCOArCH ₂	EDC, 1-HOBT, DCM

Figure 13. 1,4-alkylation and subsequent bridging

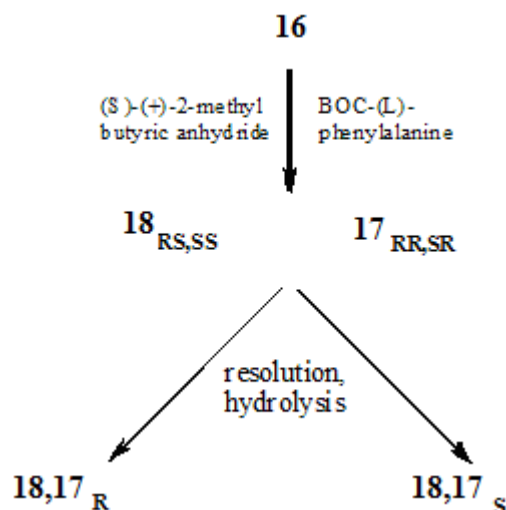


Figure 14. Synthetic resolution of racemates

Di-amide **10** was the result of an attempt at hydrolysis of **9** to produce the di-benzoic acid. Large excesses of TMAH as well as switching the solvent to DMF at reflux did not push the equilibrium toward complete hydrolysis. The $^1\text{H-NMR}$ spectrum in figure 15a shows two sets of non-equivalent amide protons in the 5-6.2 ppm region. All analogues of this particular calix[6]arene possessing C_2 symmetry will have three non-equivalent t-bu resonances in the area of 1 ppm. Heating the sample to 50°C resulted in a coalescence of amide protons owing to unrestricted CN bond rotation (figure 15b). The FT-IR spectrum shown in figure 14 shows an asymmetric/symmetric NH stretch at $3364.38/3193.11\text{ cm}^{-1}$. The absorption at 1661.97 cm^{-1} is an amide carbonyl, which has a longer CO bond length, hence, a lower energy. The amide I and II absorptions are at 1614.95 and 1569.17 cm^{-1} , respectively.

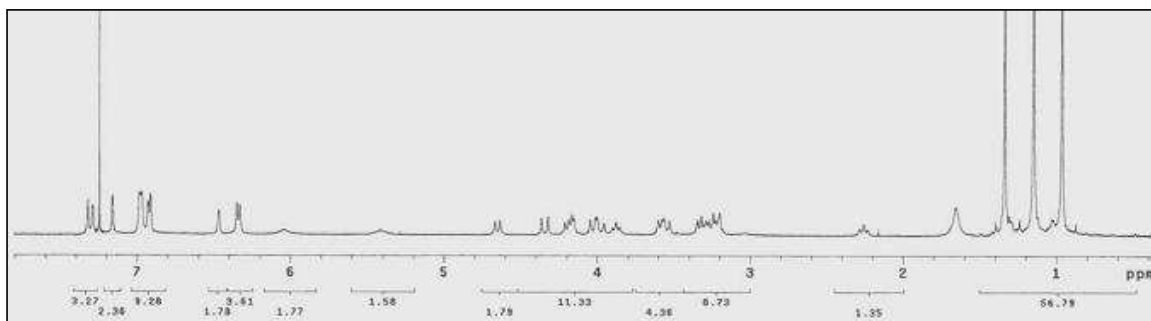


Figure 15a. **10** $^1\text{H-NMR}$ at 22°C

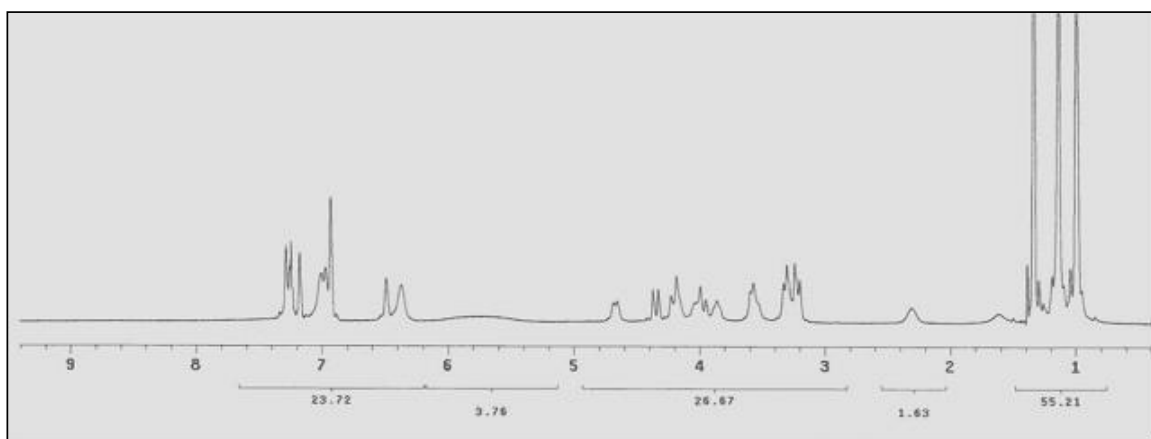


Figure 15b. **10** $^1\text{H-NMR}$ at 50°C

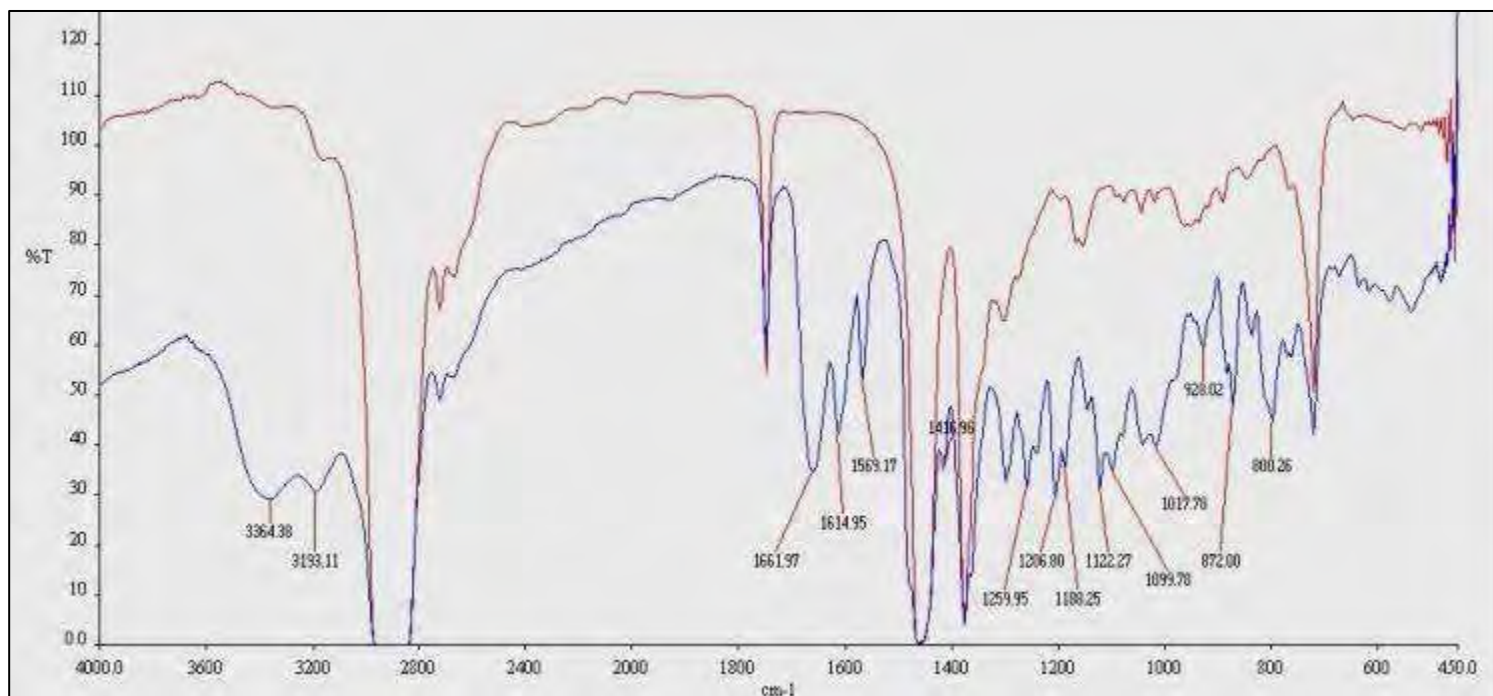


Figure 16. **10** FT-IR (nujol mull, background in red)

The ^1H -COSY spectrum in figure 17a identifies diastereotopic methylene protons, which are confirmed by matching geminal coupling constants in figure 17b. Values of 1.123, 0.624, and 0.210 ppm are found-similar values to those calculated for di-cyano **9**, which would suggest a similar conformation. The triplet peaks coupled between 2.28 and 3.33 ppm were assigned $\text{ArOCH}_2\text{CH}_2\text{OCH}_2$ since this portion of the triethyleneoxy bridge is closest to the phenolic oligomer, the chiral element of the molecule, resulting in an enhancement of the diastereotopic effect. The same rationale can be applied to the couplings at 3.59, 3.89 ppm ($\text{ArOCH}_2\text{CH}_2\text{OCH}_2$) and an obscured multiplet at 3.27 ppm ($\text{ArOCH}_2\text{CH}_2\text{OCH}_2$), the latter resonance bearing the protons closest to the rotational axis of symmetry and therefore showing weak geminal coupling. An acylation of the diamide

was attempted using (-)-menthoxyacetyl chloride as the chiral acylating agent but resulted in a mixture of byproducts. Plans to convert the racemic diamide mixture to diastereomers were ultimately abandoned.

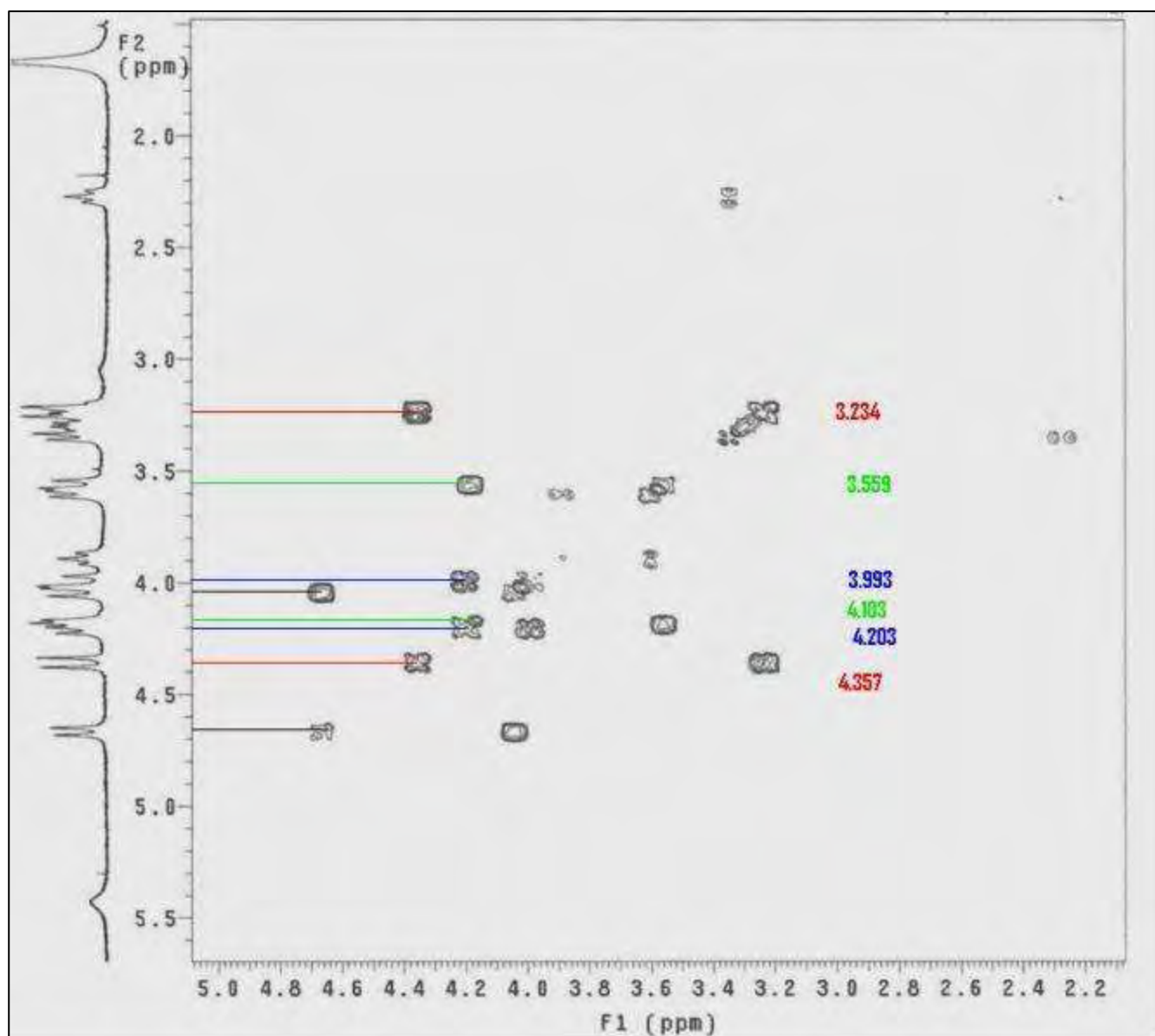


Figure 17a. **10** ^1H -COSY spectrum in the methylene region

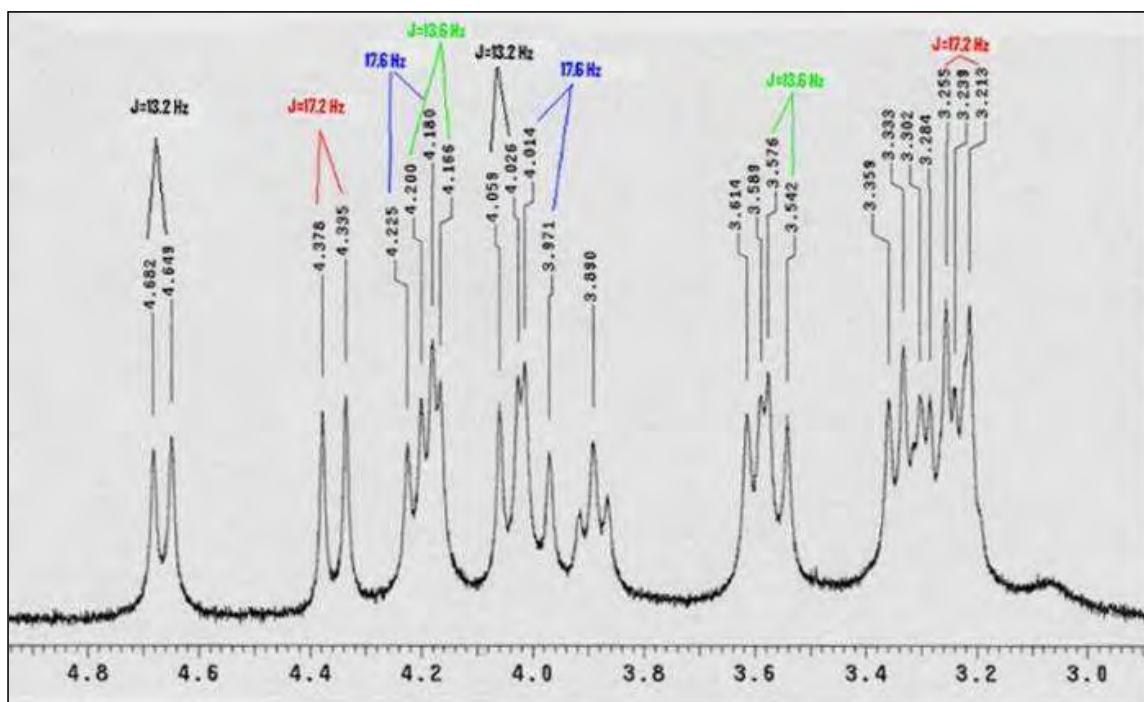


Figure 17b. **10** $^1\text{H-NMR}$ in the methylene region

The procedure for di-alkylation of the parent calixarene to produce 1,4-di-pyridine-t-bu-calix[6]arene was taken from Neri and Pappalardo²⁶, who synthesized various regioisomers using 2-(chloromethyl)pyridine hydrochloride. They obtained the 1,4-diether 5Ba2DMF complex in 80% yield. The use of $\text{BaO}/\text{Ba}(\text{OH})_2$ as base affords a stepwise alkylation, whereas K^+ bases provide a concerted 1,4-alkylation by forming a complex with the four remaining phenoxide moieties. The $^{13}\text{C-DEPT}$ spectrum for **11** shown in figure 18a shows the three methylene carbons with associated chemical shift values of 29.769, 31.731, and 38.760 ppm indicating a syn, syn/anti, anti conformation. The diastereotopic methylene protons are shown in the $^1\text{H}^{13}\text{C-HETCOR}$ spectrum of figure 18b along with the corresponding coupling constants in figure 18c. An integral value of 1.98 for the ArOH proton suggests a nBa**11** complex.

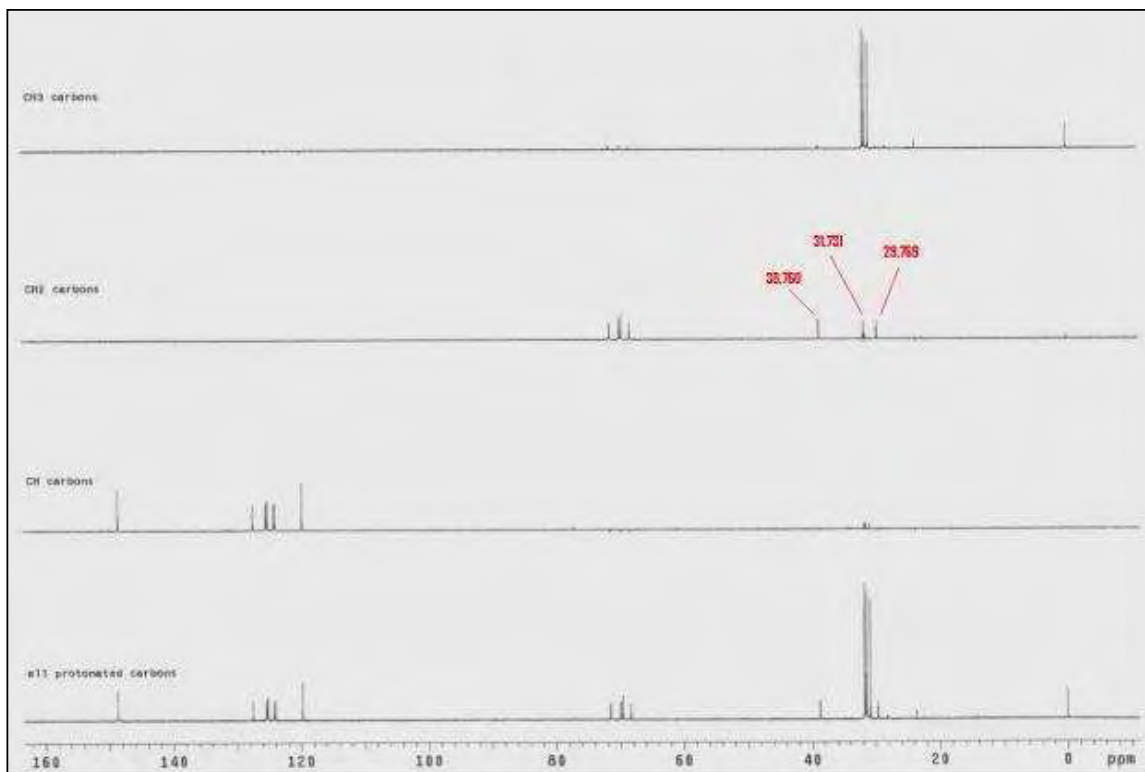


Figure 18a. **11** ^{13}C -DEPT

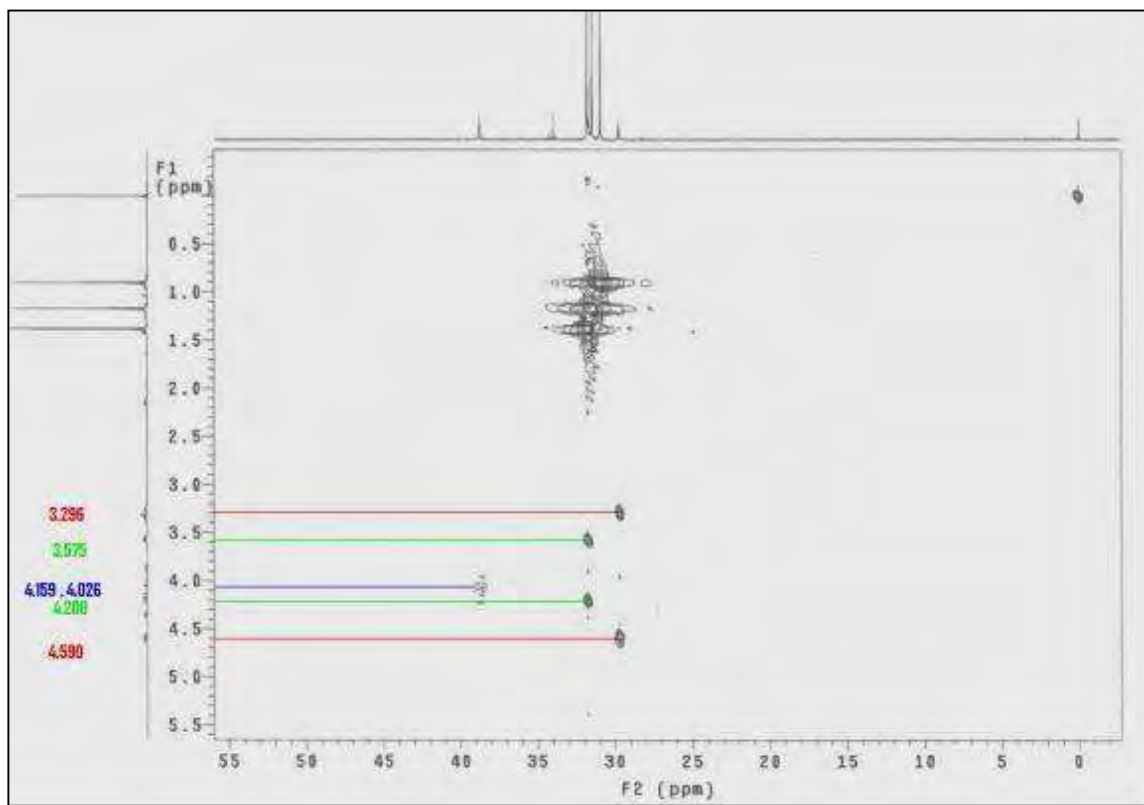


Figure 18b. $^{11} \text{ }^{13}\text{C}$ -HETCOR

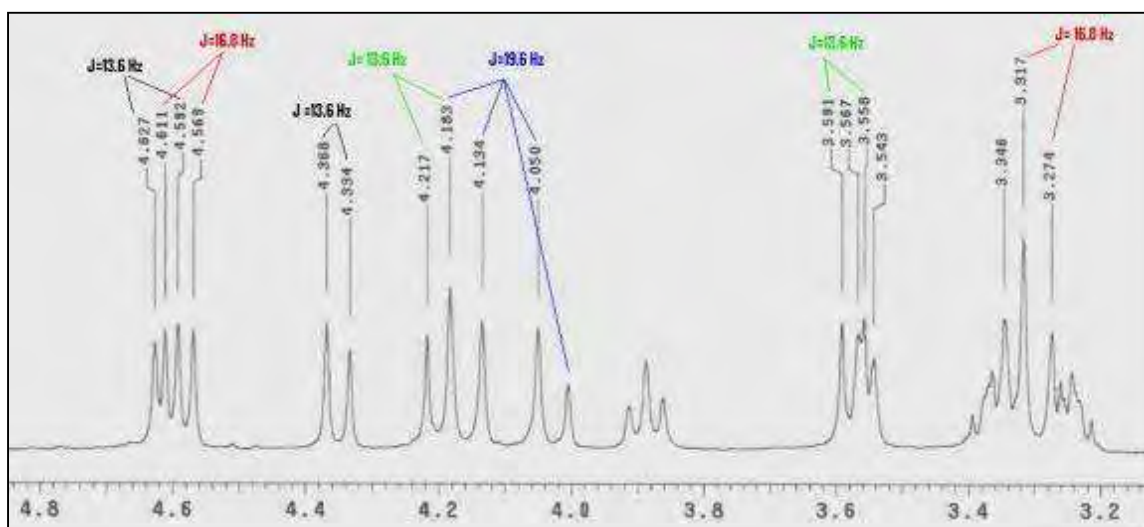


Figure 18c. $^{11} \text{ }^1\text{H}$ -NMR in the methylene region

4-bromomethyl-N-(leucine methyl ester)benzamide was synthesized to provide a chiral alkylating agent for 1,4-substitution on the parent t-bu-calix[6]arene, followed by 2,5-bridging-an alternate route to diastereomers. A DCC/DMAP coupling system was originally used, however, the resulting DCU byproduct was difficult to remove, even after chromatography. EDC is a favorable alternative because the terminal tertiary amine renders the urea byproduct water-soluble, and can be easily removed in an aqueous work-up. Using this chiral alkylating agent for 1,4-substitution did not work on a first try using the conventional synthesis.

Alkylation of t-bu-calix[6]arene with ethyl bromoacetate to produce **12** was ceased at the 12h mark and the major product was mono-substituted ester as confirmed by $^1\text{H}/^{13}\text{C}$ -NMR, as well as some starting material. It is important to maintain a dry environment for this particular reaction because the ester group will readily hydrolyze in the presence of water. Ester hydrolysis will be a recurrent obstacle throughout calixarene alkylation. BaO will form the weaker $\text{Ba}(\text{OH})_2$ in the presence of water. Altering the BaO/ $\text{Ba}(\text{OH})_2$ ratio will affect the base strength for this reaction. Attempting to bridge **12** following the synthesis for 1,4-di-pyridinyl-2,5-triethyleneoxy-t-bu-calix[6]arene **11** resulted in hydrolysis to **13** (conversion 85%).

The ^1H -NMR spectrum for **14** shows a pair of doublets at 3.52 and 4.34 ppm (8H, $\Delta J=14$ Hz, $\Delta\delta=0.826$) and a pair of doublets at 3.58 and 3.85 ppm (4H, $\Delta J=14$ Hz, $\Delta\delta=0.26$), which would suggest a 1,2,3-alt conformation at ambient temperature. The paltry yield of diastereomers of 1,4-di-tolunitrile-2,5-triethyleneoxy-3,6-(-)-menthoxy acetyl-t-bu-calix[6]arene **15** can be attributed to the two remaining hydroxyl groups on the starting molecule being shielded within the calixarene cavity, having limited

reactivity as a result. This was an observation of the Lunig group, whose phenanthroline-bridged molecule shares a similar geometry. Heating, excess reagent, and prolonged reaction times did not improve the yield. The synthesis of di-amine **16** involved the reduction of di-nitrile **9**, full conversion is confirmed by the absence of the cyano peak ~ 118 ppm and the presence of a signal at 46.31 ppm, characteristic of Ph-CH₂-NH₂. The FT-IR spectrum of **16** in figure 19 shows a stretch at 1584.23 cm⁻¹, which is a NH₂ scissor.

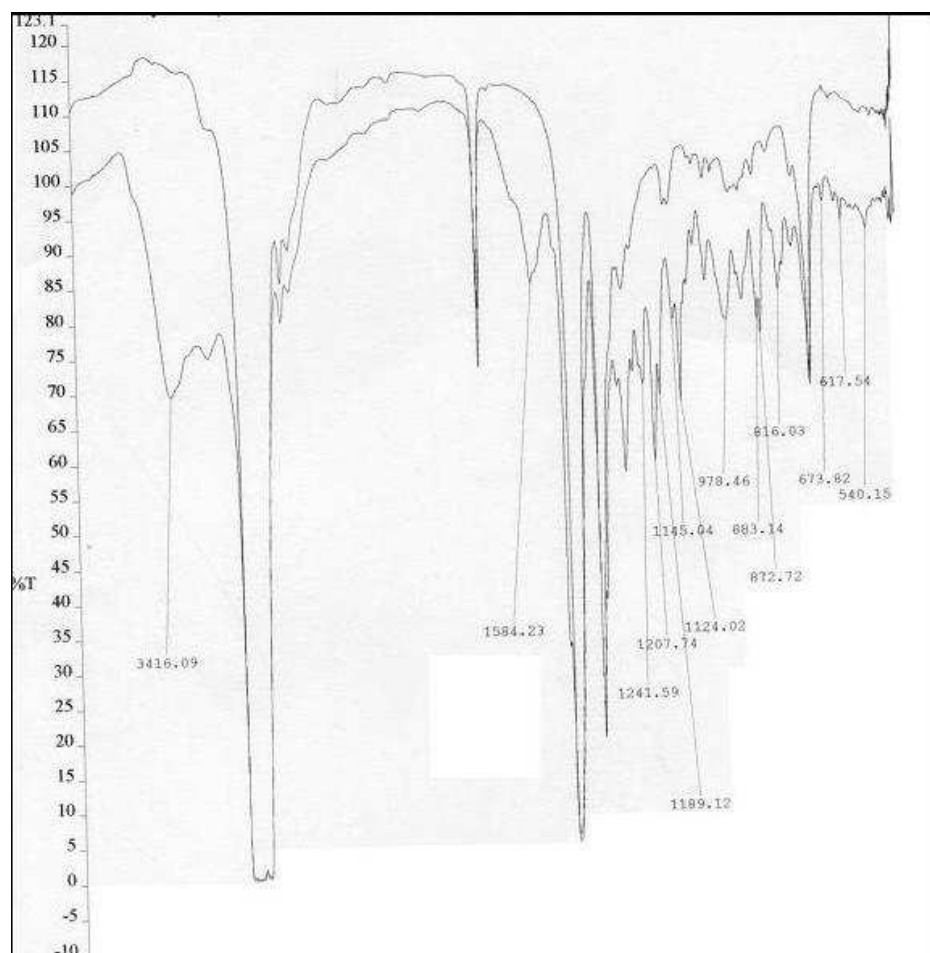


Figure 19. **16** FT-IR (nujol)

Upon isolation of a single diastereomer of **17**, attempts were made at cleaving the chiral appendages through TMAH hydrolysis. N-BOC cleavage would proceed initially as confirmed through the absence of characteristic N-BOC resonances in the ^{13}C -NMR spectrum. Extended reaction times would not cleave the remaining amide moieties. An interesting phenomenon observed in the ESI-MS of this compound (figure 20a) was two sets of fragmentations of 44 and 56. This could be a McLafferty rearrangement of N-BOC group in positive-ion mode (figure 20b).²⁷

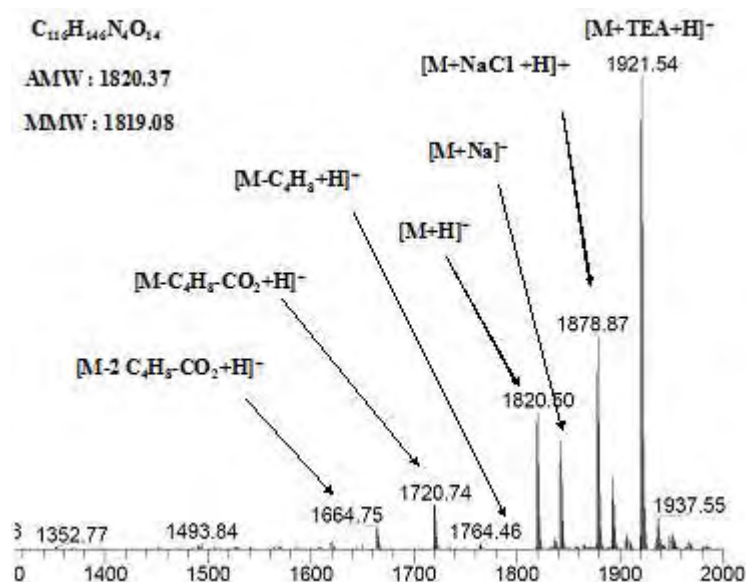


Figure 20a. **17** ESI-MS (PIM)

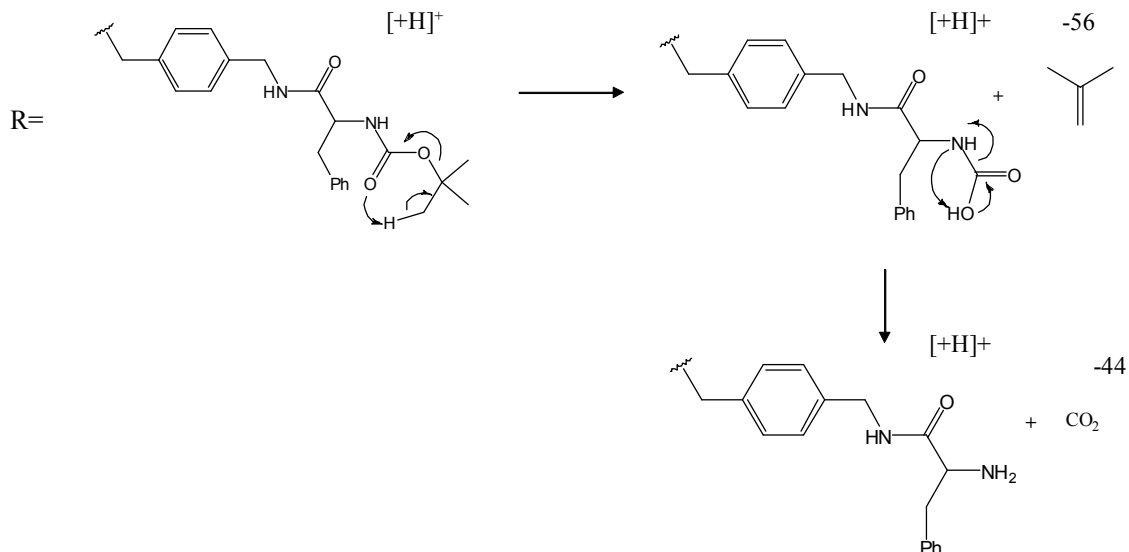


Figure 20b. McLafferty rearrangement of N-BOC group

Purification of **18** gave a single TLC spot, which would indicate that the product was a single diastereomer. To confirm this assertion, a TMAH cleavage was attempted to render an enantiomeric product, the degree of enrichment to be determined through chiral HPLC. As was the case with **17**, the amide bond was unsusceptible to base hydrolysis in binary phase. Also attempted was an acid hydrolysis using excess TFA, which was not successful. The ESI-MS for **18** shows the same $M+101$ peak as **17** (figure 20a), likely to be residual triethylamine used as a reagent or chromatography additive. The ability of this class of calix[6]arenes to retain TEA throughout the purification process and form a stable gas-phase adduct would warrant further investigation into the host-guest interaction in solution-state and solid-state.

The ease of purification/characterization of diastereomer **18** was impetus for a similar reaction of di-acid **19**, using instead (S)-(+)-2-methyl-butanol to form a di-ester, which should hydrolyze readily. However, esterification using the EDC/1-HOBt coupling system resulted in the isolation of what is believed to be anhydride **20** based,

primarily, on ESI-MS data. In PIM, the peak at 2698.1 is equivalent to a molecular formula of $C_{176}H_{208}O_{22}+Na$ while the peak at 1361.4 is the complementary $+2Na$ adduct. These results can be rationalized by the formation of intermolecular anhydride bridges ($2 C_{88}H_{106}O_{12} - 2 H_2O$). Figure 21 shows FT-IR spectra of both starting material di-acid **19** and the anhydride **20**. A combination of aromatic resonance and dimerization of **19** in the solid-state results in a lower frequency carbonyl stretch at 1694.97 cm^{-1} . The characteristic symmetric/asymmetric carbonyl stretches at 1786.37 and 1728.01 cm^{-1} support an anhydride product **20**.

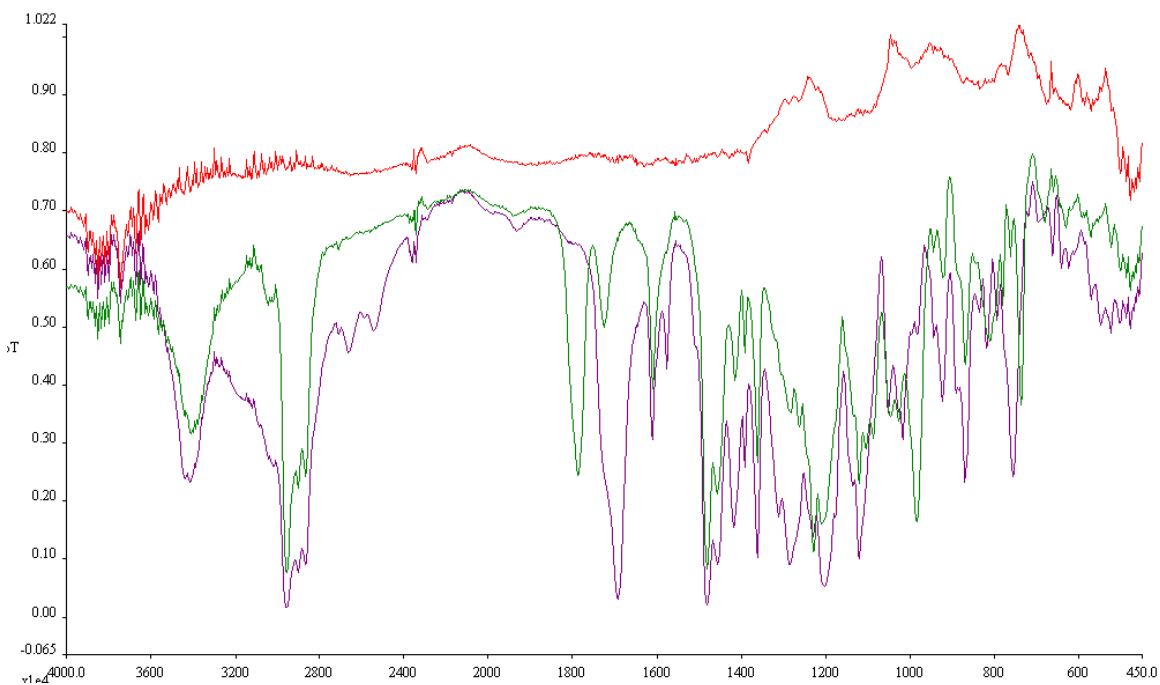


Figure 21. FT-IR overlay of di-acid **19** (purple), anhydride **20** (green), and background (red). (KBr pellets)

During the synthesis of **19**, it is believed that bridging is accompanied by rapid acid-catalyzed hydrolysis of the ester by the combination of toluenesulfonic acid generated in-situ and adventitious H₂O. The acid aqueous workup would not be responsible since the 1,4-alkylation retained the ester through similar workup conditions. For a larger scale synthesis, recrystallization from CHCl₃ is the preferred method of purification. The ease of recrystallization can be attributed to the hydrogen-bonding network that will form as can be seen in the crystal structure in figure 22b. The crystal structure also shows that chlorinated solvent contributes to the hydrogen-bonding. The notion that solvent molecules reinforce the solid-state structure agrees with experimental observation, as the crystals will collapse upon drying. Crystal growing using acetone as the base solvent with a slow diffusion of DCM resulted in nucleation at the acetone/DCM surface interface, further supporting the role of chloroform as structural reinforcement.

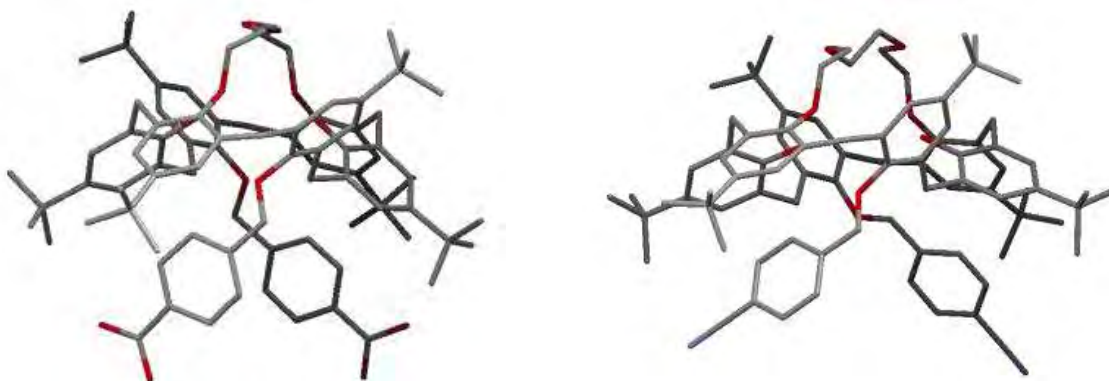


Figure 22a. (left) Unrefined crystal structure of single enantiomer of **19** with solvent molecules omitted for clarity (P2₁/c space group, $\alpha=\beta=\gamma=90^\circ$, $V=11282.7 \text{ \AA}^3$, $Z=8$, R-factor=21.13 %). (right) **9** with hydrogen atoms and solvent omitted for clarity.

19 has a similar 1,4-alt conformation to that of **9**. However, due to the carboxylic acid “sticky contacts,” the monomer is able to aggregate in the solid state as shown in the unit cell of figure 22b. O---H---O hydrogen-bonding between the free phenolic oxygen and the crown-ether oxygen of bond distance 2.759 and 2.809 angstroms in **19** compares to values of 2.791 and 2.759 angstroms for **9**. Propagation of the hydrogen-bonding network results in a linear chain, which coils into a helical structure of absolute directionality dependent on the chirality of the monomer (figure 20c). The P (clockwise) or M (counterclockwise) convention will be used when describing the helical orientation. Figure 20d shows a well-defined cavity within the supramolecular helix lined with molecules of chloroform.

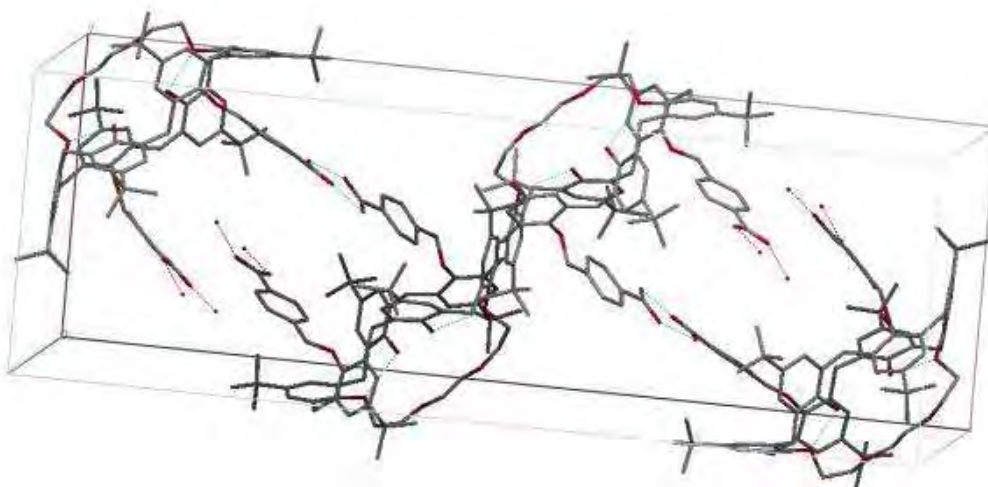


Figure 22b. The unit cell geometry of **19** shows 2 open-ended dimers. The dimer on the right contains two identical enantiomers while the dimer on the left contains two identical enantiomers of the opposite chirality [S--S R--R]. (a=14.725 red, b=17.378 green, c=44.092 blue)

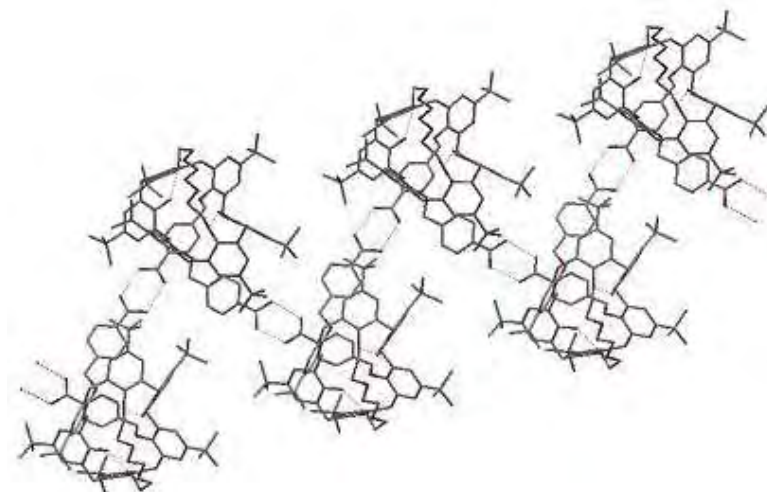


Figure 22c. **19-P** viewed orthogonally to helical axis

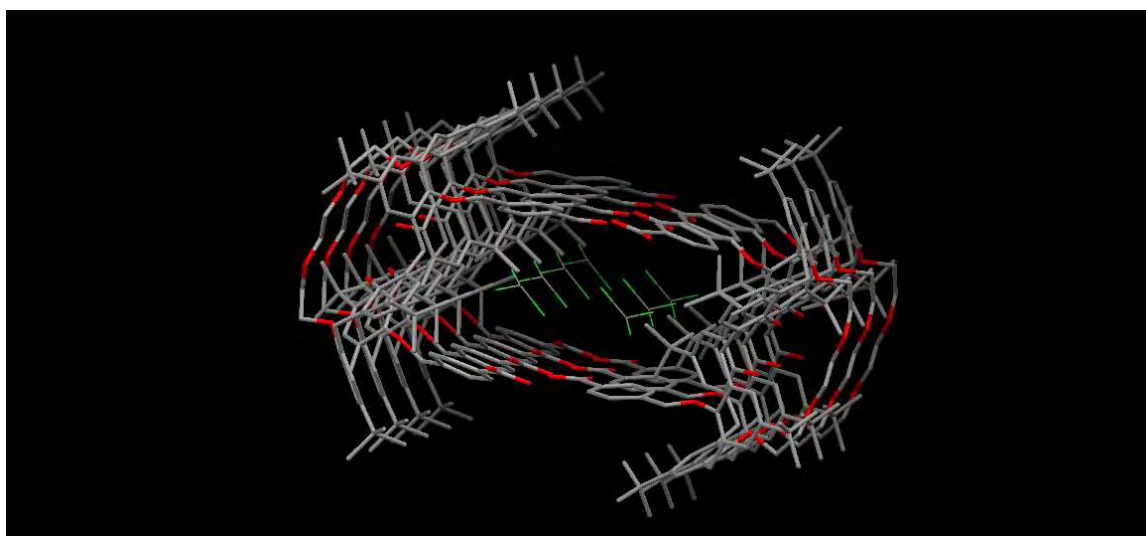


Figure 22d. **19-P** viewed parallel to helical axis (inner-cavity dimensions 9 x 7 Å)

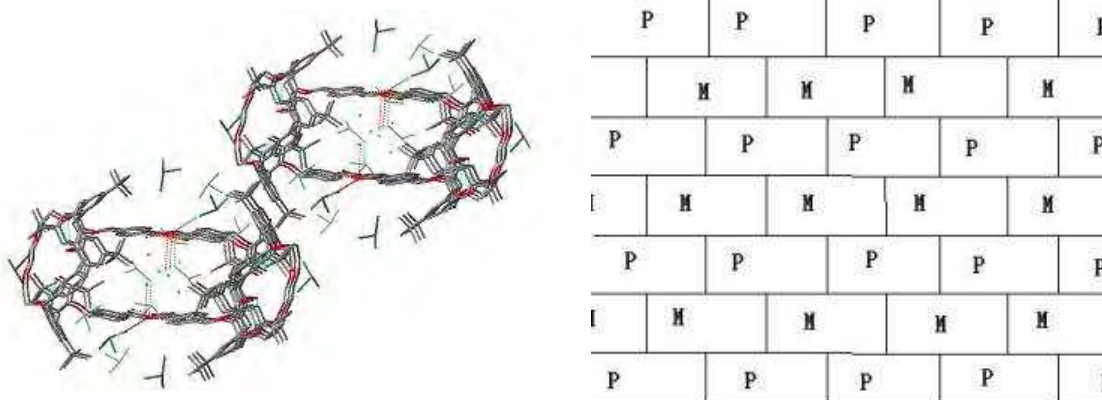


Figure 22e. Staggered P and M helicites as extrapolated from single unit cell geometry (solvent molecules included). Also shown is a crude representation of one possible helical stacking arrangement from the same perspective.

Of particular interest would be the unit cell and packing arrangement of the single enantiomers. A regular pattern of racemic unit cells as depicted in figure 22e would rule-out a conglomerate, and with it the possibility of separating the enantiomers through preferential crystallization.²⁸ Due to the ease of crystallization of **19** with a variety of solvents, separating enantiomers via a classical resolution to form the diastereomeric salts was a logical option. The ammonium-carboxylate salt-forming resolving agents quinidine, brucine, and cinchonine were screened in a variety of solvents. The **19**-brucine salt formed crystals in CHCl_3 and subsequently, the filtered crystals and mother liquor were washed with successive portions of 1 N H_2SO_4 to regenerate the free acid. The degree of enantiomeric enrichment was to be determined through chiral HPLC using a Chiral-pak AD-H column. This column efficiently resolved racemic **9** (90:10 Hex:IPA) but not **19** under identical conditions. Addition of ion-pairing reagents (TFA, DEA) as well as variation in solvent ratio would not produce a separation, which is due to the carboxylic acid groups, whose hydrogen-bonding may cohere enantiomers.

Derivatization of the carboxyl may enable resolution. A synthesis was tried where a simple alcohol, in this case isopropanol, was to be coupled to the acid using the same coupling reagents as that of the esterification of **19** with (S)-(+)-2-methyl-butanol. This reaction produced the same non-polar byproducts, however, if the formation of anhydride is confirmed, this species may serve as the derivatized chromatography aid.

Low enantiomeric excess (e.e.) values resulting from classical resolution can be improved with successive recrystallizations, although yields will depreciate significantly throughout this technique. Due to the complementary structural relationship between **19** and the diamine **16**, it would be worthwhile to study the thermotropic properties of their diastereomeric salts, provided a small chiral pool of both can be attained. Preparative chiral HPLC, though costly, can provide such a chiral pool in the event that trial-and-error diastereomeric resolutions don't yield sufficient e.e. values.

In theory, a mixture of the R enantiomer of **19** with the complementary R enantiomer of **16** would likely form a crystalline arrangement similar in structure to that of figures 22c and 22d. The alternate RS diastereomer would likely form a crystal with different packing arrangements and intermolecular dispersion forces. Differential scanning calorimetry (DSC) is a technique that provides the temperature change associated with phase transitions and is predictive of ideal eutectic behavior, where two components crystallize in separate domains. A binary mole fraction (x_A) vs. temperature (T) phase diagram can be constructed from the DSC data, and the shape of the graph can indicate the performance of that particular diastereomeric resolution system. The experimental phase-diagram can be compared to a calculated phase diagram using the Schröder-Van Laar equation (1):²⁹

$$\ln x_A = \frac{H_A}{R} \left(\frac{1}{T_A} - \frac{1}{T} \right)$$

Where H_A is the latent heat of fusion of pure A, R is gas constant and T_A is the melting temperature of pure A. The “closeness of fit” between the two plots determines a eutectic mixture. The efficiency of the resolution can be approximated through equation (2):³⁰

$$R_{\max} = \frac{0.5 - x_{\text{eu}}}{1 - x_{\text{eu}}} \times 100\% \quad (R_{\max} = 0 - 50\%)$$

$$S = kt = \frac{1 - 2x_{\text{eu}}}{1 - x_{\text{eu}}} \quad (S = 0 - 1)$$

Where x_{eu} is the eutectic composition, k is the chemical yield (k=2, 100% yield), and t is the optical purity (t=1, 100% e.e.). Figure 23 shows an example phase diagram of an ibuprofen-(S)-phenylglycinol diastereomer salt. The solid line represents an ideal eutectic calculated from H_A , H_B and T_A , T_B values of the pure diastereomers through equation (1). The dotted points are experimental values that follow the ideal eutectic closely, indicating an efficient resolution system.

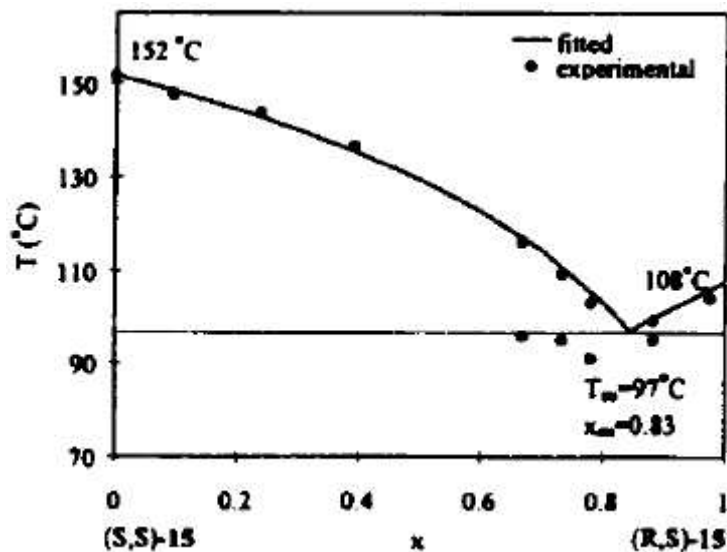


Figure 23. Ibuprofen-(S)-phenylglycinol phase diagram with characteristics of ideal eutectic behavior-high $\Delta T_{A,B}$ values between pure diastereomers, steep slope of eutectic point and substantial shift from $x_A=0.5$.

Certain factors such as the formation of solvates, additional polymorphs, and the presence of mesophases will complicate such phase diagrams. The formation of solvates can be detected through NMR or elemental analysis. The nature and thermotropic behavior of the mesophase can be correlated with polarized light optical microscopy to generate more elaborate phase diagrams.^{31,32} The practical application of such thermotropic study would be towards efficient classical resolution of **16**, which in turn would be used to resolve **19** in a reciprocal process.

A ^1H - ^1H -ROESY NMR experiment was conducted on a sample of **19** in THF-d₈ to ascertain intermolecular hydrogen-bonding in the solution-state. The specific NOE interactions, along with proton assignments using a crystal structure as a model, are outlined in figures 24-33. The crystal structure of **9** was used since the unrefined crystal structure for **19** does not include hydrogens but shares a similar geometry. Figure 24

shows the complete ROESY spectrum with the t-butyl to aromatic NOEs drawn. Each t-butyl proton resonance has two corresponding aromatic protons in close proximity, however, the t-Bu resonance furthest downfield has a third.

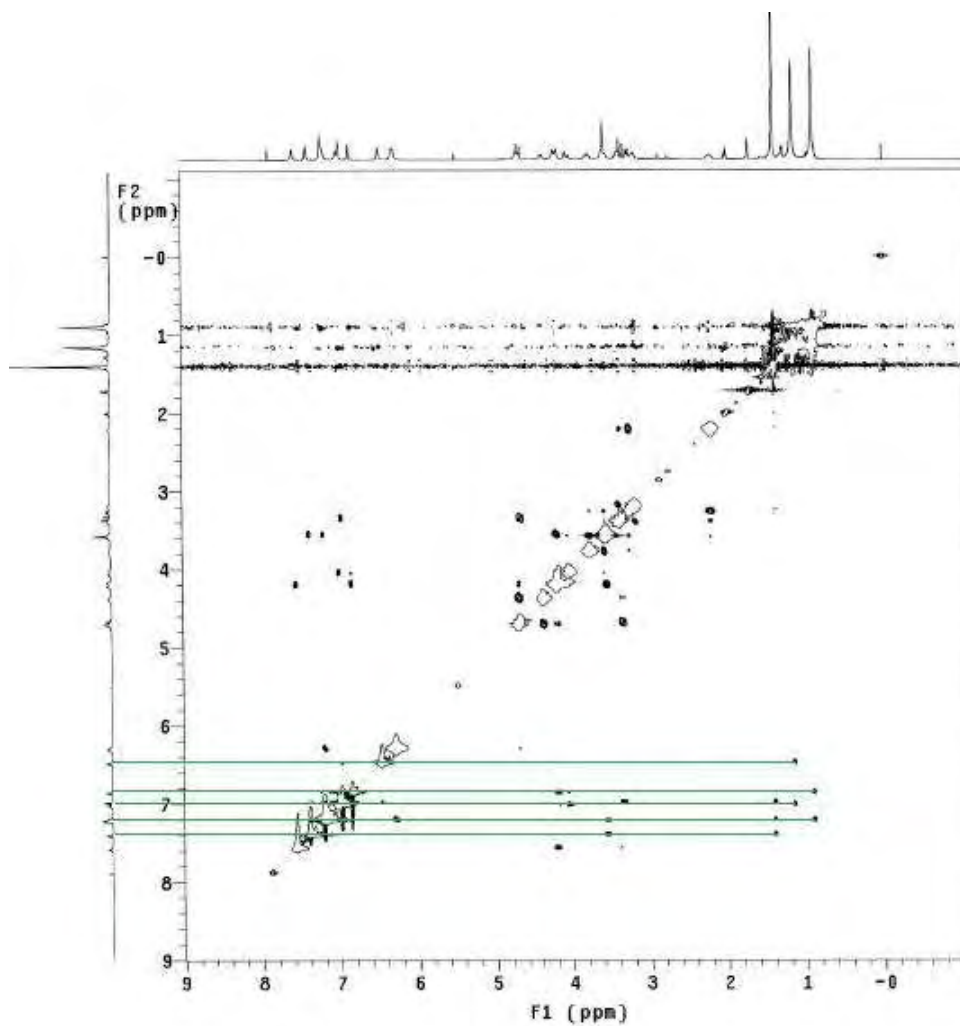


Figure 24. ROESY spectrum with t-butyl to aromatic NOEs

Figure 25 shows a close-up of the methylene to aromatic region with the specific interactions labeled. The wide doublets at 3.4 and 4.7 ppm can be assigned as the syn

methylene protons based off the COSY data in figure 26 and their large chemical shift difference.

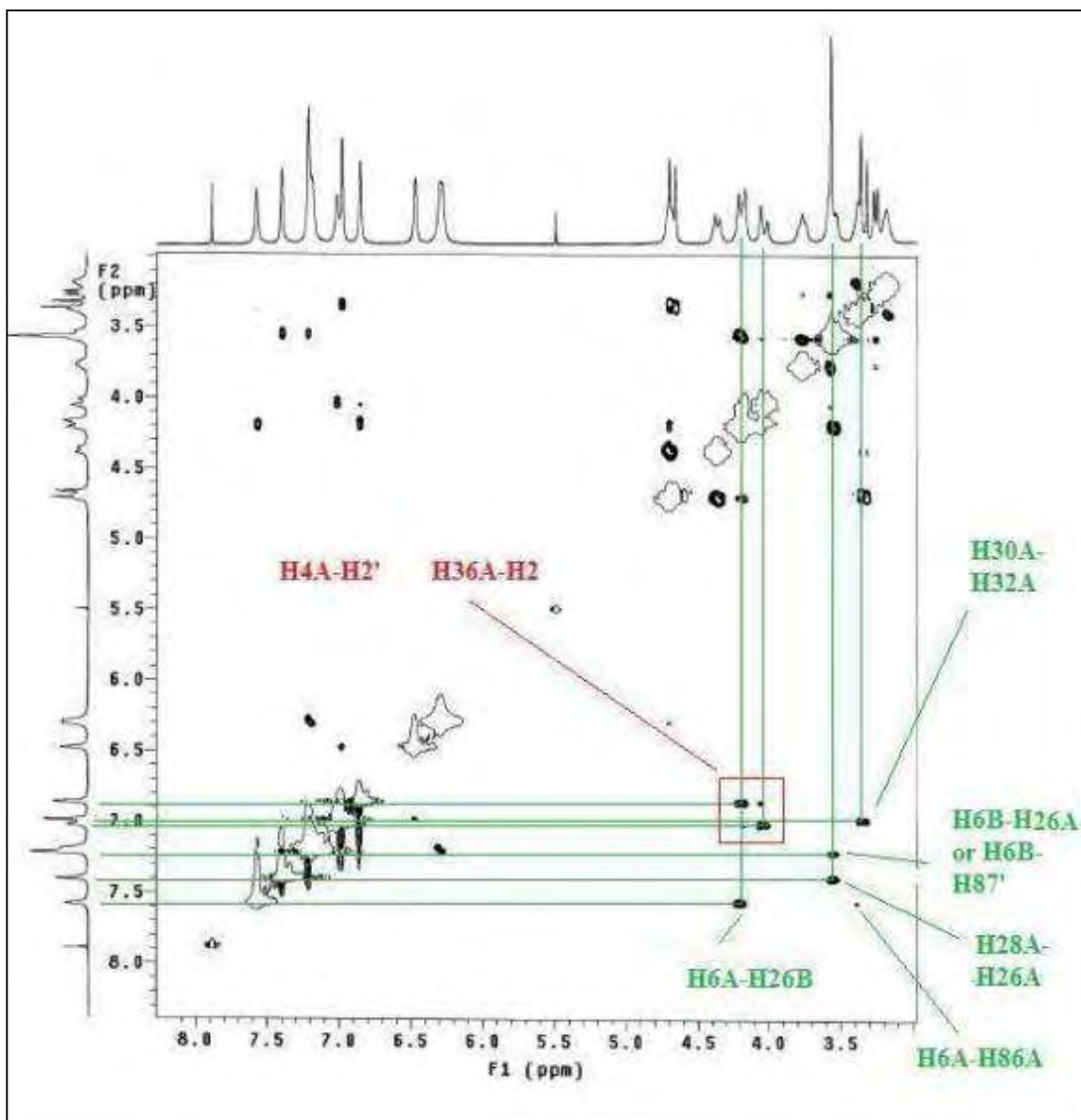


Figure 25. ROESY spectrum in methylene-aromatic region

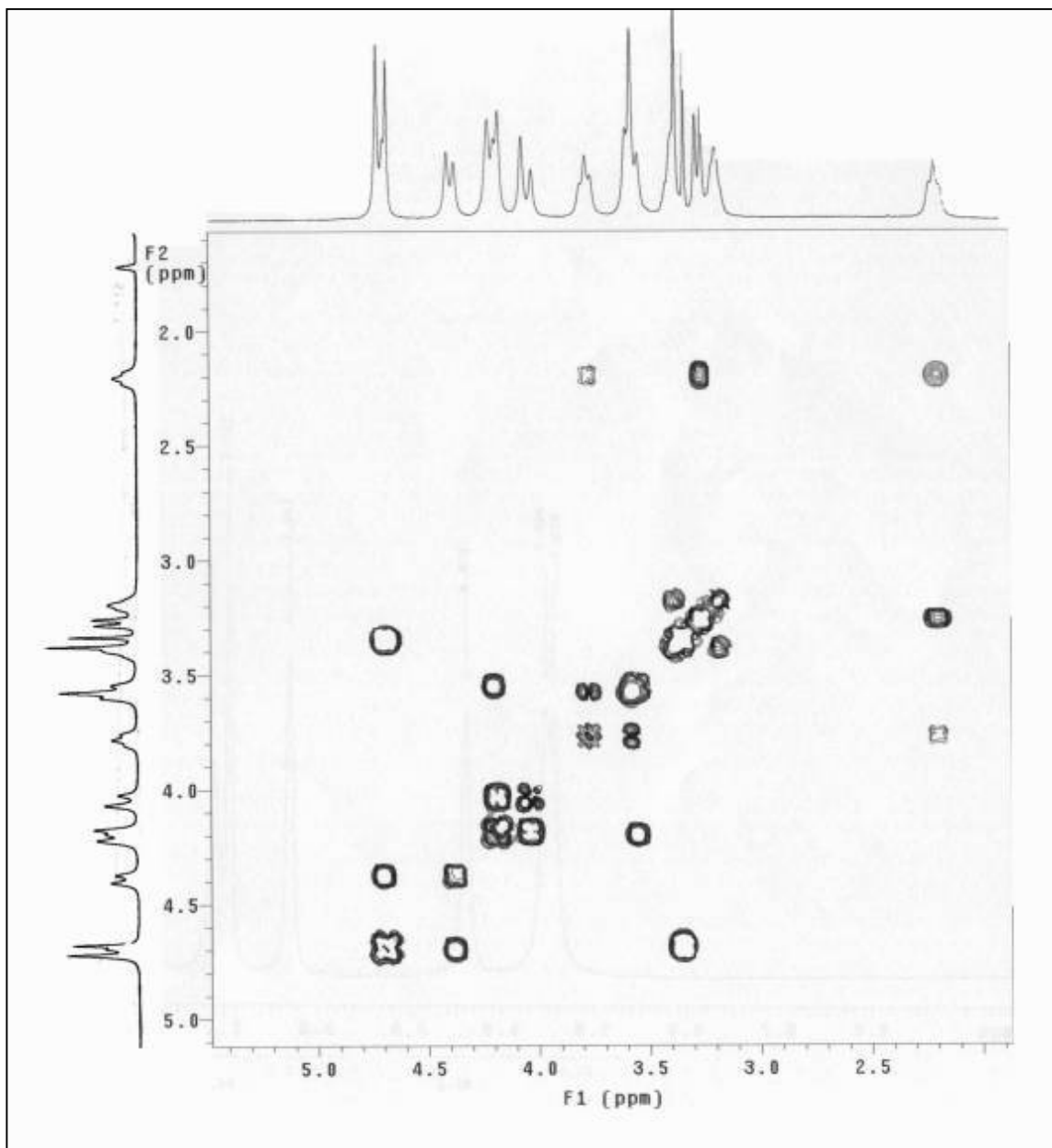


Figure 26. COSY spectrum in the methylene region

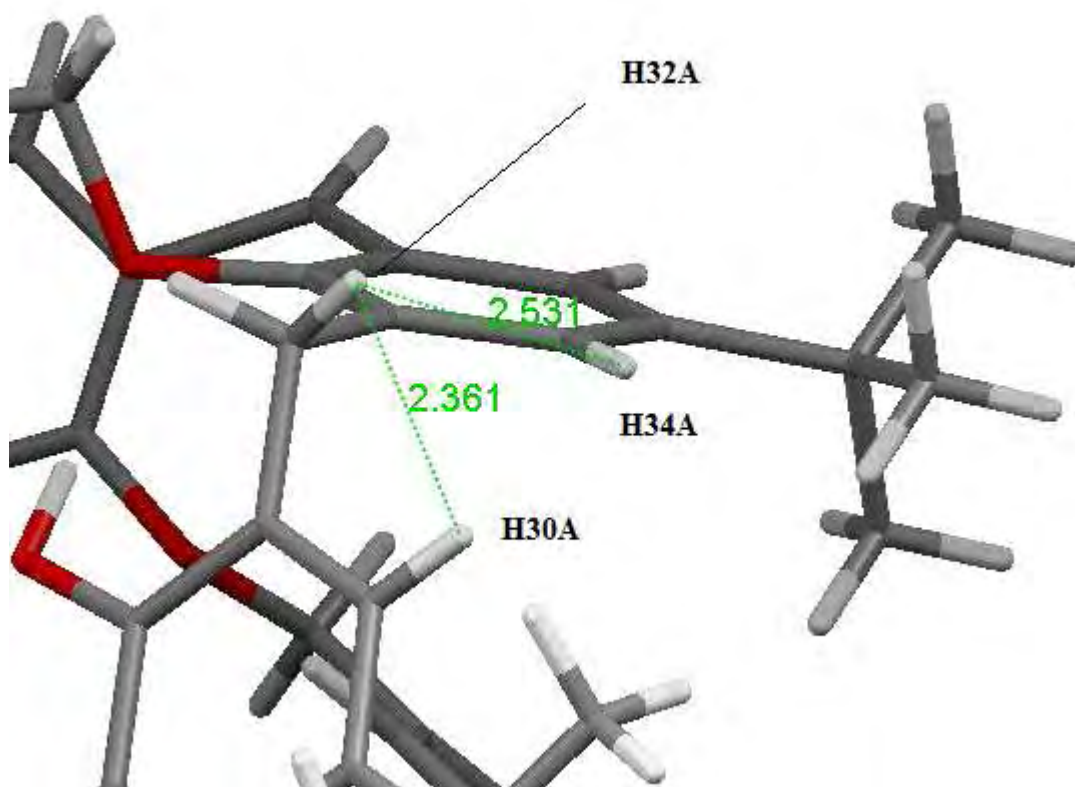


Figure 27. Solid-state structure in methylene(syn) region with NOE interactions and bond distances labeled

The H30A-H32A interaction gives an estimate of the ROESY through-space bond distance under the given experimental parameters. Based off this interaction, the aromatic signal at 6.99 ppm can be labeled H30A. Figure 28 shows a COSY spectrum in the aromatic region. Weak meta-coupling exists between H30A and the signal at 7.41 ppm, which can be labeled H28A. The red box in figure 25 shows the methylene(anti)-aromatic interactions. The stronger aromatic-methylene interaction reflects a dihedral angle closer to zero degrees. Also shown in figure 25 is the

methylene(syn/anti)-aromatic interaction H28A-H26A. That portion of the molecule is shown in figure 29.

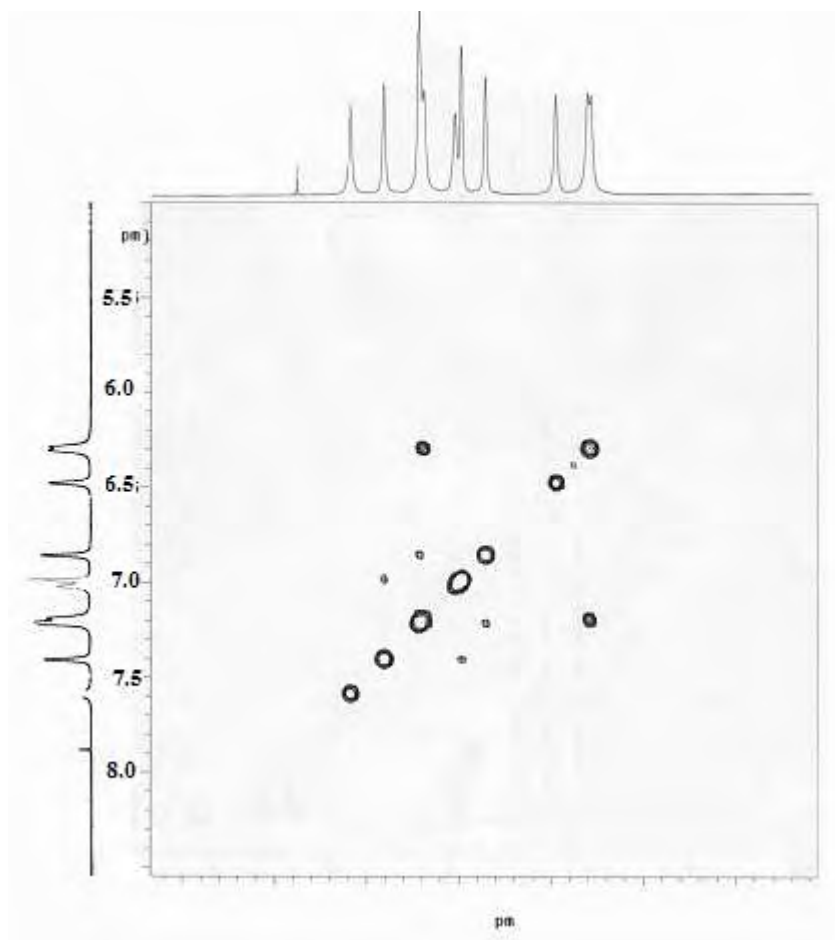


Figure 28. COSY spectrum in the aromatic region

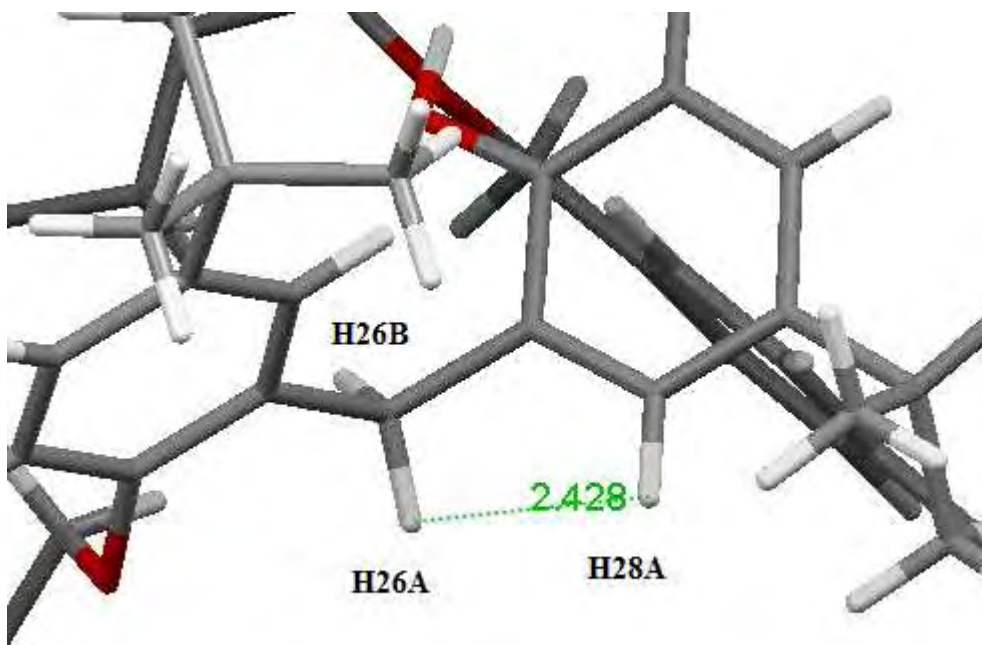


Figure 29. Syn/anti system

Based off COSY data, the corresponding methylene(syn/anti) proton H26B, which is directed toward the inside of the cavity, is the obscured signal located at 4.19 ppm. The phenolic proton (7.60 ppm) shows a strong NOE peak in this region, which deviates from the solid-state conformation where the closest methylene proton would be H32B, the syn methylene proton directed toward the center of the cavity (wide doublet ~4.7 ppm). This would indicate that in solution, the phenolic proton is directed toward the center of the calixarene cavity, in close proximity to H26B (figure 30). COSY data shows a faint coupling between the signal at 7.41 ppm (H28A) and the signal at 7.22 ppm, which can be labeled as the adjacent oligomer aryl proton that has the benzoic acid residue (H6B in figure 31). From this information, the remaining aromatic resonances, as well as the t-bu resonances, can be assigned (figures 32, 33).

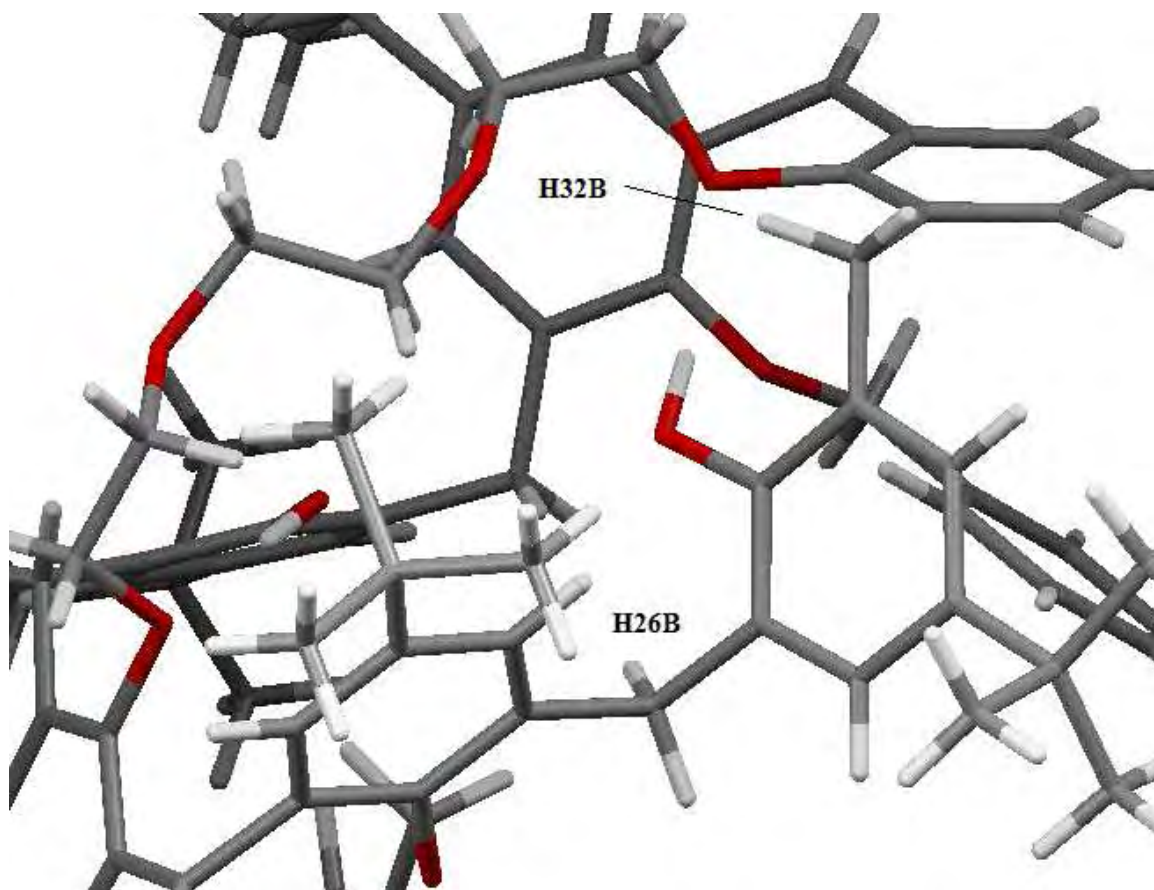


Figure 30. Phenolic proton with adjacent inner cavity methylene protons labeled

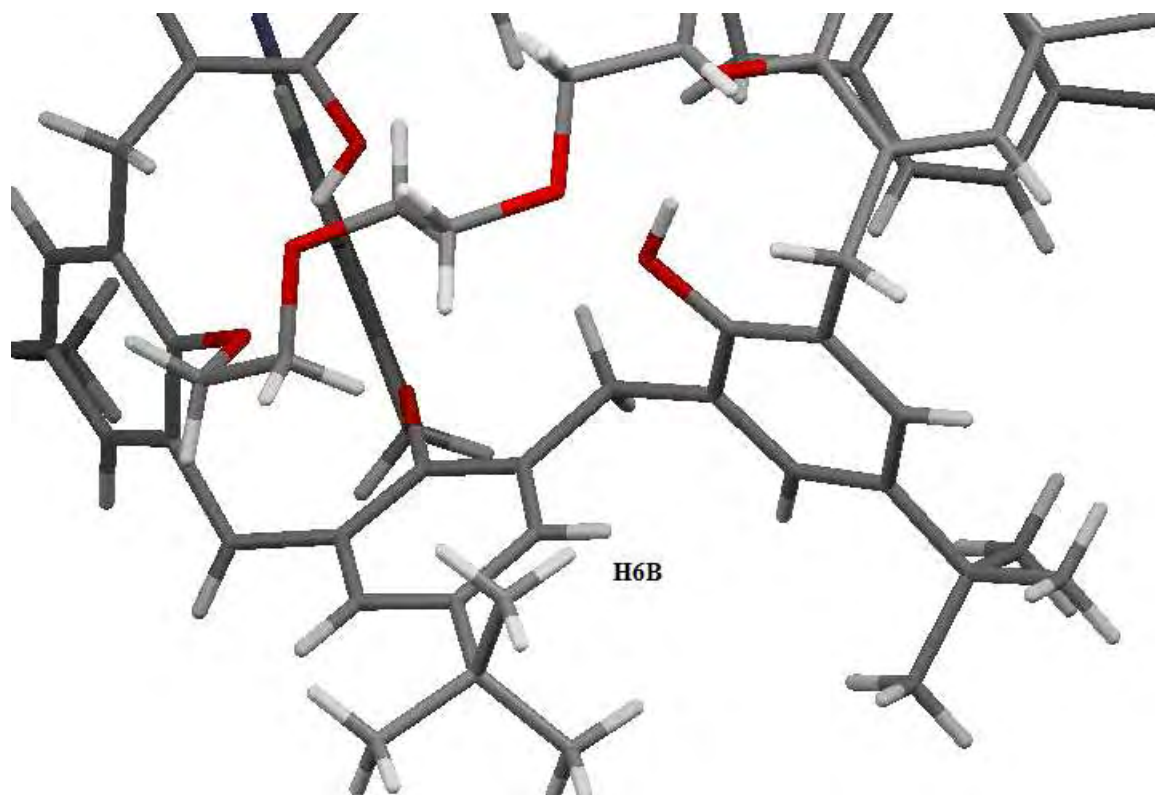


Figure 31. Syn/anti portion of the molecule

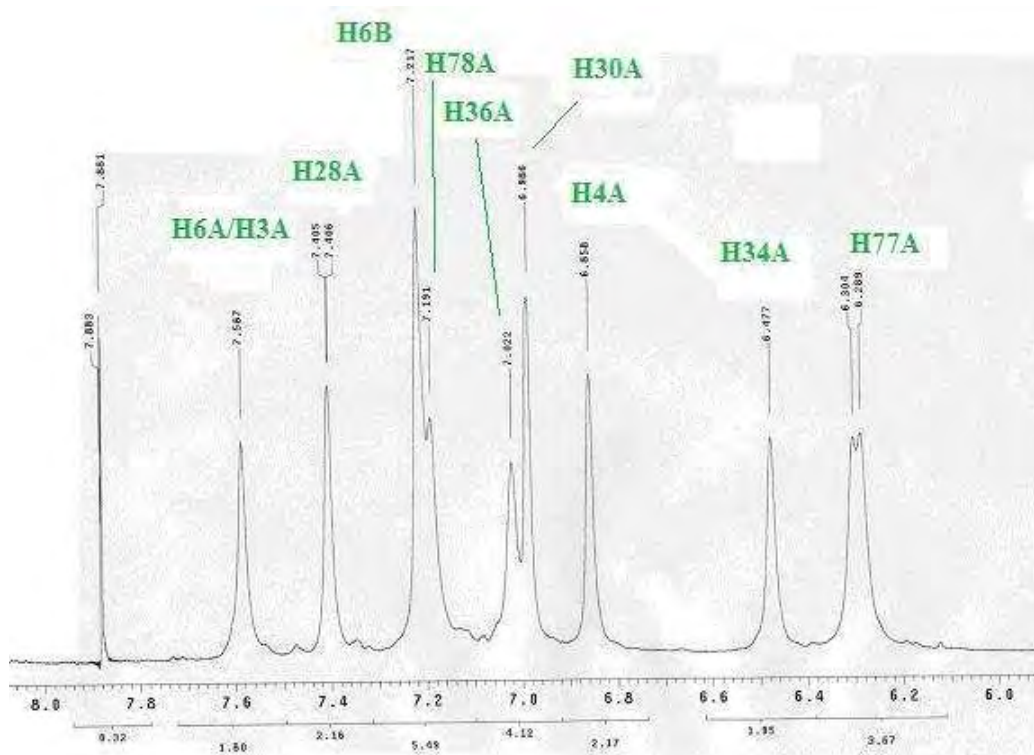


Figure 32. $^1\text{H-NMR}$ in the aromatic region

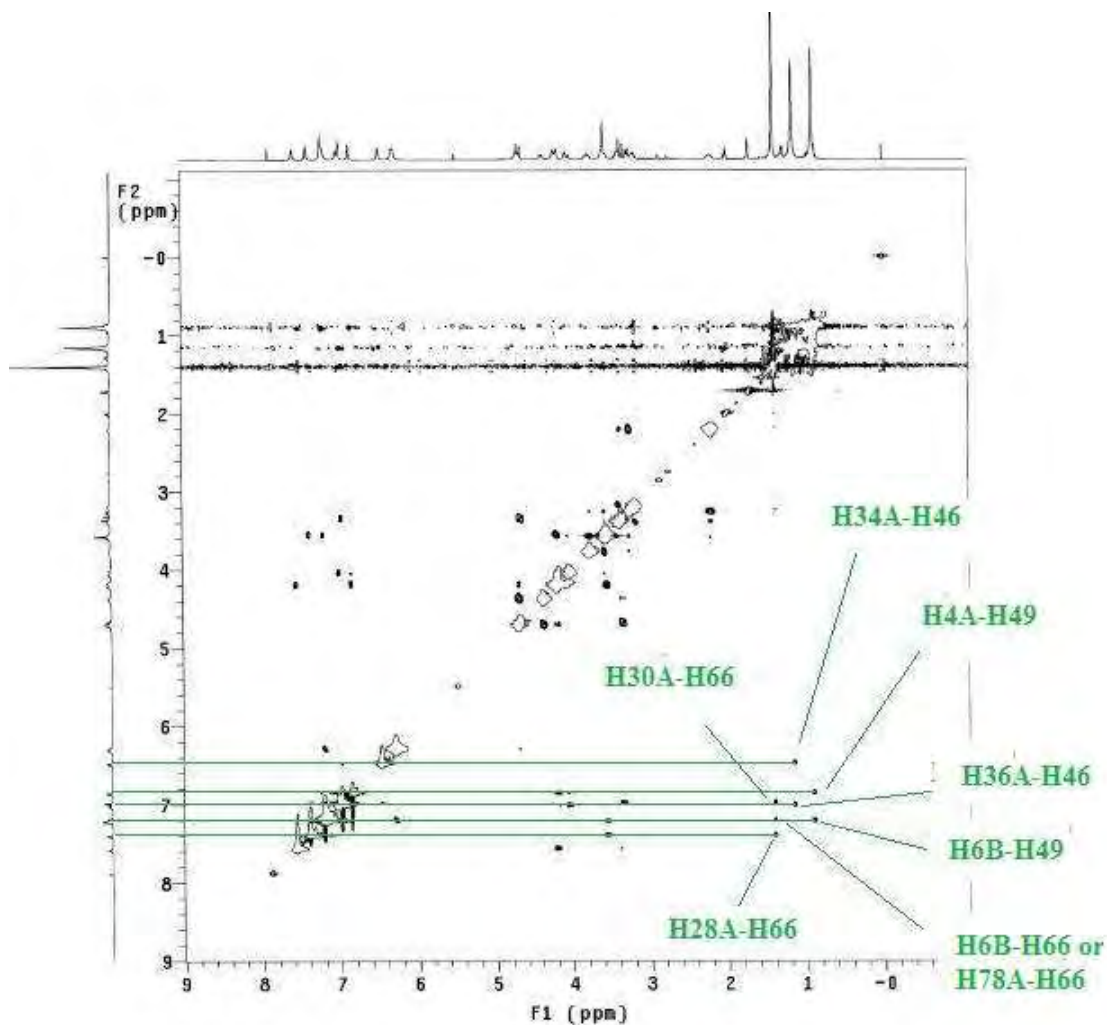


Figure 33. ROESY t-bu-aromatic labeled

The third aromatic NOE interaction on the aryl unit with the phenolic residue is likely the ortho proton on the benzoic acid. Altering the parameters of these ROESY experiments can show longer distance NOE cross-peaks that may reveal intermolecular interactions, providing evidence that **19** aggregates in solution.

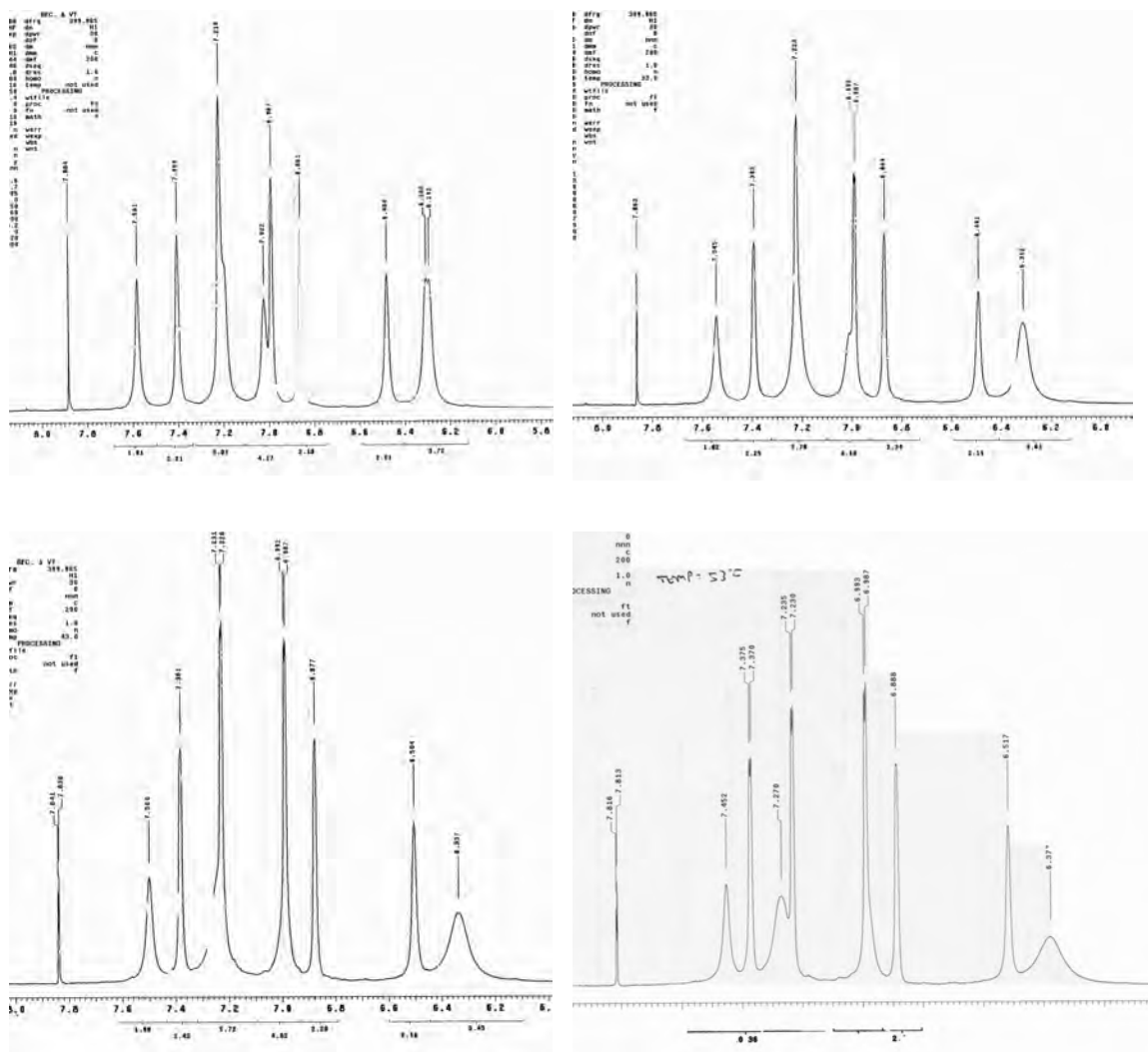


Figure 34. Variable temperature $^1\text{H-NMR}$ in aromatic region 23°C (top left), 33°C (top right), 43°C (bottom left), 53°C (bottom right)

A variable temperature $^1\text{H-NMR}$ experiment on **19** was performed on at 23, 33, 43, 53°C in THF- d_8 . Figure 34 shows the aromatic region. Upon heating, the resonances for the aromatic protons on the phenolic aryl unit H28A, H30A (7.41, 6.99 ppm) and the benzoic acid aryl unit H6B (7.22 ppm) split. The other benzoic acid aryl proton H4A (6.86 ppm) partially splits while the resonances for the bridging aryl unit H36A, H34A (7.02, 6.48 ppm) remain the same. As temperature increases, the intermolecular

hydrogen-bonding between benzoic acid groups and intramolecular hydrogen-bonding of the phenolic protons is disrupted, resulting in conformational flexing of their corresponding oligomer aryl units and splitting of their NMR signals. The bridging aryl unit remains fixed and no splitting occurs. The signal for H4A partially splits due to the adjacent bridging aryl unit, which restricts flexing in that region of the molecule somewhat. To confirm this theory, protic solvent, which also disrupts hydrogen-bonding, could be added to the sample and similar patterns should arise. Increasing temperature shifts the phenolic proton from 7.58 ppm to 7.45 ppm as electron density is increased. The benzoic acid aromatic protons coalesce and shift downfield (more so in the ortho position) with heating, which is caused by a decrease in electron density. This can be explained by disruption of hydrogen-bonding of the carboxylic acid. A carboxylic acid substituent is more deactivating, in terms of electrophilic aromatic substitution, than a carboxylate substituent. Figure 35 displays the temperature experiment in the methylene region. The obscured singlet at ~4.2 ppm which is the inner-cavity methylene(syn/anti) proton H26B shifts upfield slightly with heating which indicates an interaction between that proton and the phenolic oxygen. The proton H75A ($\text{OCH}_2\text{ArCOOH}$) shifts downfield somewhat, attributable to the decreased electron density imparted by the non-dimerized benzoic acid.

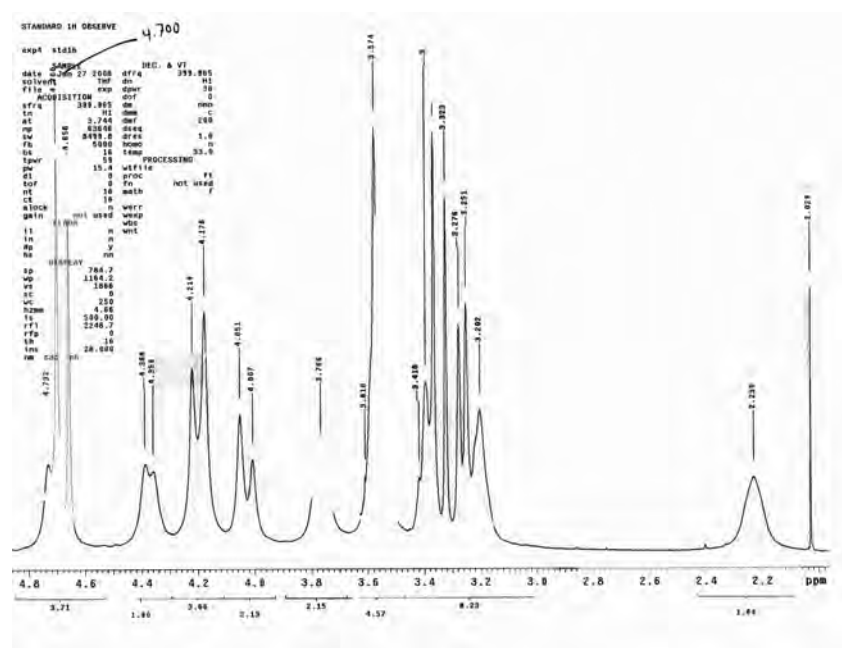
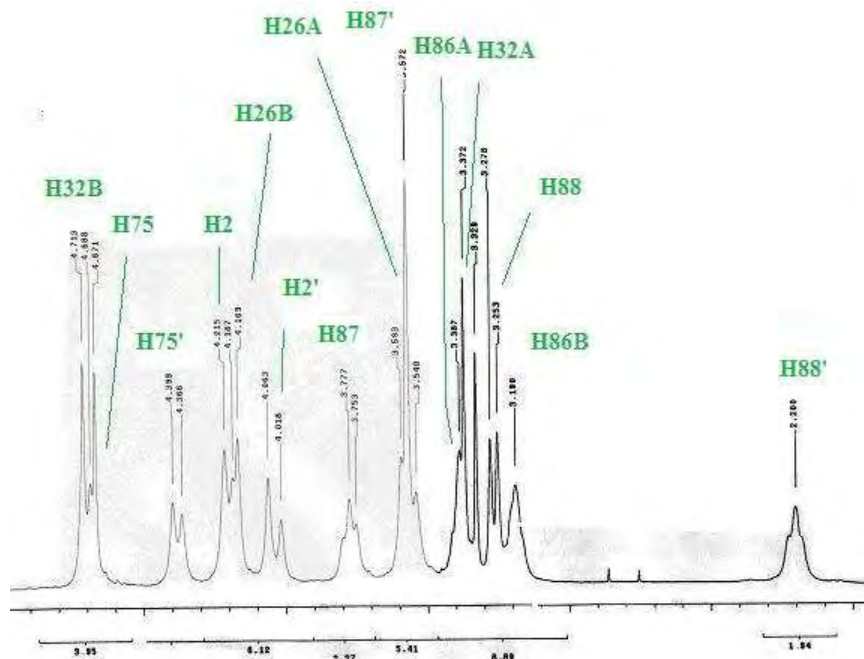


Figure 35. Variable temperature $^1\text{H-NMR}$ in methylene region 23°C (top), 33°C (bottom)

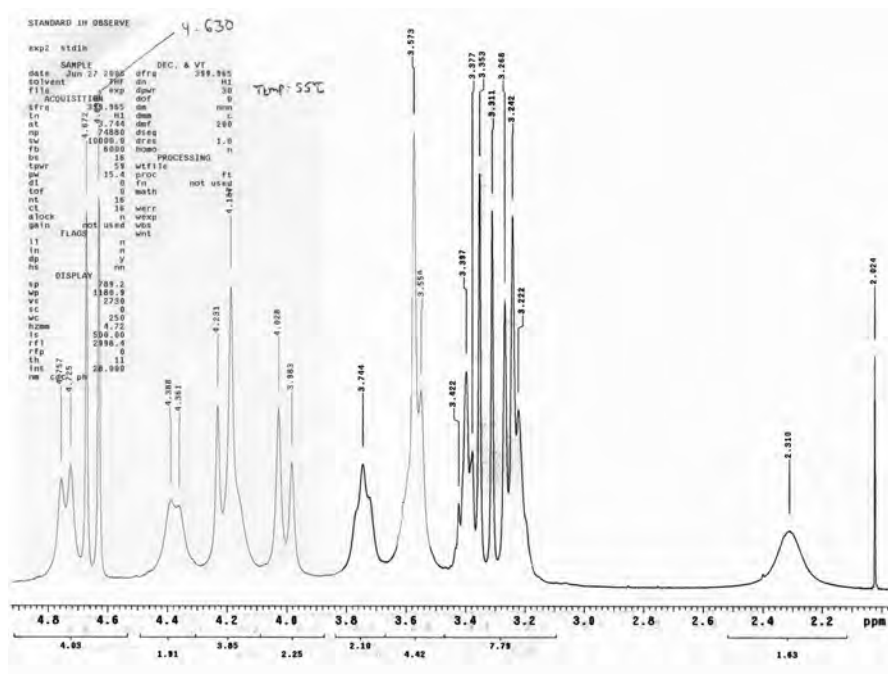
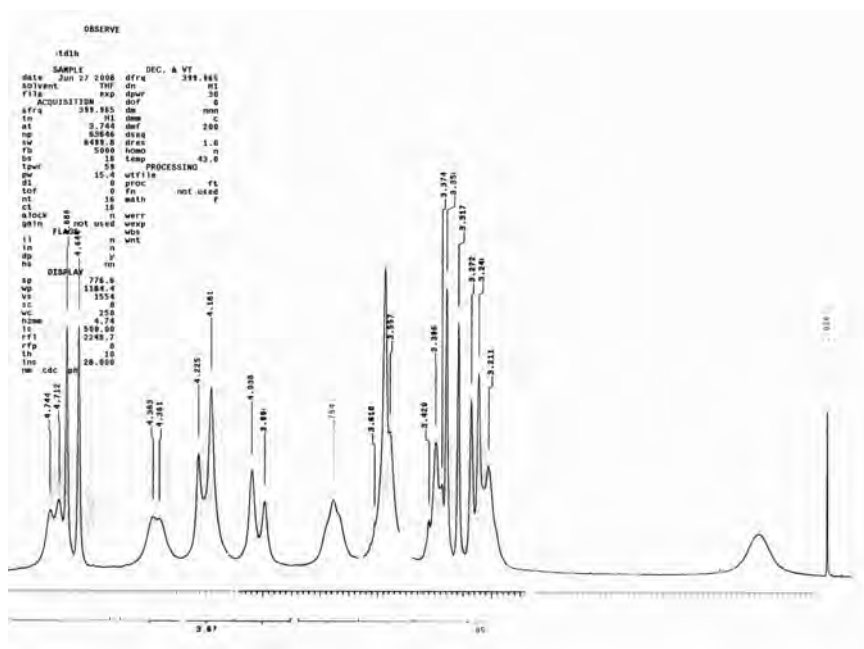


Figure 35. (continued) 43°C (top), 53°C (bottom)

CHAPTER III

CONCLUSIONS AND FUTURE WORK

Racemic, inherently chiral calix[6]arene dicarboxylic acid and diamine derivatives have been prepared. Strategies for optical resolution of the racemates were described based on conversion to diastereomers by classical salt formation or by appending chiral auxiliaries. X-ray crystallography and ^1H and ^{13}C NMR spectra indicated the racemic diacid and diamine adopt a rare 1,4-alternate conformation. The novel architecture orients the two proton donor or acceptor arms in opposite direction and makes the monomers good molecular tectons in self-assembly processes. The di-acid tecton self-assembled, through hydrogen bonding, into left-handed and right-handed helical nanotubes in the solid-state. Furthermore, the nanotubes were shown to encapsulate solvent (chloroform) molecules hinting at their potential as molecular containers.

When reviewing applications for these nanotubes, the two unique properties are taken into consideration: a) the enclosed environment b) the helical sense of the outer walls. A starting point for our group would be the study of encapsulation of small guest molecules. A combination of ROESY and X-ray diffraction crystallography would be a good approach. The through-space interactions between guest and host would help

determine if asymmetry is being transferred from the lining of the chiral nanotube to the entrapped guest. Strong host-guest NOEs would support an anisotropic orientation of guest molecules. The arrangement of guest molecules within the inner cavity that is inferred through NMR could be reinforced by host-guest crystal structures.

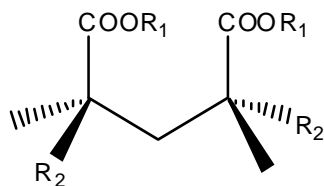
Polymer templating is a possible application for a calixarene nanotube. The helical **19^P** or **19^M** would serve as a nanostructured self-organized medium to shape polymeric reactions within the cavity. The interest in polymer templating resides in the specific properties that a template would impart on the final product that is not possible in bulk polymerizations. In our case, the transfer of asymmetry into the cavity results in an asymmetric product, in some form. Monomer/guest preorganization is the primary objective for such a system,³³ which can be determined from NOE experiments. A thermally-driven reaction would be undesirable in our template, since it is to be demonstrated that high temperatures disrupt the hydrogen-bonding in the aggregate and the template collapses before asymmetric polymerization can occur.

Photopolymerization provides a non-invasive means of initiating the reaction. The literature reports template-assisted photopolymerizations where a liquid crystal (LC) mesophase serves as a non-reactive organizing medium and upon completion of the reaction, the LC is removed from the final product.³⁴ Although no mesophase has been identified in our class of molecules, running a traditional photopolymerization in bulk solvent that favors hydrogen-bonding along with a single enantiomer of **19**, which will serve as a asymmetric catalyst, may result in a polymer of prescribed tacticity. Methacrylate derivatives would be a good series of monomer to screen for such a goal.

The conversion of methyl methacrylate to polymethyl methacrylate (PMMA) can proceed as a photo-induced free-radical polymerization.³⁵

ESI-MS can determine chiral host/guest binding. When a chiral host molecule is mixed with racemic guest molecules, diastereomeric complexes will form in solution. If the host-guest interaction is particularly strong, stable gas-phase adducts will form that can be detected and the host-adduct stoichiometry can be applied to the host-guest system in solution, to an extent.³⁶ A single one of the guest enantiomers can be isotopically labeled to distinguish the two diastereomeric adducts and enantioselectivity can then be calculated.³⁷ The host-guest stoichiometry can be confirmed and the specific interactions determined through NMR and x-ray diffraction crystallography. Analogues of **21_{S,S}** (see figure 36) and the corresponding enantiomer **21_{R,R}** would be the initial guest species to study since their polymethacrylates are the focus of our asymmetric catalysis studies.

Figure 36. Diastereomer **21_{S,S}**



It would be preferable to place the deuterium label on the R₁ group, away from the stereocenter, as to not influence the chiral recognition. Chiral TEA analogues would be a logical choice of guest for enantioselectivity studies due to their presence in the ESI-MS of amide analogues, perhaps due to the crown ether moiety, which is known to form positively-charged adducts with alkali salts as well as ammonium ion.³⁸

CHAPTER IV

EXPERIMENTAL

Melting points are uncorrected. $^1\text{H-NMR}$ and $^{13}\text{C-NMR}$ were performed on a Varian Unity INOVA 400 instrument using TMS as an internal standard at a frequency of 399.96 Hz and 100.58 Hz, respectively. ROESY experiments were performed on **19** using a concentration of 30mg substrate/0.75mL THF, mix time of 0.250s, relax delay of 1.00s, 16 repetitions, and 2x200 increments. ROESY were processed using Gaussian apodization methods. Preparative column chromatography separations were performed on Fluka flash chromatography silica gel 60 (230-400 mesh), while precoated silica gel plates (60 F₂₅₄) were used for analytical TLC. ESI mass spectra were performed in positive ion mode (PIM) using CHCl_3 as the matrix solvent. The data crystal for **19** was prism that had approximate dimensions; 0.30 x 0.24 x 0.12 mm. The data was collected on a Nonius Kappa CCD diffractometer using a graphite monochromator with $\text{MoK}\alpha$ radiation ($\lambda = 0.71073\text{\AA}$). A total of 785 frames of data were collected using ω -scans with a scan range of 0.8° and a counting time of 73 seconds per frame. The data were collected at 153 K using an Oxford Cryostream low temperature device. THF was purified via distillation over sodium metal/benzophenone. DMF was dried over 3 angstrom molecular sieve. DCM was purified via distillation over CaH_2 . Sodium hydride was stripped of mineral oil using anhydrous pentane or hexanes via cannula

transfer. All other chemicals were commercially available and used without further purification.

t-bu-calix[6]arene

SYNTHESIS: 100g of p-t-bu-phenol was added to a 3000 mL 3-neck round bottom flask fitted with a mechanical stirrer, a Dean-Stark trap, and a reflux condenser. 42g of paraformaldehyde was added then 1000 mL xylenes. Argon was introduced and heat was applied. 34 mL of RuOH solution (50% by weight in H₂O) was added and reflux started. The initial orange solution turned a thick white precipitate as water collected in the Dean-Stark trap. Heating was discontinued after 4h of reflux. The reaction mixture was filtered to give a pale white powder. The powder was reconstituted in 3000 mL CHCl₃/1000 mL 1 N HCl, washed, and the organic phase separated. The organic phase was washed a second time with 500 mL brine. The organic was dried over anhydrous MgSO₄, filtered, and concentrated to 500 mL under vacuum to form a precipitate. 300 mL of MeOH was added to further precipitation. The precipitate was filtered and dried to give 85 g of t-bu-calix[6]arene as a fine, white powder (yield 79%). ¹H-NMR (CDCl₃) δ 1.25 (s, 54H, C(CH₃)₃), 3.88 (s, 12H, CH₂), 7.15 (s, 12H, ArH), 10.55 (s, 6H, ArOH).

1,4-di-tolunitrile-t-bu-calix[6]arene

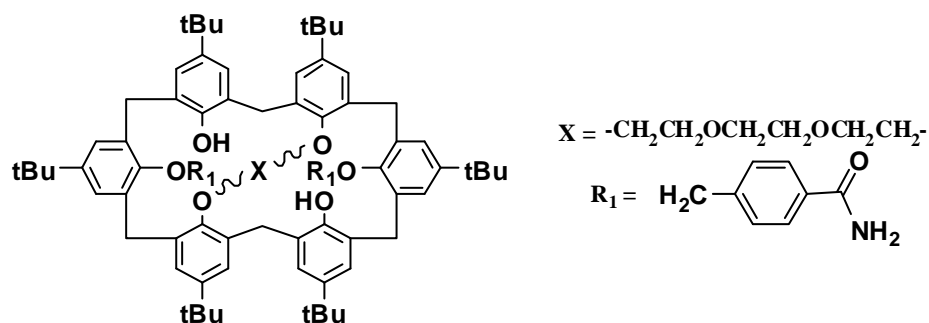
SYNTHESIS: 10 g of t-bu-calix[6]arene was added to 2000 mL 2-neck round bottom flask and then added 900/100 mL THF/DMF. The flask was immersed in an ice-water bath then added 9 g of potassium trimethyl silanolate ($\text{KOSi}(\text{Me})_3$) under magnetic stirring to form a yellow solution. 6 g of 4-bromomethyl tolunitrile was dissolved in 100 mL THF and added to an addition funnel and dripped into the reaction over a period of 2h under argon. A precipitate would form and the reaction color became pink. At the 3h mark, the THF was removed under reduced pressure in a 45°C rotavap bath. The DMF was then stripped under vacuum pump pressure. The residue was reconstituted in 600/200 mL CHCl_3 /2N HCl (some ethanol was added to ease the emulsion) and the organic washed/separated. The organic was washed a second time with 200 mL brine. The organic was separated, dried over anhydrous MgSO_4 , filtered, and concentrated to 20 mL in a 65°C rotavap bath. The oil was slowly added to 500 mL of stirring MeOH to form a precipitate. The precipitate was filtered and dried to give 8.2 g of 1,4-di-tolunitrile-t-bu-calix[6]arene as a white powder (yield 66%). $^1\text{H-NMR}$ (CDCl_3) δ 1.12 (s, 18H), 1.25 (s, 36H), 3.48 (d, 2H, $J=14.0$ Hz), 3.54 (d, 2H, $J=14.0$ Hz), 3.91 (d, 2H, $J=14.0$ Hz), 4.29 (d, 4H, $J=14.0$ Hz), 6.98 (s, 4H), 7.10 (d, 8H, $J=2.5$ Hz), 7.47 (d, 4H, $J=8.5$ Hz), 7.55 (d, 4H, $J=8.5$ Hz), 7.71 (s, 4H)

1,4-di-tolunitrile-2,5-triethyleneoxy-t-bu-calix[6]arene **9**

SYNTHESIS: 2.0 g of NaH (60% oil dispersion) was added to a dry 2000 mL 2-neck round bottom flask under argon. The NaH was washed several times with anhydrous pentane via canula. 700/70 mL THF/DMF was added along with 8.2 g of 1,4-di-tolunitrile-t-bu-calix[6]arene to form a mixture. The reaction flask was outfitted with a reflux condenser and an addition funnel. The reaction was brought to reflux to form an orange solution. 3.8g triethylene glycol di-p-tosylate was dissolved in 100mL of THF in the addition funnel and the contents dripped into the refluxing reaction flask over a period of 2h under argon. A precipitate would form during the addition. At the 5h mark, the reaction was cooled and the THF removed under reduced vacuum. The remaining DMF solution was slowly added to 2 L of cold, stirring 0.12 N HCl to form a precipitate. The precipitate was dried and reconstituted in 500/125 mL CHCl₃/Brine and the organic washed/separated. The organic was dried over anhydrous MgSO₄, filtered, and concentrated to 20 mL in a 65°C rotavap bath. The oil was slowly added to 500 mL of stirring MeOH to form a precipitate. The precipitate was filtered and dried to give 8.7 g of 1,4-di-tolunitrile-t-bu-calix[6]arene as a white powder (yield 80%). ¹H-NMR (CDCl₃) δ 7.54 (s, 2H), 7.34, 7.03 (AXq, J = 2.4 Hz), 7.14, 6.80 (AXq, J = 2.0 Hz, 4H), 7.00, 6.48 (AXq, J = 2.0 Hz, 4H), 6.70, 6.38 (AXq, J = 8.0 Hz, 8H), 4.65, 4.49 (ABq, J = 13.6 Hz, 4H), 4.59, 3.26 (AXq, J = 17.2 Hz, 4H), 4.19, 3.56 (AMq, J = 17.6 Hz, 4H), 4.16, 4.03 (ABq, J = 16.8 Hz, 4H), 3.87 (t, J = 10 Hz, 2H), 3.51 (t, J = 10 Hz, 2H), 3.33–3.35, (m,

3H), 3.23–3.21 (m, 3H), 2.10 (t, $J = 10$ Hz, 2H), 1.42 (s, 18H), 1.17 (s, 18H), 0.89 (s, 18H)

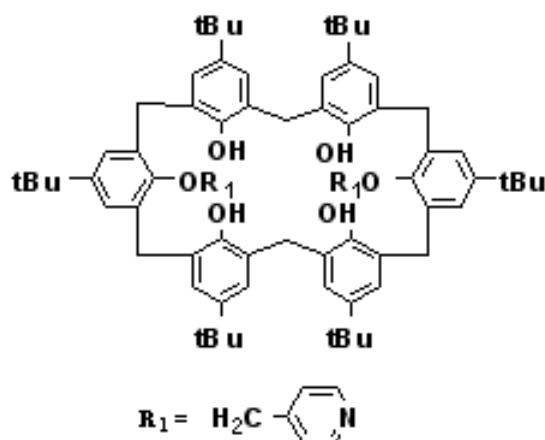
1,4-di-benzamide-2,5-triethyleneoxy-t-bu-calix[6]arene **10**



SYNTHESIS: 500 mg of 1,4-di-tolunitrile-2,5-triethyleneoxy-t-bu-calix[6]arene was added to a 100 mL round-bottom flask equipped with a magnetic stirrer. 20 mL of THF was added to form a yellow solution and 682 μL of tetramethyl ammonium hydroxide (TMAH, 25% by weight in H_2O) was added. The reaction was left to reflux under argon for 48h, during which time a precipitate would form. The solvent was removed under reduced pressure and the residue was reconstituted in 15/8 mL $\text{CHCl}_3/2\text{N HCl}$. The organic was washed and separated, then washed a second time with 8 mL 2N HCl. The organic was dried over anhydrous MgSO_4 , filtered, and concentrated to an oil in a 65°C rotavap bath. 50 mL of MeOH was added to form a precipitate, which was filtered to recover 287 mg of 1,4-di-benzamide-2,5-triethyleneoxy-t-bu-calix[6]arene as a white

powder (yield 56%). Left in the filtrate was unreacted starting material as well as mono-substituted amide. $^1\text{H-NMR}$ (CDCl_3) δ 7.33 (s, 2H, ArOH), 7.30 (d, 2H, ArH, 2.4 Hz), 7.17 (d, 2H, ArH, 2.0 Hz), 7.00 (d, 4H, $\text{OCH}_2\text{ArHHCONH}_2$, 8 Hz), 6.99 (s, 2H, ArH), 6.93 (d, 2 H, ArH, 2.4 Hz), 6.93 (d, 2H, ArH, 2.0 Hz), 6.48 (s, 2H, ArH), 6.35 (d, 4H, $\text{OCH}_2\text{ArHHCONH}_2$, 8 Hz), 6.07 (bs, 2H, NH_2), 5.63 (bs, 2H, NH_2), 4.67 (d, 2H, OCH_2Ar 13.2 Hz), 4.36 (d, 2H, $\text{HOArCH}_2\text{ArOX}$, 17.2 Hz), 4.21 (d, 2H, $\text{XOArCH}_2\text{ArOR}_1$, 17.6 Hz), 4.19 (d, 2H, $\text{HOArCH}_2\text{ArOR}_1$, 13.6 Hz), 4.05 (d, 2H, OCH_2Ar 13.2 Hz), 3.99 (d, 2H, $\text{XOArCH}_2\text{ArOR}_1$, 17.6 Hz), 3.89 (t, 2H, $\text{ArOCH}_2\text{CH}_2\text{OCH}_2$), 3.59 (t, 2H, $\text{ArOCH}_2\text{CH}_2\text{OCH}_2$), 3.56 (d, 2H, $\text{HOArCH}_2\text{ArOR}_1$, 13.6 Hz), 3.33 (t, 2H, $\text{ArOCH}_2\text{CH}_2\text{OCH}_2$), 3.27 (m, 4H, $\text{ArOCH}_2\text{CH}_2\text{OCH}_2$), 3.24 (d, 2H, $\text{HOArCH}_2\text{ArOX}$, 17.2 Hz), 2.28 (t, 2H, $\text{ArOCH}_2\text{CH}_2\text{OCH}_2$), 1.35 (s, 18H, CH_3), 1.16 (s, 18H, CH_3), 0.98 (s, 18H, CH_3) $^{13}\text{C-NMR}$ (CDCl_3) δ 30.43 ($\text{HOArCH}_2\text{ArOX}$), 31.09 (CH_3), 31.52 (CH_3), 31.82 (CH_3), 33.95, 38.78 ($\text{XOArCH}_2\text{ArOR}_1$), 69.55 ($\text{ArOCH}_2\text{CH}_2\text{OCH}_2$), 69.94 ($\text{ArOCH}_2\text{CH}_2\text{OCH}_2$), 70.23 (OCH_2Ar), 71.64 ($\text{ArOCH}_2\text{CH}_2\text{OCH}_2$), 124.10, 124.31, 124.91, 125.32, 125.44, 125.79, 126.54, 127.02, 130.77, 130.94, 132.17, 133.65, 135.14, 141.82, 142.38, 145.43, 147.73, 150.06, 151.17, 153.51, 169.57 (CONH_2) ESI-MS m/z 1353.6 (M+1), 1375.6 (M+Na)

1,4-di-pyridinyl-t-bu-calix[6]arene



SYNTHESIS: 7.0 g (7.2 mmol) of t-bu-calix[6]arene was added to 1000 mL 3-neck round bottom flask and then added 100 mL anhydrous DMF under argon. The reaction flask was outfitted with a reflux condenser and an addition funnel. 4.8g (30.4 mmol) BaO and 2.6g (14.9 mmol) Ba(OH)₂ was added to form a suspension. The flask was immersed in an oil bath under stirring and brought to 50-60 °C. To the addition funnel was added a yellow solution of 3.8g (14.6 mmol) of 4-bromomethyl-pyridine HCl in 100 mL anhydrous DMF. The reagent was dripped in over the course of 1h, during which the reaction color went from pink → green → dark purple. After 16h, the reaction was removed from the heat and 100 mL MeOH was added. 2L H₂O was added to form a thick, dark green slurry. The precipitate was filtered, washed with successive portions of MeOH and H₂O, and then dried to give 12g of crude brown powder. The crude was dissolved in minimal CHCl₃ and loaded onto a silica gel column using 50:50 CHCl₃:Acetone as eluent to isolate 1.3g of 1,4-di-pyridine-t-bu-calix[6]arene as a white

powder (yield 16%). ^{13}C -NMR (CDCl_3) δ 31.19, 31.54, 32.15, 33.90, 75.25, 121.27, 125.54, 125.88, 126.13, 126.90, 132.24, 142.86, 149.76

1,4-di-pyridinyl-2,5-triethyleneoxy-t-bu-calix[6]arene **11**

SYNTHESIS: 490 mg of NaH (60% oil dispersion) was added to a dry 250 mL 3-neck round bottom flask under argon. The NaH was washed several times with anhydrous pentane via canula. 150 mL acetone was added along with 1.0025 g of 1,4-di-pyridine-t-bu-calix[6]arene to form a clear solution. The reaction flask was outfitted with a reflux condenser and an addition funnel. The reaction was brought to reflux to form a yellow solution. 568 mg triethylene glycol di-p-tosylate was dissolved in 25mL of acetone in the addition funnel and the contents dripped into the refluxing reaction flask over a period of 2h under argon. A precipitate would form during the addition. At the 12h mark, the reaction was cooled and the acetone removed under reduced vacuum. The remaining oil was reconstituted in 200/100 mL CHCl_3 /0.12 N HCl and the organic washed/separated. The organic was washed a second time with 100 mL brine. The organic was dried over anhydrous MgSO_4 , filtered, and concentrated in a 50°C rotavap bath. The oil was loaded

onto a silica gel column using 70:30 CHCl_3 :Acetone as eluent to isolate 278.4mg of 1,4-di-pyridine-2,5-triethyleneoxy-t-bu-calix[6]arene as a white powder (yield 25%). $^1\text{H-NMR}$ (CDCl_3) δ 0.8-1.4 (3s, 54H, CH_3), 2.13 (t, 2H, $\text{ArOCH}_2\text{CH}_2\text{OCH}_2$), 3.30 (d, 2H, $\text{HOArCH}_2\text{ArOX}$, 16.8 Hz), 3.32 (m, 4H, $\text{ArOCH}_2\text{CH}_2\text{OCH}_2$), 3.35 (t, 2H, $\text{ArOCH}_2\text{CH}_2\text{OCH}_2$), 3.56 (t, 2H, $\text{ArOCH}_2\text{CH}_2\text{OCH}_2$), 3.58 (d, 2H, $\text{HOArCH}_2\text{ArOR}_1$, 13.6 Hz), 3.89 (t, 2H, $\text{ArOCH}_2\text{CH}_2\text{OCH}_2$), 4.09 (q, 4H, $\text{XOArCH}_2\text{ArOR}_1$, 19.6 Hz), 4.20 (d, 2H, $\text{HOArCH}_2\text{ArOR}_1$, 13.6 Hz), 4.35 (d, 2H, OCH_2Ar , 13.6 Hz), 4.59 (d, 2H, $\text{HOArCH}_2\text{ArOX}$, 16.8 Hz), 4.61 (d, 2H, OCH_2Ar , 13.6 Hz), 6.16 (d, 4H, OCH_2ArHHN , 5.6 Hz), 6.49 (d, 2H, ArH , 2.0 Hz), 6.81 (d, 2H, ArH , 2.4 Hz), 7.00 (d, 2H, ArH , 2.4 Hz), 7.01 (d, 2H, ArH , 2.4 Hz), 7.17 (d, 2H, ArH , 2.0 Hz), 7.33 (d, 2H, ArH , 2.4 Hz), 7.51 (s, 2H, ArOH), 7.68 (d, 4H, OCH_2ArHHN , 5.6 Hz) $^{13}\text{C-NMR}$ (CDCl_3) δ 29.73 ($\text{HOArCH}_2\text{ArOX}$), 30.84 (CH_3), 31.16 ($\text{C}(\text{CH}_3)$), 31.50 (CH_3), 31.60 ($\text{C}(\text{CH}_3)$), 31.66 ($\text{C}(\text{CH}_3)$), 31.73 ($\text{HOArCH}_2\text{ArOR}_1$), 31.80 (CH_3), 33.98, 38.74 ($\text{XOArCH}_2\text{ArOR}_1$), 68.30 (OCH_2Ar), 69.59 ($\text{ArOCH}_2\text{CH}_2\text{OCH}_2$), 69.90 ($\text{ArOCH}_2\text{CH}_2\text{OCH}_2$), 71.47 ($\text{ArOCH}_2\text{CH}_2\text{OCH}_2$), 119.78 ($\text{OCH}_2\text{Ar}(\text{CC})\text{N}$), 124.03 (ArCH), 124.21 (ArCH), 124.90, 125.21 (ArCH), 125.25 (ArCH), 125.44 (ArCH), 126.40, 127.52 (ArCH), 130.13, 131.35, 133.46, 135.59, 141.77, 145.75, 146.78, 147.61, 148.68 ($\text{OCH}_2\text{Ar}(\text{CC})\text{N}$), 149.99, 151.31, 153.05

4-bromomethyl-benzoic acid

SYNTHESIS: 1.5115 g (7.7mmol) of 4-bromomethyl-tolunitrile was added to a 100 mL round bottom flask. 10/10/10 mL H₂O/AcOH/H₂SO₄ was added and a reflux condenser attached. The reaction was brought to reflux to form a solution. A precipitate would form after 1h. Heat was removed and the reaction flask immersed in an ice-water bath. The mixture was diluted with 50 mL H₂O and then filtered. The filter cake was dissolved in 2N NaOH and then acidified with 2 N HCl to form a precipitate. The mass was filtered, washed three times with H₂O, and dried. The precipitate was recrystallized from 95% EtOH to recover 1.2387g (5.76mmol) of 4-bromomethyl-benzoic acid as colorless crystals (yield 75%). ¹³C-NMR (DMSO) δ 33.26, 129.42, 129.69, 130.58, 142.81, 166.89

4-bromomethyl-N-(leucine methyl ester)benzamide

SYNTHESIS: 1.5870 g (7.01 mmol) of 4-bromomethyl-benzoic acid was added to a dry, argon-charged, 500 mL round bottom flask. 1.175g (7.69mmol) of 1-hydroxy-benzotriazole hydrate (HOBt) and 1.3733g (7.02mmol) of 1-ethyl-3(3-dimethylaminopropyl) carbodiimide HCl (EDC) was added. 165 mL of anhydrous THF and 120 mL anhydrous CH₂Cl₂ was added to form a solution. 2.1 mL of TEA was added.

In a separate 100 mL round-bottom flask was added 1.4015g (7.71mmol) of leucine methyl ester HCl and then dissolved in 45 mL CH₂Cl₂. The reaction flask was immersed in an ice-water bath and the reagent dripped in over 45 minutes via addition funnel. At the 16h mark, the solvent was stripped under vacuum to recover an oil, which was reconstituted in 100 mL CH₂Cl₂ and washed 3 times with 30 mL H₂O. The organic phase was dried over MgSO₄, filtered, and rotovapped to leave an oil. 100 mL of hexanes was added to form a white precipitate, which was filtered and dried to give 1.29g of 4-bromomethyl-N-(leucine methyl ester)benzamide as a white powder (yield 54%). ¹³C-NMR (CDCl₃) δ 21.86, 22.86, 24.99, 51.26, 52.41, 64.06, 126.55, 127.22, 132.34, 145.26, 167.61, 174.09

1,4-di-ethyl acetyl-t-bu-calix[6]arene **12**

SYNTHESIS: 2.41 g (2.48 mmol) of t-bu-calix[6]arene was added to a dry 250 mL round bottom flask and then added 80 mL anhydrous DMF under argon. 1.52g (9.92 mmol) BaO and 0.867g (4.96 mmol) Ba(OH)₂ was added to form a suspension. The contents were left under magnetic stirring for 10 minutes. 580 μL (5.14 mmol) of ethyl bromoacetate was dripped in over the course of 10 minutes. After 16h, the reaction contents were dumped into 300 mL H₂O to form a thick precipitate. The precipitate was filtered, reconstituted in 150/50 mL CHCl₃/2 N HCl, and washed with 50 mL portions of

2 N HCl/brine. Typical workup followed by $\text{CHCl}_3/\text{MeOH}$ precipitation would give 1.62g of white powder. The crude was dissolved in minimal CHCl_3 and loaded onto a silica gel column using CHCl_3 as eluent to isolate 800 mg of 1,4-di-ethyl acetyl-t-bu-calix[6]arene as a white powder (yield 27%). $^{13}\text{C-NMR}$ (CDCl_3) δ 14.01, 31.28, 31.54, 32.10, 32.27, 33.92, 34.25, 61.39, 70.89, 125.52, 125.83, 125.95, 132.24, 142.57, 147.72, 149.27, 151.80, 169.63

1,4-di-ethanoic acid-t-bu-calix[6]arene **13**

$^{13}\text{C-NMR}$ (CDCl_3) δ 31.15, 31.31, 31.39, 32.19, 33.79, 34.30, 70.32, 124.80, 125.27, 126.62, 127.10, 127.18, 132.57, 142.99, 148.10, 151.74, 172.33

4-bromomethyl-methyl benzoate

SYNTHESIS: 21 g (93 mmol) of 4-bromomethyl-benzoic acid was added to a 1000 mL round bottom flask. 300/6 mL $\text{MeOH}/\text{H}_2\text{SO}_4$ was added to form a slurry and a reflux condenser attached. The reaction was brought to reflux under stirring to form a solution.

After 1.5h, heating was discontinued and the solvent was concentrated to 50 mL on a rotavap. 760 mL H₂O was added to form a precipitate. The precipitate was filtered and the crude filter cake was recrystallized from MeOH to give 10.4g of 4-bromomethyl-methyl benzoate as colorless crystals (yield 50%). mp 48-50°C lit 56 °C

1,4-di-methyl benzoate-t-bu-calix[6]arene **14**

SYNTHESIS: A similar synthesis to that of 1,4-di-tolunitrile-t-bu-calix[6]arene was followed to afford 11.25g of 1,4-di-methyl benzoate-t-bu-calix[6]arene as a white powder (yield 86%). ¹H-NMR (CDCl₃) δ 1.07 (s, 18H, C(CH₃)₃), 1.26 (s, 36H, C(CH₃)₃), 3.52 (d, 4H, HOArCH₂ArOR₁, 14 Hz), 3.58 (d, 2H, HOArCH₂ArOH, 14.4 Hz), 3.85 (d, 2H, HOArCH₂ArOH, 14 Hz), 3.89 (s, 6H, OCH₃), 4.34 (d, 2H, HOArCH₂ArOR₁, 14 Hz), 6.94 (s, 4H, ArH), 7.09 (bs, 8H, ArH), 7.50 (d, 4H, OCH₂ArHHCOOMe, 8 Hz), 7.91 (d, 4H, OCH₂ArHHCOOMe, 8 Hz), 8.03 (s, 4H, ArOH)

1,4-di-tolunitrile-2,5-triethyleneoxy-3,6-(-)menthoxy acetyl-t-bu-calix[6]arene **15**

SYNTHESIS: To a dry 250mL RB flask was added 1.4g(1.06 mmol) of 1,4-ditolunitrile-2,5-triethyleneoxy-t-bu-calix[6]arene. The flask was flushed with argon under stirring and 90/10 mL THF/DMF was added to form a clear solution. 300mg(7.5 mmol) of NaH (60% mineral oil dispersion) was washed with hexanes and added to form a yellow solution. 1.186mL(5.2 mmol) of (-)-menthoxy acetyl chloride was dripped into the flask over 2h and the solution became turbid. The reaction was left to stir under argon for 12h, at which point, a few drops of MeOH was added to destroy the excess hydride. The solution was rotavapped to dryness and then reconstituted in 200/100 mL of CHCl₃/H₂O. The binary was mixed in a sep funnel and then the organic was separated. The organic was washed a second time with 100mL H₂O then brine. The organic was dried over anhydrous MgSO₄, filtered, then rotavapped to dryness. The crude was reconstituted in minimal CH₂Cl₂ and purified through flash chromatography (60:40 DCM:hexanes) to isolate 150 mg of mixed diastereomers. ¹³C-NMR (CD₂Cl₂) δ 15.36, 19.92, 19.98, 21.34, 22.49, 22.52, 27.89, 27.96, 28.56, 28.65, 28.84, 28.90, 30.17, 30.19, 30.27, 30.30, 30.61, 30.67, 30.72, 33.43, 33.57, 33.59, 39.21, 39.49, 47.32, 47.38, 64.11, 64.73, 68.09, 68.21, 69.28, 69.43, 71.58, 73.81, 73.88, 79.43, 80.09, 111.15, 111.20, 117.79, 117.83, 123.53, 123.59, 123.93, 124.18, 124.26, 124.31, 124.77, 125.03, 130.96, 131.00, 131.06, 131.10, 131.67, 131.71, 132.14, 132.28, 132.63, 132.66, 142.10, 142.20, 142.51, 142.58, 145.49, 145.55, 145.62, 145.68, 147.06, 150.46, 153.11, 168.87

1,4-di-benzylamine-2,5-triethyleneoxy-t-bu-calix[6]arene **16**

SYNTHESIS: To a dry 250 mL 3-neck RB flask under a stream of argon was charged 30 mL of freshly distilled THF and then slowly added 1.32g (33.0 mmol) LiAlH₄ under stirring (caution-frothing will occur) to form a grey slurry. In a separate 50 mL RB flask was added 2.73g(2.07mmol) of 1,4-di-tolunitrile-2,5-triethyleneoxy-t-bu-calix[6]arene and 20 mL THF to form a colorless solution. The substrate was dripped into the LiAlH₄ mixture over the course of 2h under argon to form an initially green mixture that would turn orange with time. At the 7h mark, the reaction flask was immersed in an ice-water bath and diluted with 30 mL THF. 2.3 mL of 10% NaOH was cautiously dripped in over a stream of argon under stirring (rapid evolution of H₂), followed by 4.2 mL of H₂O to form white solids. The lithium salts were filtered off and washed several times with THF. The THF was rotavapped off to leave a white residue. The residue was reconstituted in minimal CHCl₃ and precipitated from MeOH. The precipitate was filtered to give 2.25g of 1,4-di-benzylamine-2,5-triethyleneoxy-t-bu-calix[6]arene as a white powder (yield 82%). ¹H-NMR (CDCl₃) δ 7.38 (bs), 7.26 (s), 7.15 (d, 2 Hz), 6.94 (bs), 6.87 (s), 6.46 (bs), 6.24 (s), 4.65 (s), 4.54 (d, 16.8 Hz), 4.27 (s), 4.18 (bs), 4.00 (bs), 3.86 (bs), 3.53 (s), 3.31 (d, 12 Hz), 3.24 (s), 2.22 (bs, 2H), 1.66 (bs, 4H, NH₂), 1.34 (s, 18H, CH₃), 1.15 (s, 18H, CH₃), 0.95 (s, 18H, CH₃) ¹³C-NMR (CDCl₃) δ 30.34, 31.07, 31.49, 31.61, 31.70, 31.82, 33.92, 34.16, 38.83, 46.24 (CH₂NH₂), 69.70, 69.90, 71.62, 124.05, 124.25, 124.99, 125.42, 126.27, 127.07, 130.50, 131.76, 133.56, 135.50, 136.43, 141.44, 145.32, 147.25, 151.20, 153.90

1,4-di-N-BOC-phenylalanine-2,5-triethyleneoxy-t-bu-calix[6]arene **17**

SYNTHESIS: To a dry 250 mL RB flask was added 101.6 mg (0.665 mmol) of HOBt, followed by 176 mg (0.665 mmol) of N-BOC-phenylalanine. 8 mL of anhydrous DCM was added to form a solution. In a separate 50 mL RB flask under argon was added 130 mg (0.665 mmol) of EDC, followed by 10 mL DCM to form a solution. 111 μ L of TEA was added to the EDC solution. The EDC solution was transferred to the HOBt/N-BOC-phenylalanine solution via canula. To a separate 500 mL RB flask was added 400 mg (0.302 mmol) of 1,4-di-benzylamine-2,5-triethyleneoxy-t-bu-calix[6]arene, which was then dissolved in 100 mL of DCM. The reagent solution was then dripped into the reaction. The reaction was left to stir under argon for 24h. The solvent was concentrated to 50 mL under vacuum, and the organic was washed with 15 mL of 0.1 N HCl, followed by 15 mL of brine. The organic was dried over anhydrous MgSO₄, filtered, then rotavapped to a crystalline oil. The crude was purified by silica gel flash chromatography using a 90:10 \rightarrow 75:25 \rightarrow 0:100 hexanes:EtOAc solvent system. 1.3g of a single diastereomer was isolated (yield 28%). ¹³C-NMR (CDCl₃) δ 28.21 (OC(CH₃)₃), 30.80, 31.15 (ArC(CH₃)₃), 31.48 (ArC(CH₃)₃), 31.76 (ArC(CH₃)₃), 33.83 (ArC(CH₃)₃), 33.96 (ArC(CH₃)₃), 34.10 (ArC(CH₃)₃), 38.81, 42.96 (ArCH₂NHCOOR), 55.92 (ArCH₂CH(NHR)(COOR)), 69.61 (ArOCH₂CH₂OCH₂), 69.85 (ArOCH₂CH₂OCH₂), 70.67 (ArOCH₂Ar), 71.69 (ArOCH₂CH₂OCH₂), 79.55 (OC(CH₃)₃), 123.90, 124.25, 124.90, 125.34, 125.75, 125.95, 126.57, 127.08, 128.33 Ar(CH_m)CH₂CH(NHR)(COOR), 129.33 Ar(CH₀)CH₂CH(NHR)(COOR), 130.59, 132.00, 133.78, 135.28, 137.04, 141.44,

145.08, 147.35, 150.20, 151.07, 153.88, 155.47 (RNHCOOtBu), 171.31 (CH₂NHCOOR)

ESI-MS m/z 1921.54 (M+1+TEA, 100), 1878.87 (M+1+C₄H₈, 50), 1820.50 (M+1, 34)

Anal. Calcd for C₁₁₆H₁₄₆N₄O₁₄: C, 76.53; H, 8.08; N, 3.08 Found: C, 73.47; H, 7.82; N, 2.93

1,4-di-(+)-2-methyl-butylamide-2,5-triethyleneoxy-t-bu-calix[6]arene **18**

SYNTHESIS: To a dry 100 mL RB flask was added 346 mg (2.26 mmol) HOBt with 3 Å molecular sieve. The flask was charged with argon and then 20 mL of DCM was added to form a slurry. The slurry was stirred under argon for 10 minutes. 201 µL of pyridine was added to form a solution. 512 µL (2.41 mmol) of (S)-(+)-2-methyl-butiric anhydride was dripped into the reaction and the reagent solution was allowed to stir for 1h. In a separate 250 mL RB flask, 1.3127g (0.990 mmol) of 1,4-di-benzylamine-2,5-triethyleneoxy-t-bu-calix[6]arene was added and charged with argon. 100 mL DCM was added followed by mild heating to form a solution. Argon was bubbled through the stirring solution for 5 minutes. The reagent solution was transferred to the substrate via canula. The reagent residue was washed with 5 mL DCM and transferred to the substrate. The reaction was left to mix under argon for 14h, during which time, a precipitate would form. The solvent was removed under vacuum and the crude was purified via silica gel flash chromatography using 95:4:1 DCM:MeOH:NH₄OH, followed

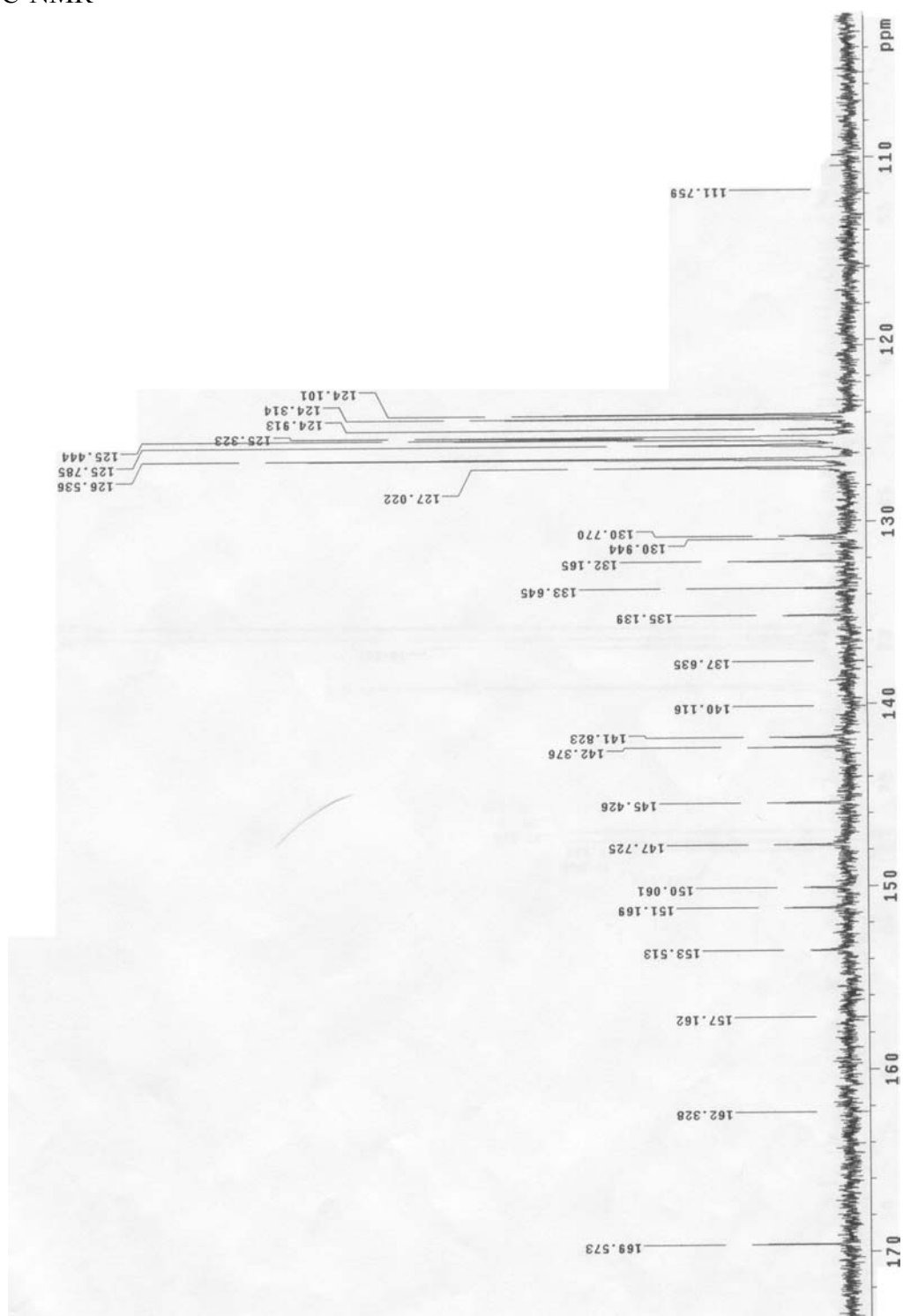
by recrystallization from DCM to recover 370 mg of 1,4-di-[(+)-(2-methyl)-butylamide]-2,5-triethyleneoxy-t-bu-calix[6]arene as a white crystalline solid (yield 25%). ^{13}C -NMR (CDCl_3) δ 11.95 (CH_2CH_3), 17.45 (CH_2CH_3), 27.31 (CHCH_3), 27.33 (CHCH_3), 30.52 ($\text{HOArCH}_2\text{ArOX}$), 31.09 ($\text{C}(\text{CH}_3)_3$), 31.50 ($\text{C}(\text{CH}_3)_3$), 31.83 ($\text{C}(\text{CH}_3)_3$), 33.93 ($\text{C}(\text{CH}_3)_3$), 34.19 ($\text{C}(\text{CH}_3)_3$), 38.88 ($\text{ROArCH}_2\text{ArOX}$), 43.18 ($\text{ArCH}_2\text{NHCOOR}$), 43.37 (CHCH_3), 69.69 ($\text{ArOCH}_2\text{CH}_2\text{OCH}_2$), 69.91 ($\text{ArOCH}_2\text{CH}_2\text{OCH}_2$), 71.70 ($\text{ArOCH}_2\text{CH}_2\text{OCH}_2$), 124.07, 124.30, 125.08, 125.40, 126.50, 127.28, 131.80, 133.57, 135.52, 137.46, 141.53, 145.38, 147.29, 175.93 (RNHCOOR) ESI-MS m/z 1493.62 ($\text{M}+1$), 1515.83 ($\text{M}+\text{Na}$), 1594.57 ($\text{M}+\text{TEA}$) high-res MS 1493.9618 $\text{C}_{98}\text{H}_{128}\text{N}_2\text{O}_{10}$ H^+ , 1510.9908 $\text{C}_{98}\text{H}_{128}\text{N}_2\text{O}_{10}$ NH_4^+ , 1515.9442 $\text{C}_{98}\text{H}_{128}\text{N}_2\text{O}_{10}$ Na^+

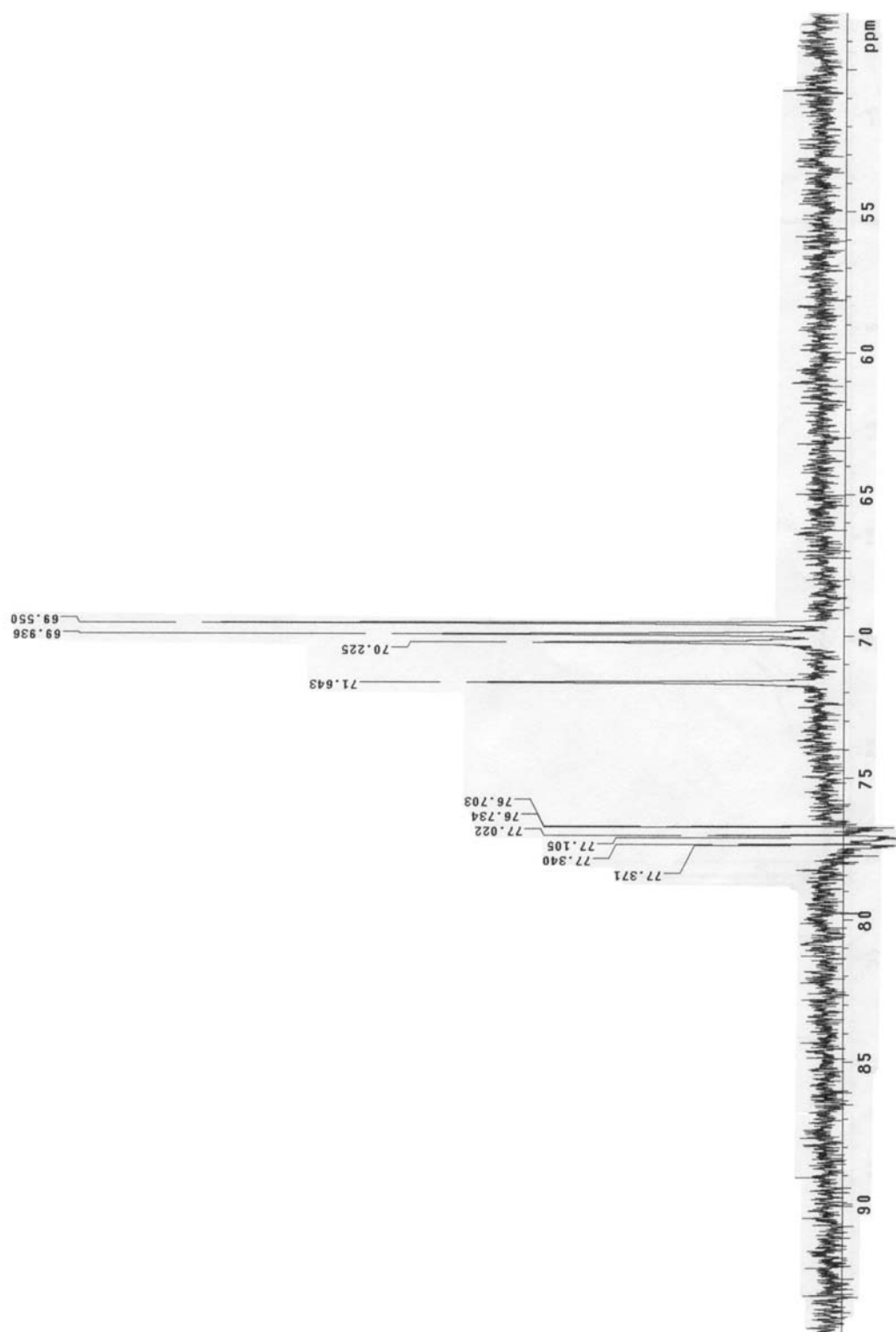
1,4-di-benzoic acid-2,5-triethyleneoxy-t-bu-calix[6]arene **19**

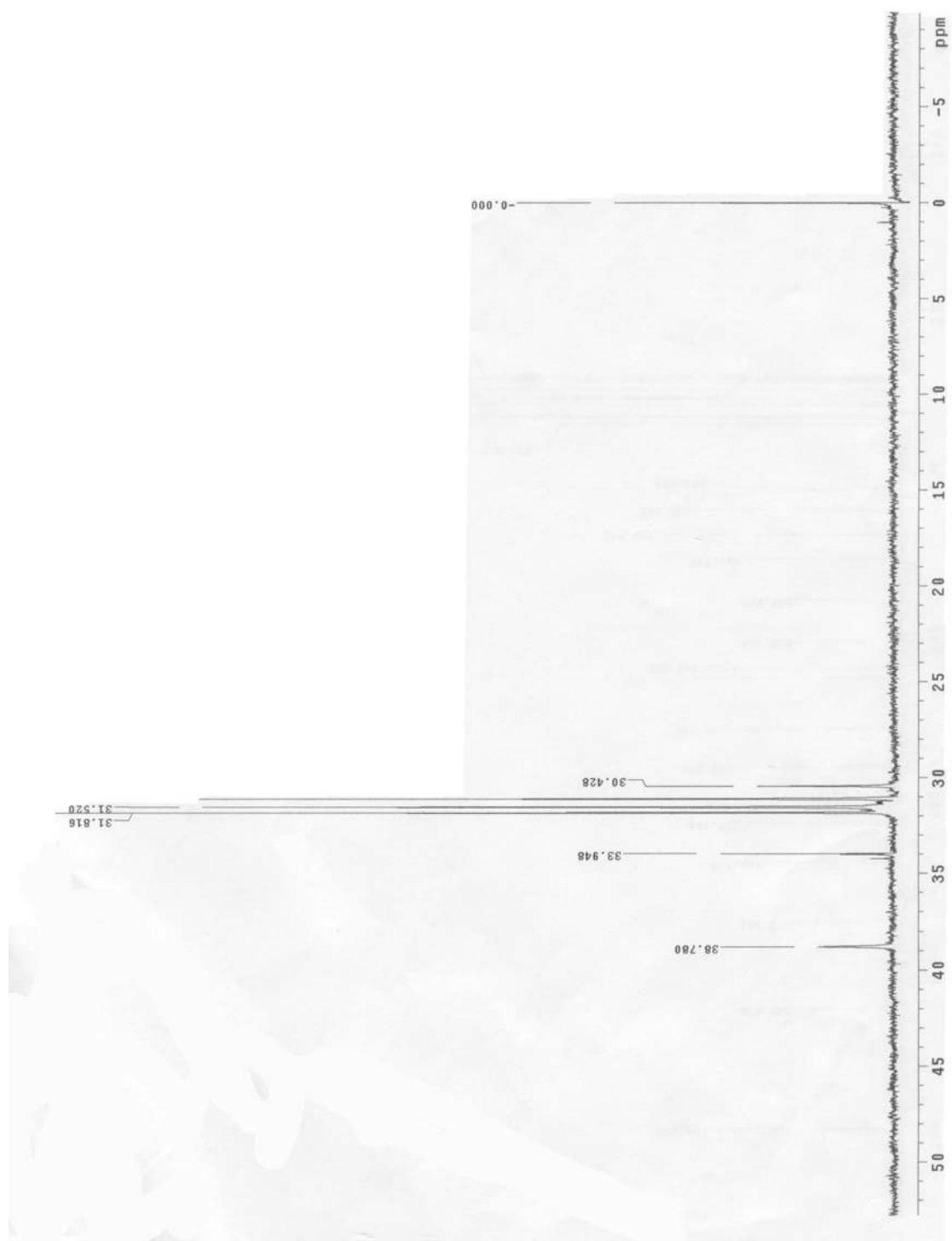
SYNTHESIS: To a dry 100 mL RB flask equipped with a stir bar was added 200 mg (0.157 mmol) of 1,4-di-methyl benzoate-t-bu-calix[6]arene. The flask was charged with argon and 10 mL freshly distilled THF and 1 mL dry DMF was added to form a solution. 60 mg NaH (60% mineral oil dispersion) was added to form a slurry. 100 mg (0.218 mmol) of triethylene glycol di-p-tosylate was dissolved in 2 mL THF and then added 91 μL TEA. The reagent solution was dripped into the reaction and left to mix under argon for 6h. The solvent was stripped under vacuum and the residue was reconstituted in

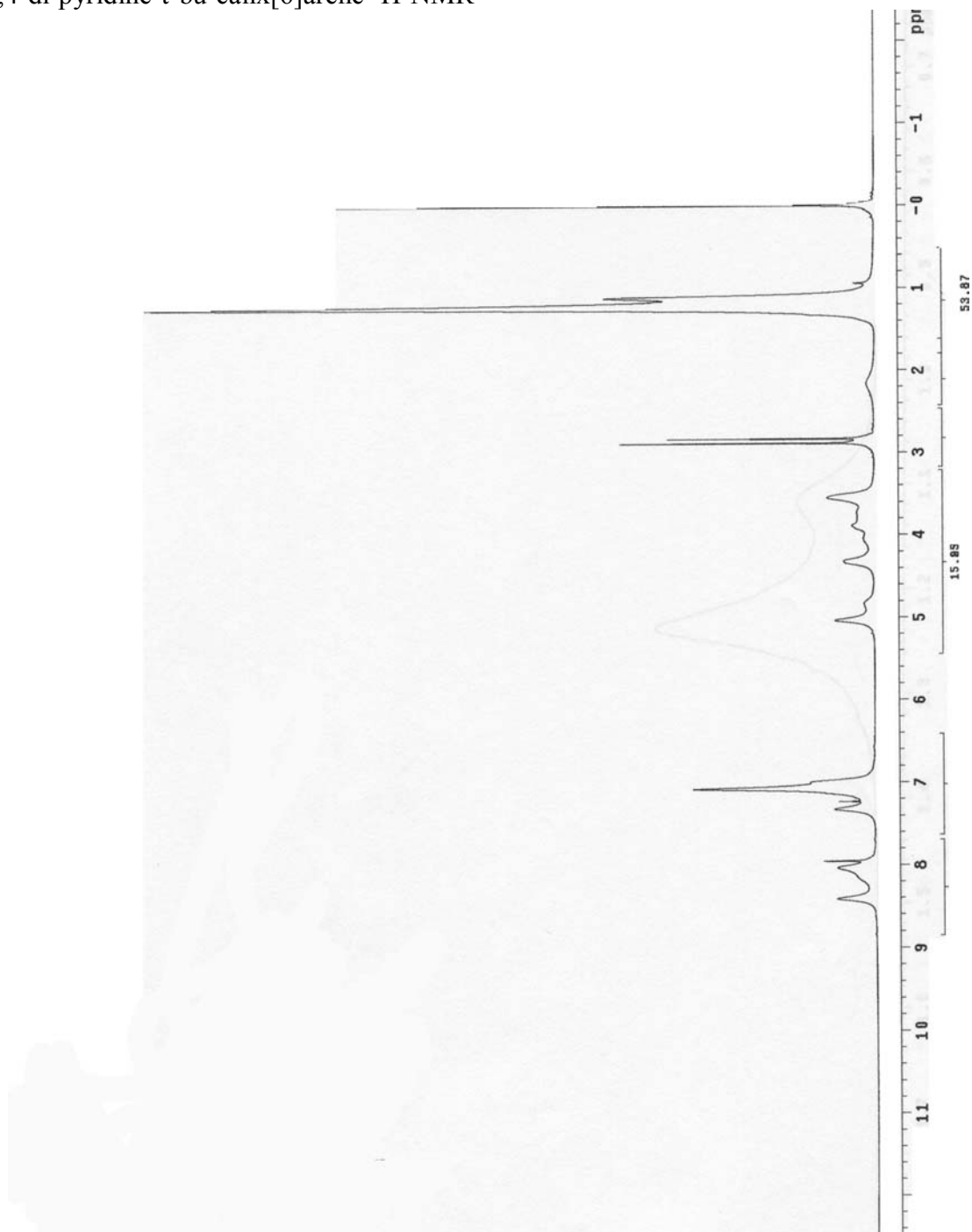
50/25 mL CHCl₃/2 N HCl. The organic was washed twice with 2 N HCl followed by a brine wash. The organic was dried over anhydrous MgSO₄, filtered, and rotavapped dryness to give a light orange crude solid. The crude solid was purified by silica gel flash chromatography using a 59:39:2 hexanes:EtOAc:AcOH solvent system. 270 mg of a desired product was isolated as a white solid (yield 62%). ¹H-NMR (THF-d₈) δ 7.59 (s, 2H, ArOH), 7.41 (s, 2H, HOArH), 7.22 (s, 2H, ROArH), 7.20 (d, 4H, OCH₂ArHHCOOH), 7.02 (s, 2H, XArH), 6.99 (s, 2H, HOArH), 6.86 (s, 2H, RArH), 6.48 (s, 2H, XArH), 6.30 (d, 4H, OCH₂ArHHCOOH, 6.8 Hz), 4.70 (d, 2H, ArOCH₂, 13.2 Hz), 4.69 (d, 2H, HOArCH₂ArOX, 16.8 Hz), 4.39 (d, 2H, ArOCH₂, 13.2 Hz), 4.19 (s, 2H, HOArCH₂ArOR), 4.19 (d, 2H, XOArCH₂ArOR, 18.2 Hz), 4.04 (d, 2H, ROArCH₂ArOX, 18.2 Hz), 3.78 (t, 2H, ArOCH₂CH₂OCH₂), 3.57 (t, 2H, ArOCH₂CH₂OCH₂), 3.57 (s, 2H, HOArCH₂ArOR), 3.38 (bs, 2H, ArOCH₂CH₂OCH₂), 3.30 (d, 2H, HOArCH₂ArOX, 16.8 Hz), 3.27 (d, 2H, ArOCH₂CH₂OCH₂, 10 Hz), 3.19 (bs, 2H, ArOCH₂CH₂OCH₂), 2.20 (t, 2H, ArOCH₂CH₂OCH₂), 1.41 (s, 18H, HOArC(CH₃)₃), 1.16 (s, 18H, XOArC(CH₃)₃), 0.89 (s, 18H, ROArC(CH₃)₃) ¹³C-NMR (THF-d₈) δ 29.85 (HOArCH₂ArOX), 30.41 (C(CH₃)₃), 30.93 (C(CH₃)₃), 31.15 (C(CH₃)₃), 33.48 (C(CH₃)₃), 33.62 (C(CH₃)₃), 33.79 (C(CH₃)₃), 38.14 (ROArCH₂ArOX), 69.49 (ArOCH₂CH₂OCH₂), 69.83 (ArOCH₂CH₂OCH₂), 71.47 (ArOCH₂CH₂OCH₂), 123.76, 124.01, 124.44, 125.02, 125.33, 126.59, 127.04, 128.32, 128.79, 130.25, 131.62, 133.39, 135.36, 141.24, 142.93, 144.67, 146.86, 150.26, 151.45, 153.70, 166.55 (COOH)

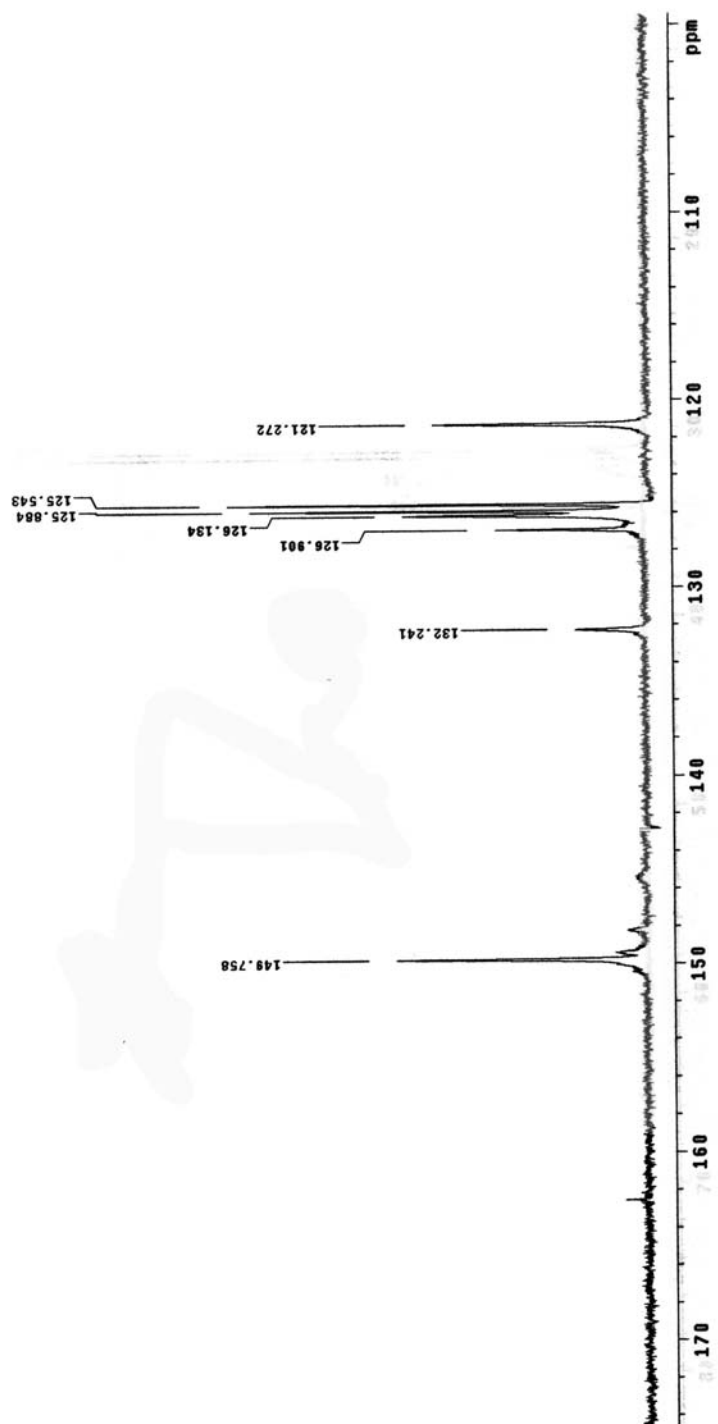
SUPPLEMENTAL MATERIAL

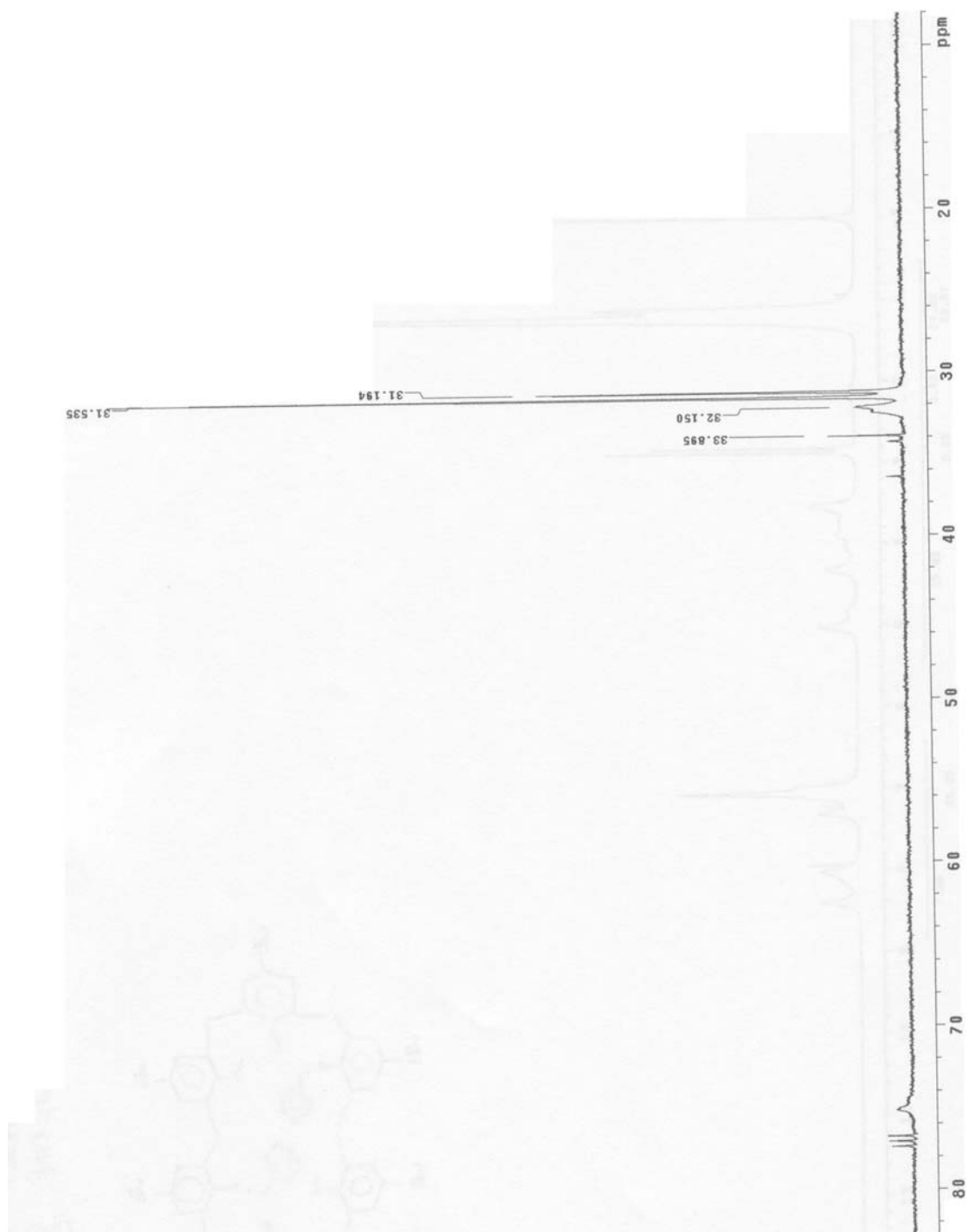
 $^{10} \text{ }^{13}\text{C-NMR}$ 

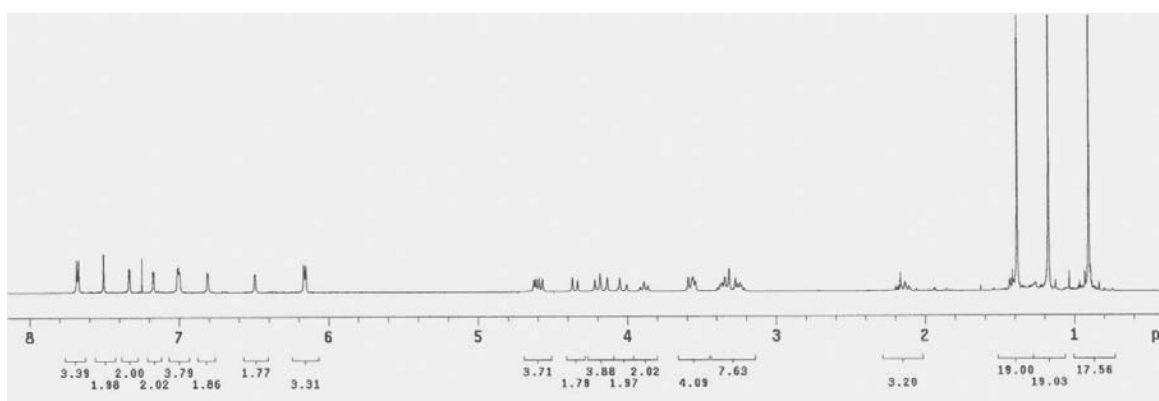
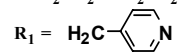
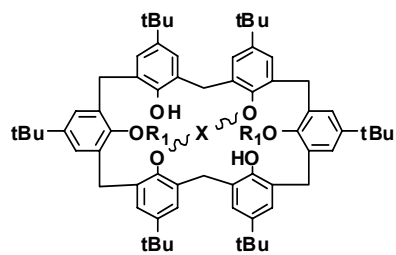
^{13}C -NMR

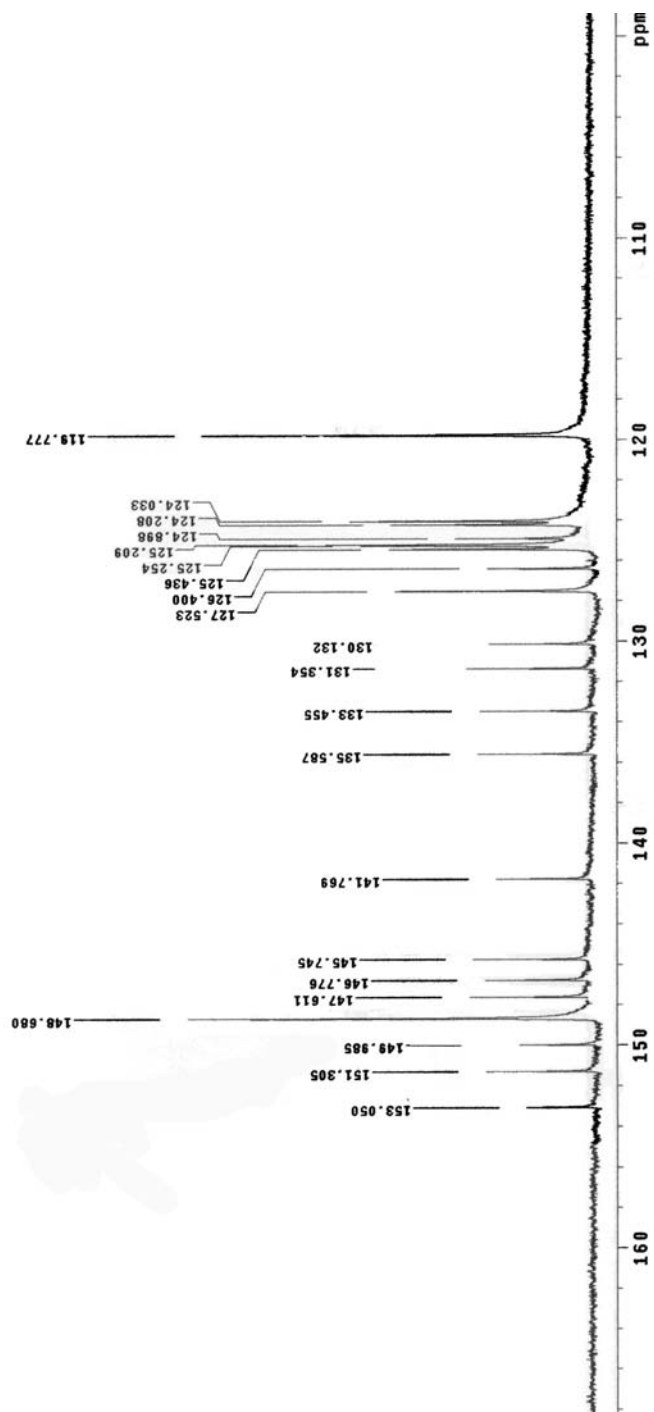
^{13}C -NMR

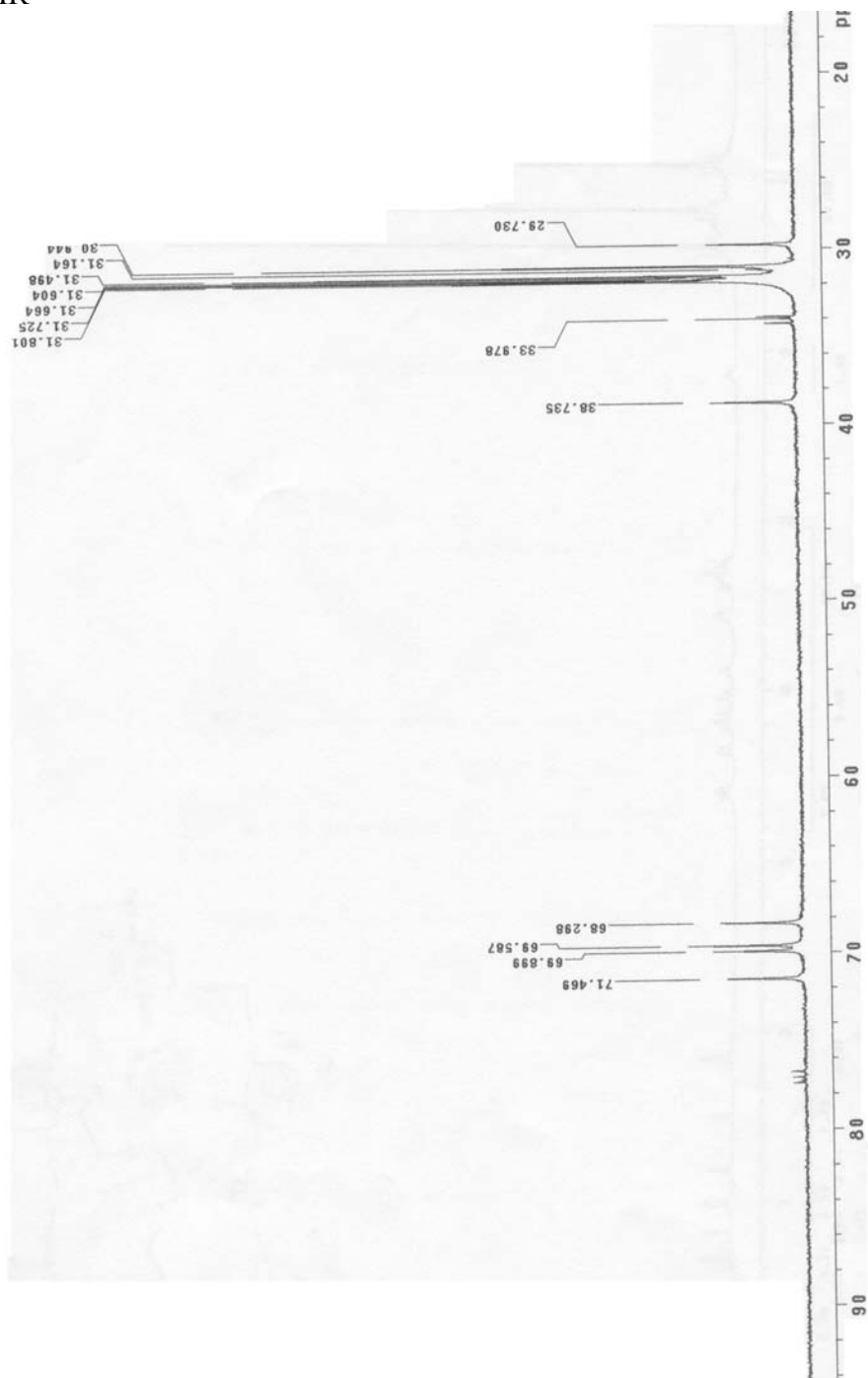
1,4-di-pyridine-t-bu-calix[6]arene $^1\text{H-NMR}$ 

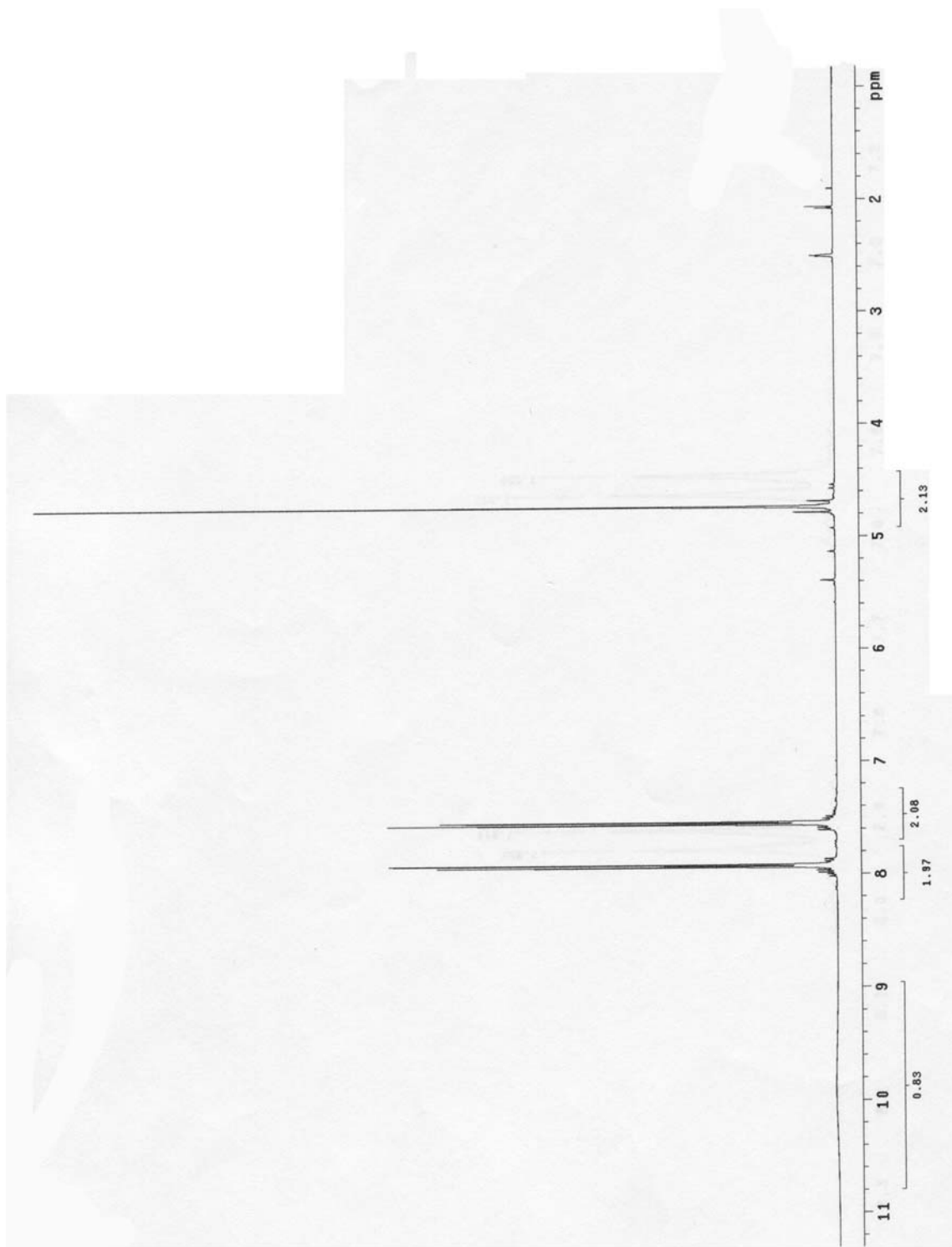
1,4-di-pyridine-t-bu-calix[6]arene ^{13}C -NMR

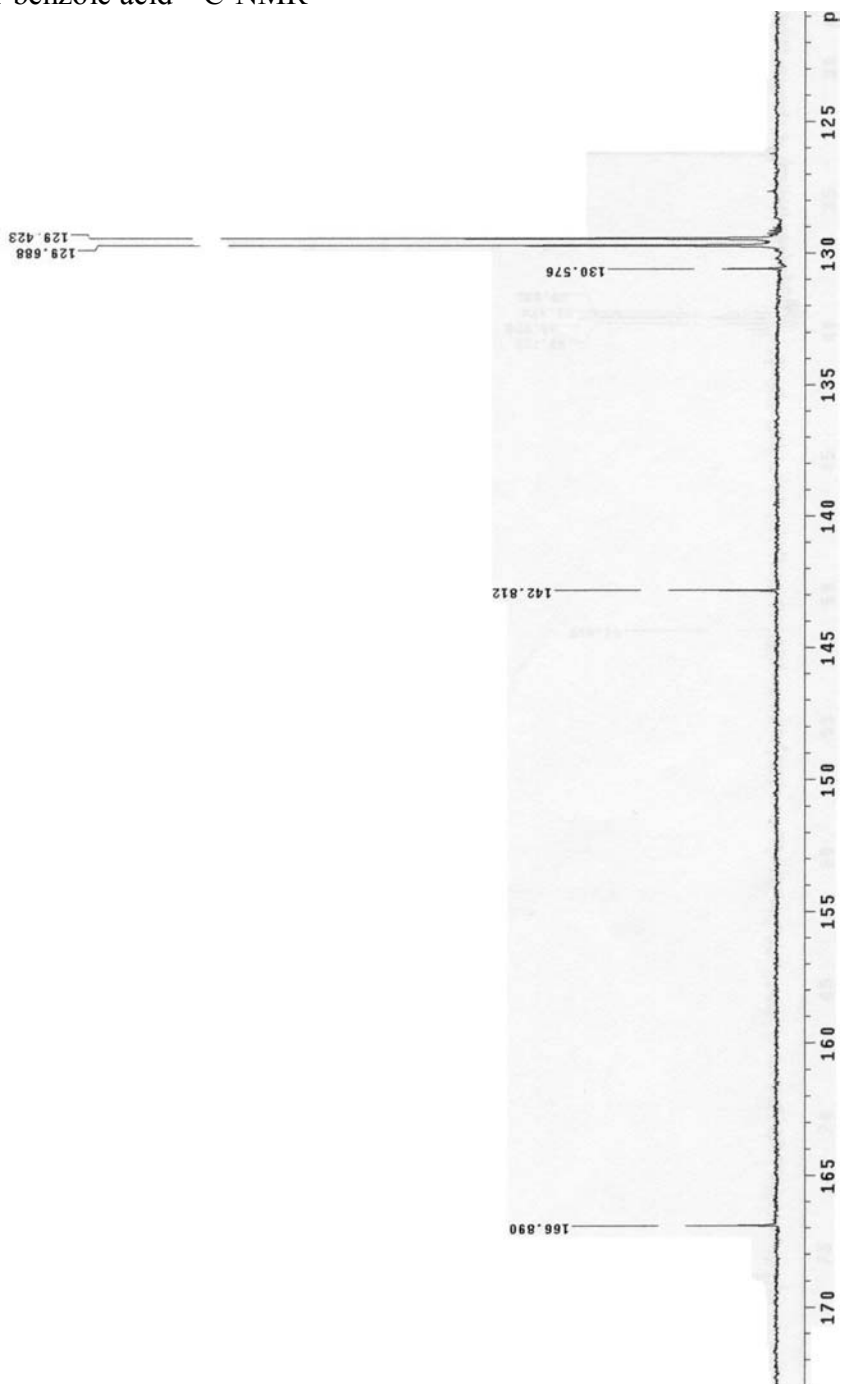
1,4-di-pyridine-t-bu-calix[6]arene ^{13}C -NMR

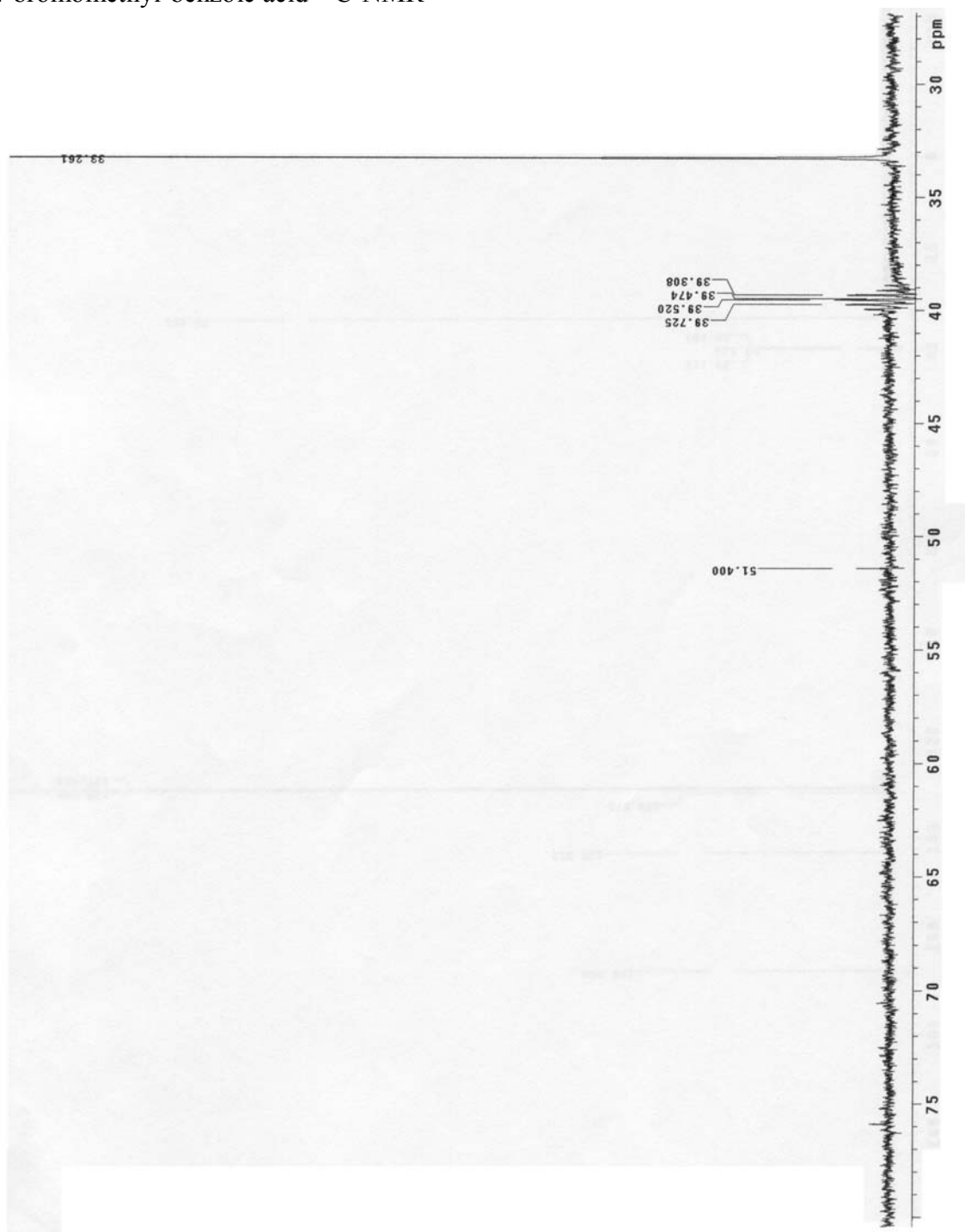
11 $^1\text{H-NMR}$ 

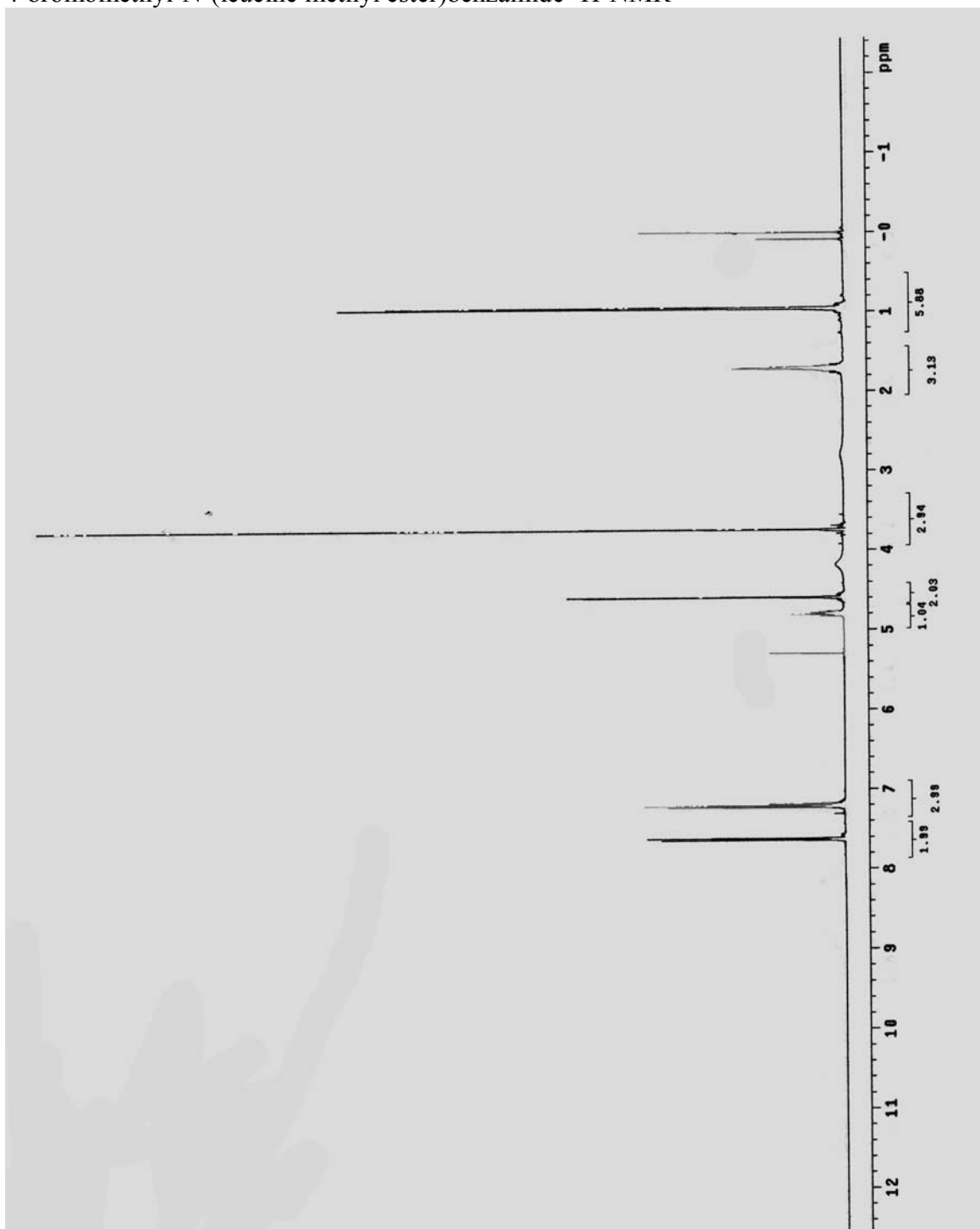
11 ^{13}C -NMR

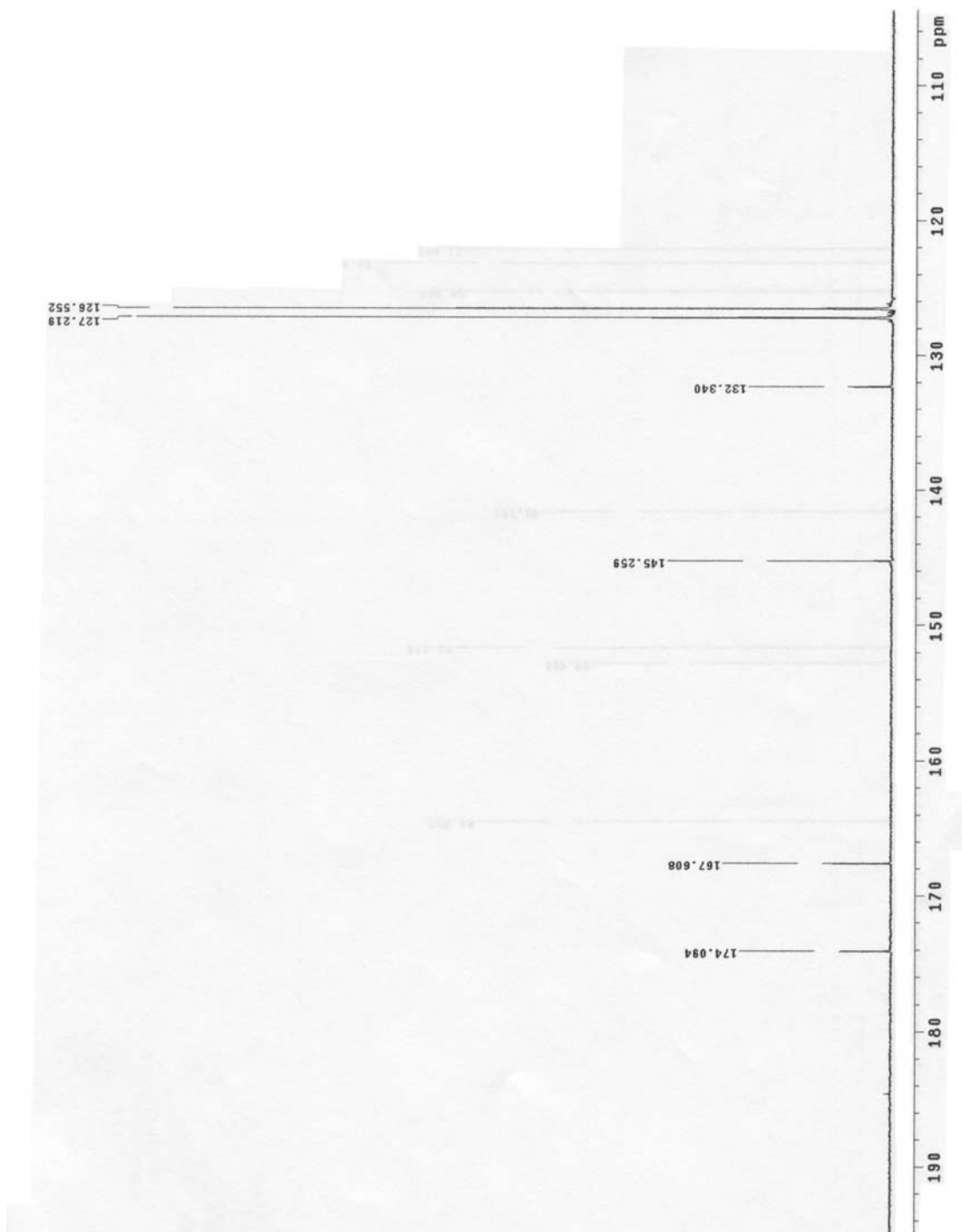
11 ^{13}C -NMR

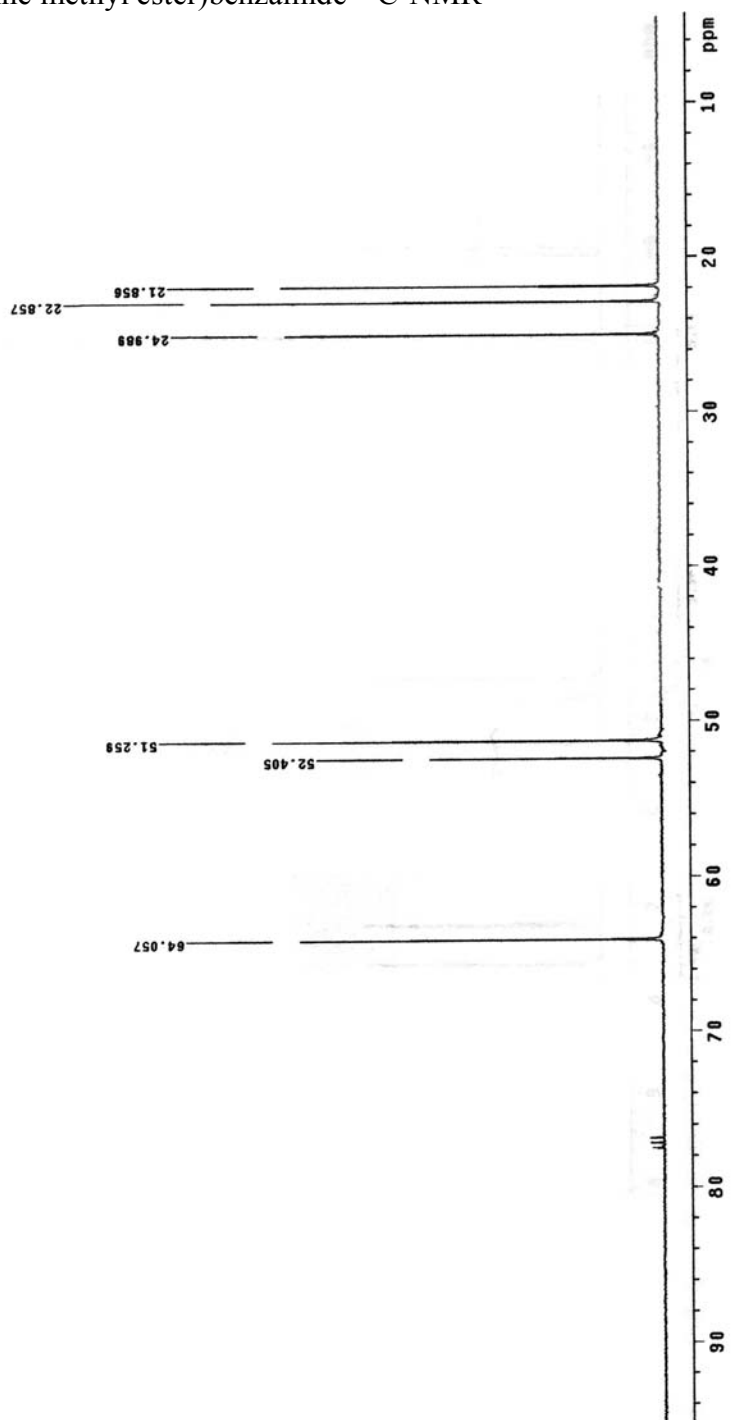
4-bromomethyl-benzoic acid $^1\text{H-NMR}$ 

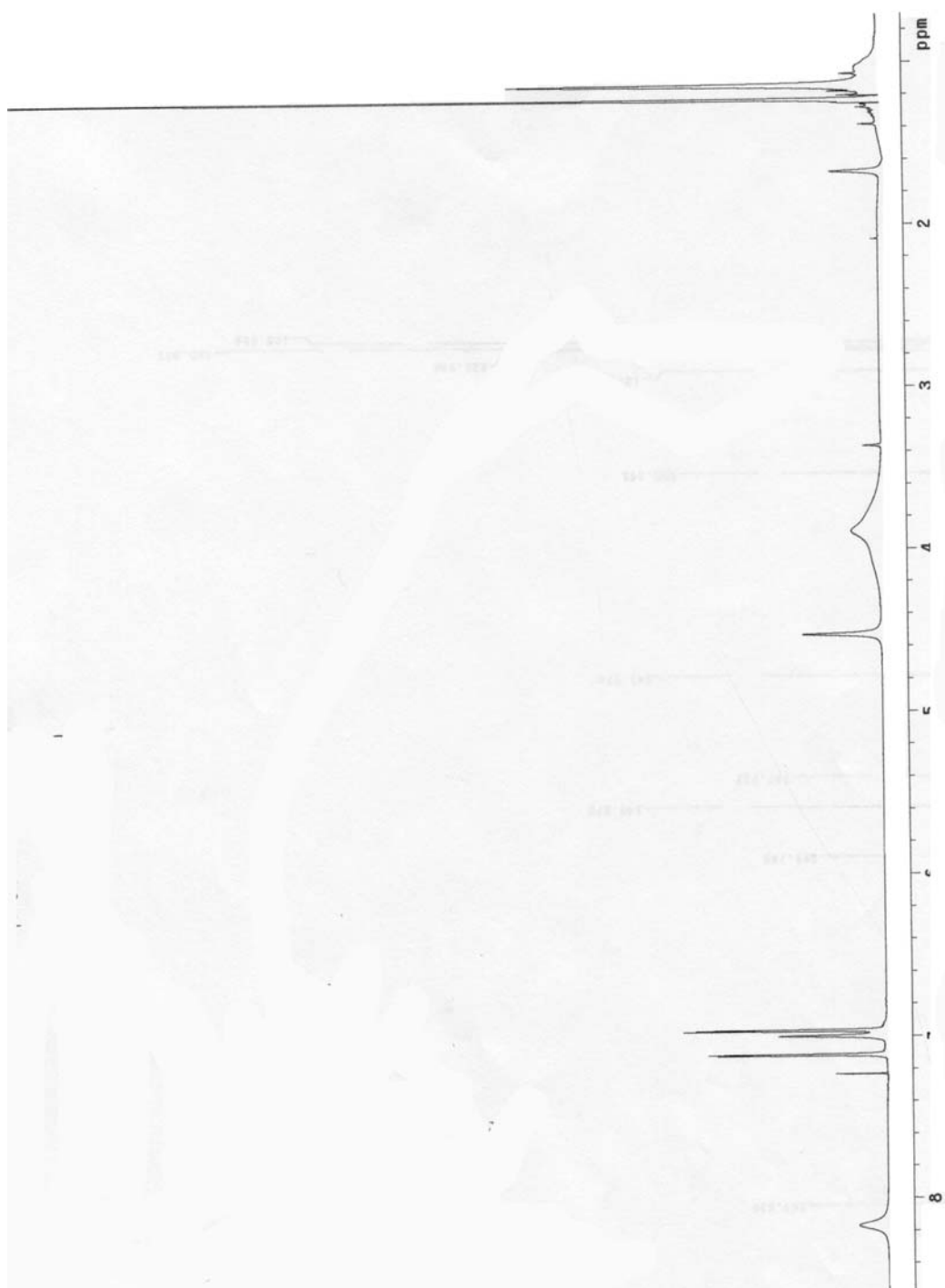
4-bromomethyl-benzoic acid ^{13}C -NMR

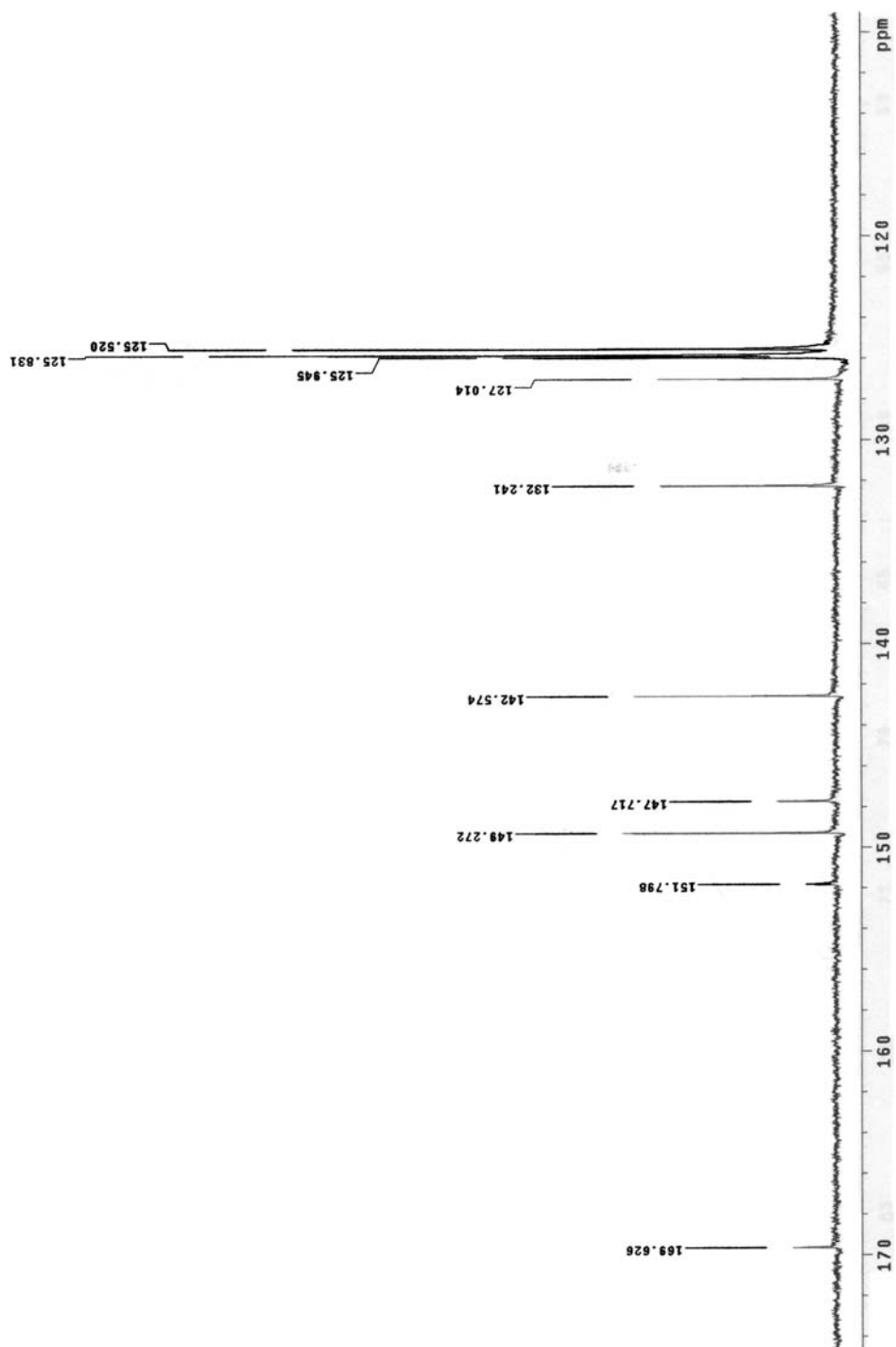
4-bromomethyl-benzoic acid ^{13}C -NMR

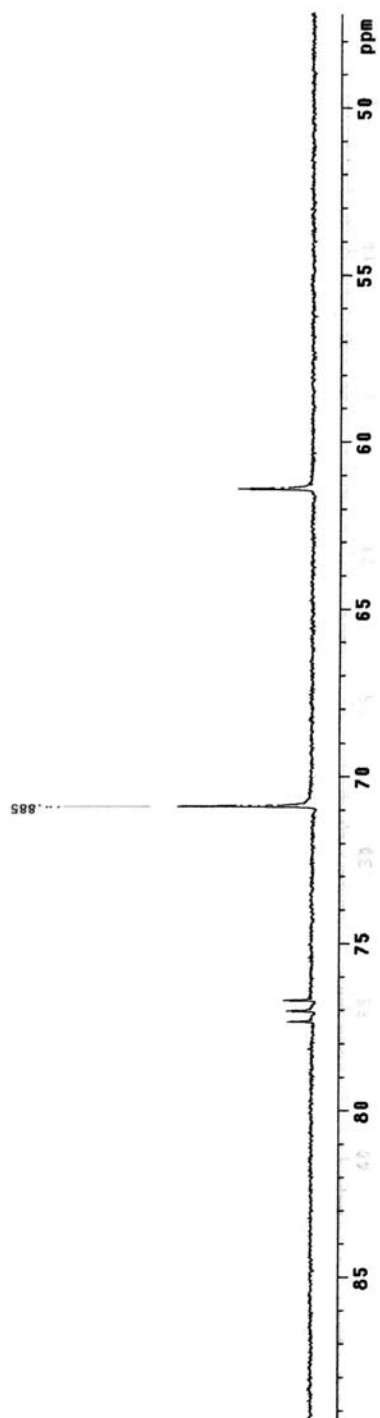
4-bromomethyl-N-(leucine methyl ester)benzamide $^1\text{H-NMR}$ 

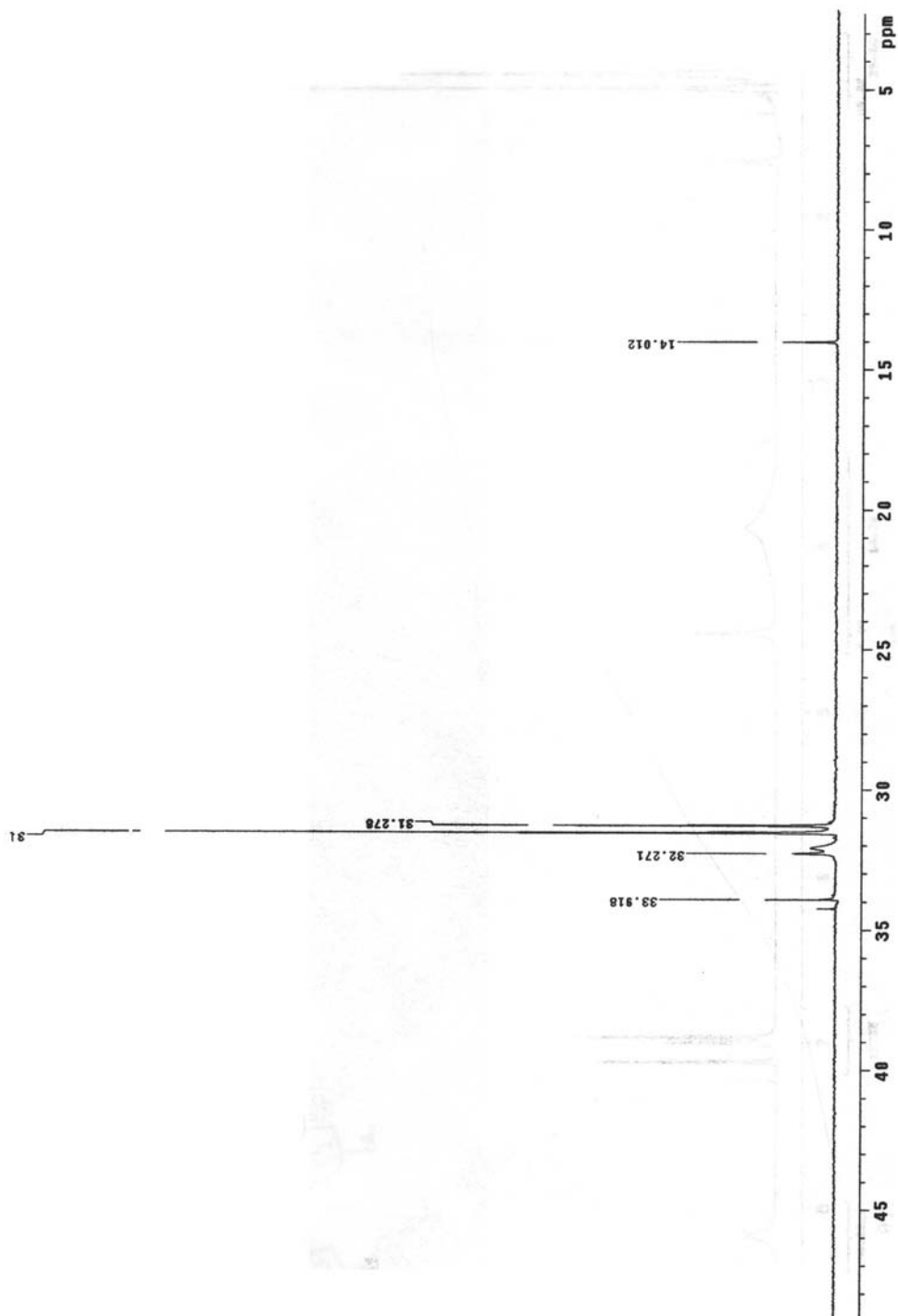
4-bromomethyl-N-(leucine methyl ester)benzamide ^{13}C -NMR

4-bromomethyl-N-(leucine methyl ester)benzamide ^{13}C -NMR

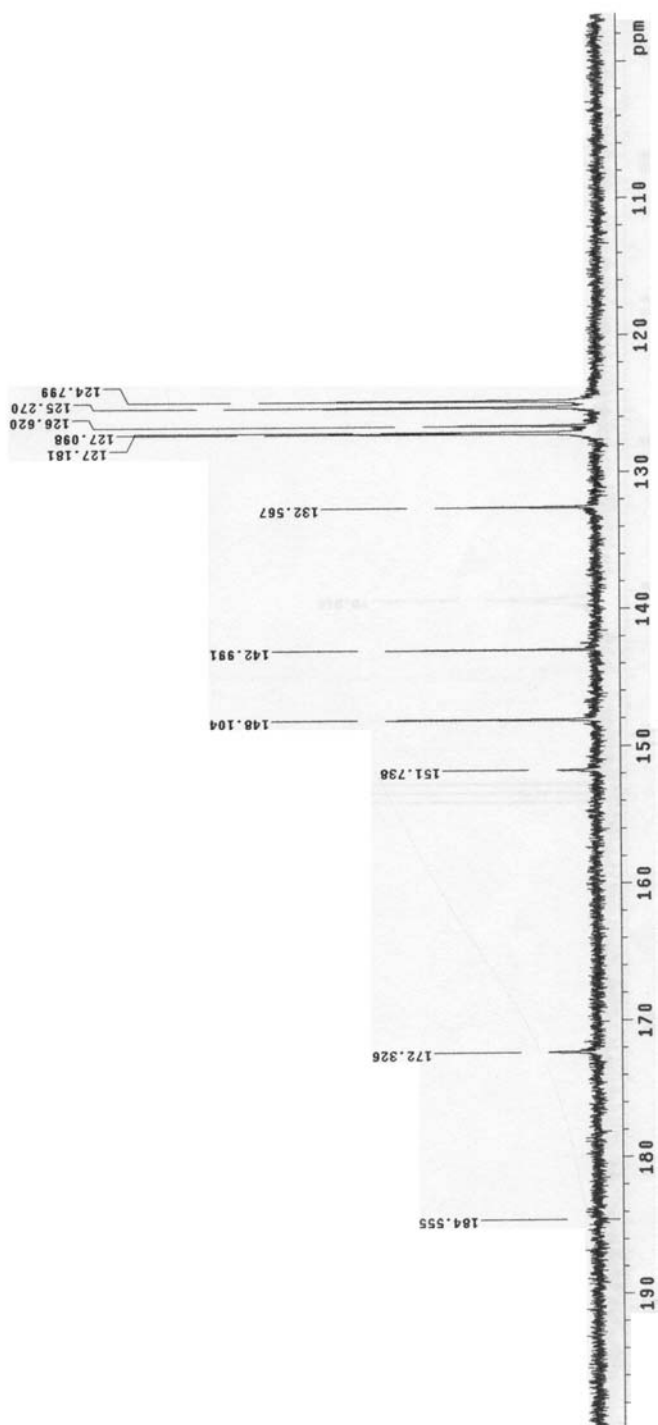
12 $^1\text{H-NMR}$ 

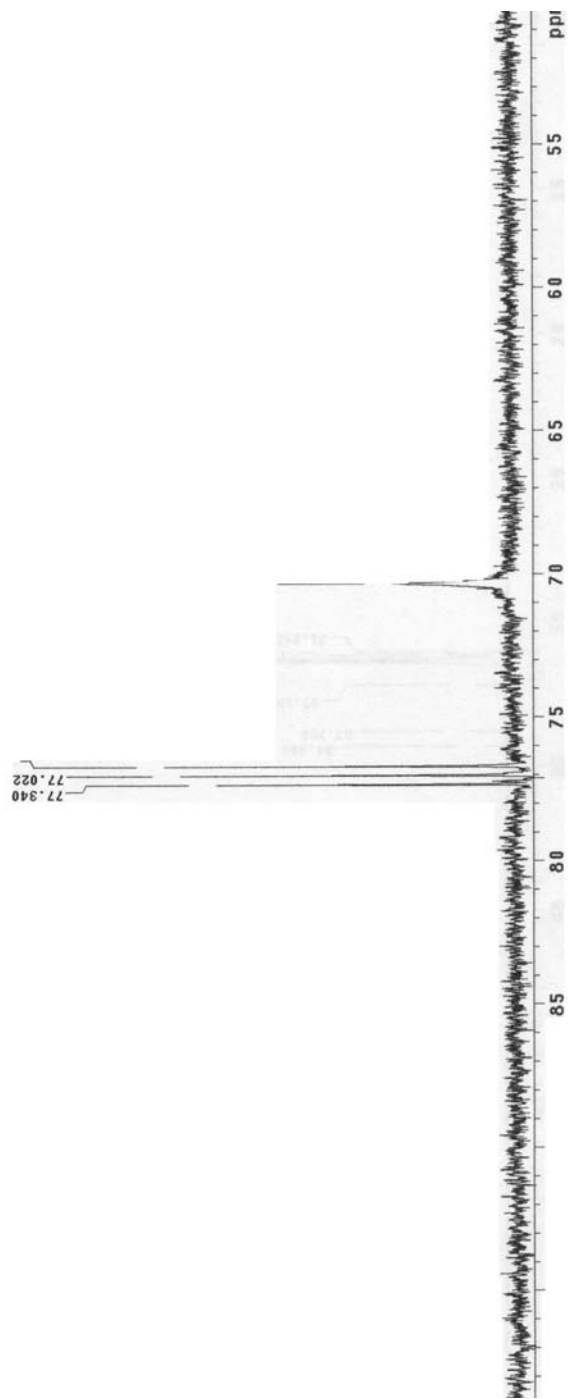
^{13}C -NMR

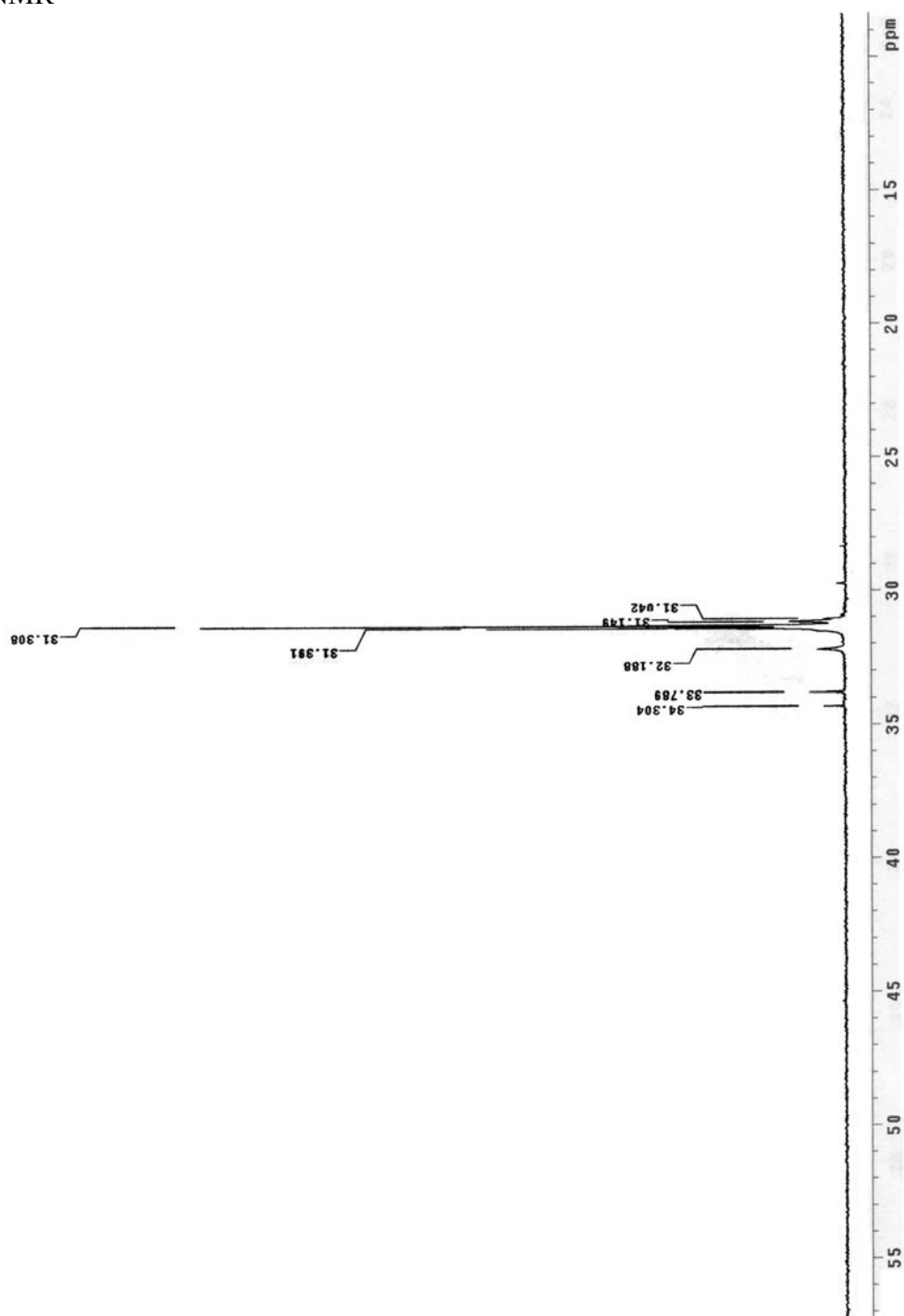
^{13}C -NMR

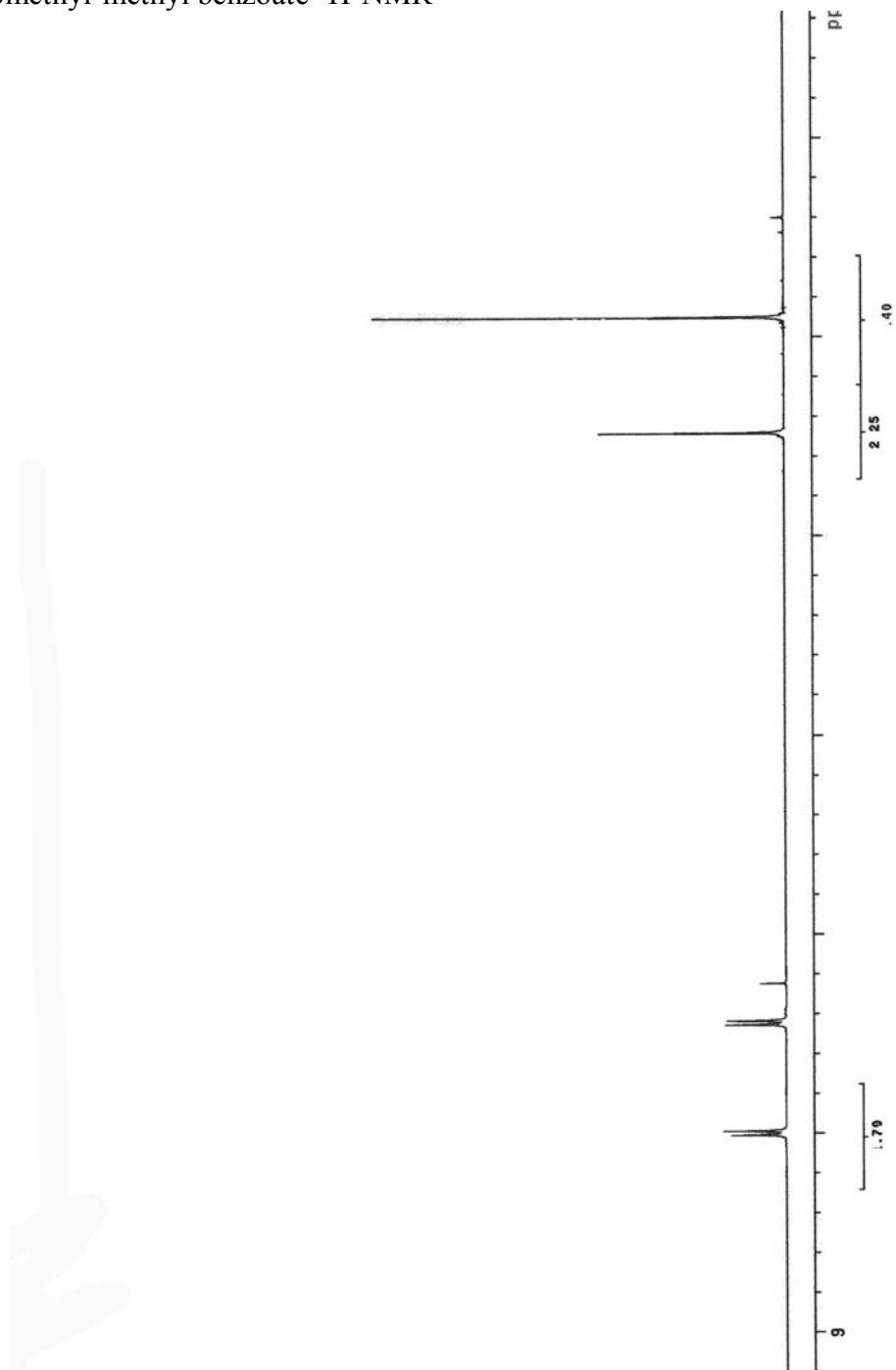
$^{13}\text{C-NMR}$ 

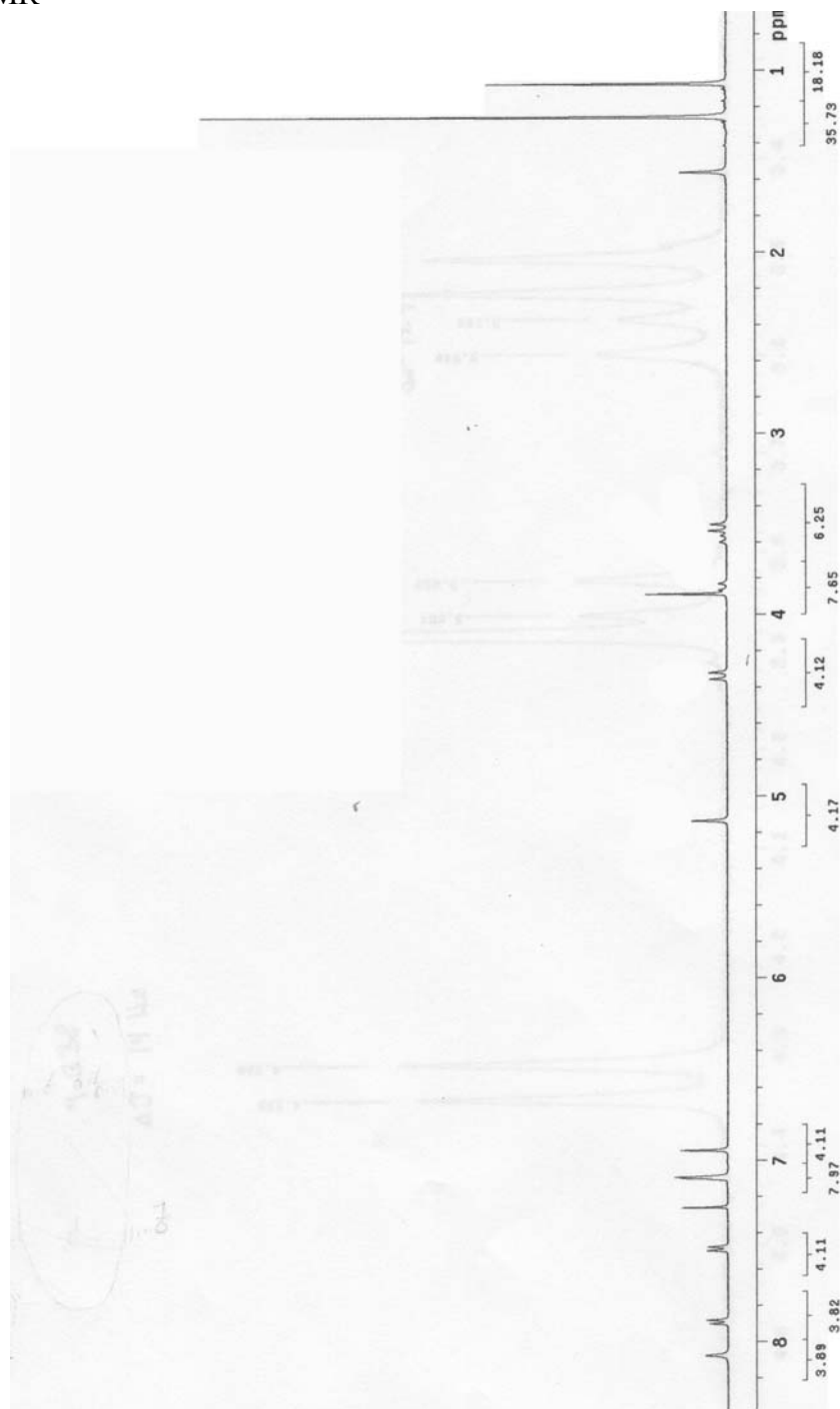
^{13}C -NMR

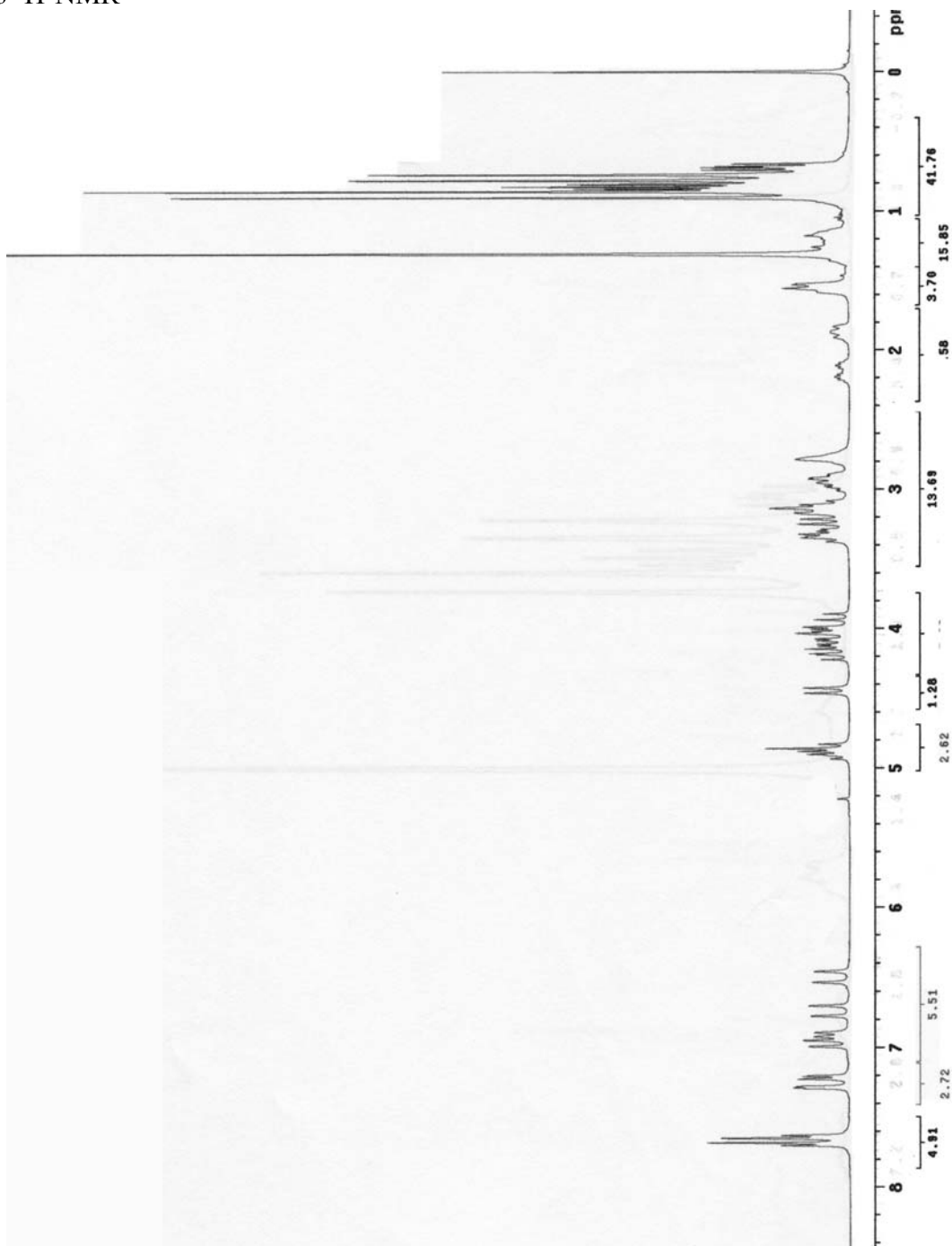
^{13}C -NMR

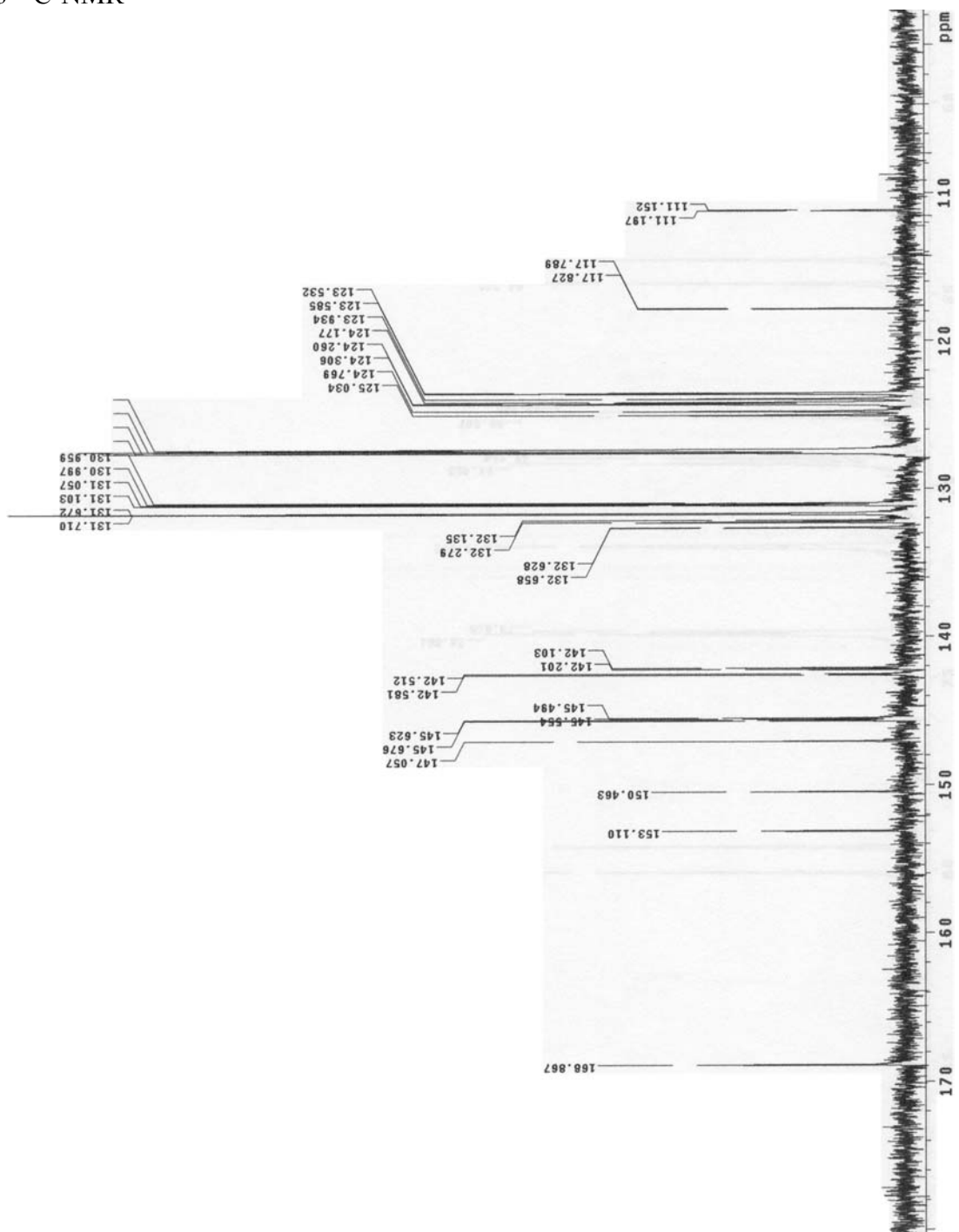
^{13}C -NMR

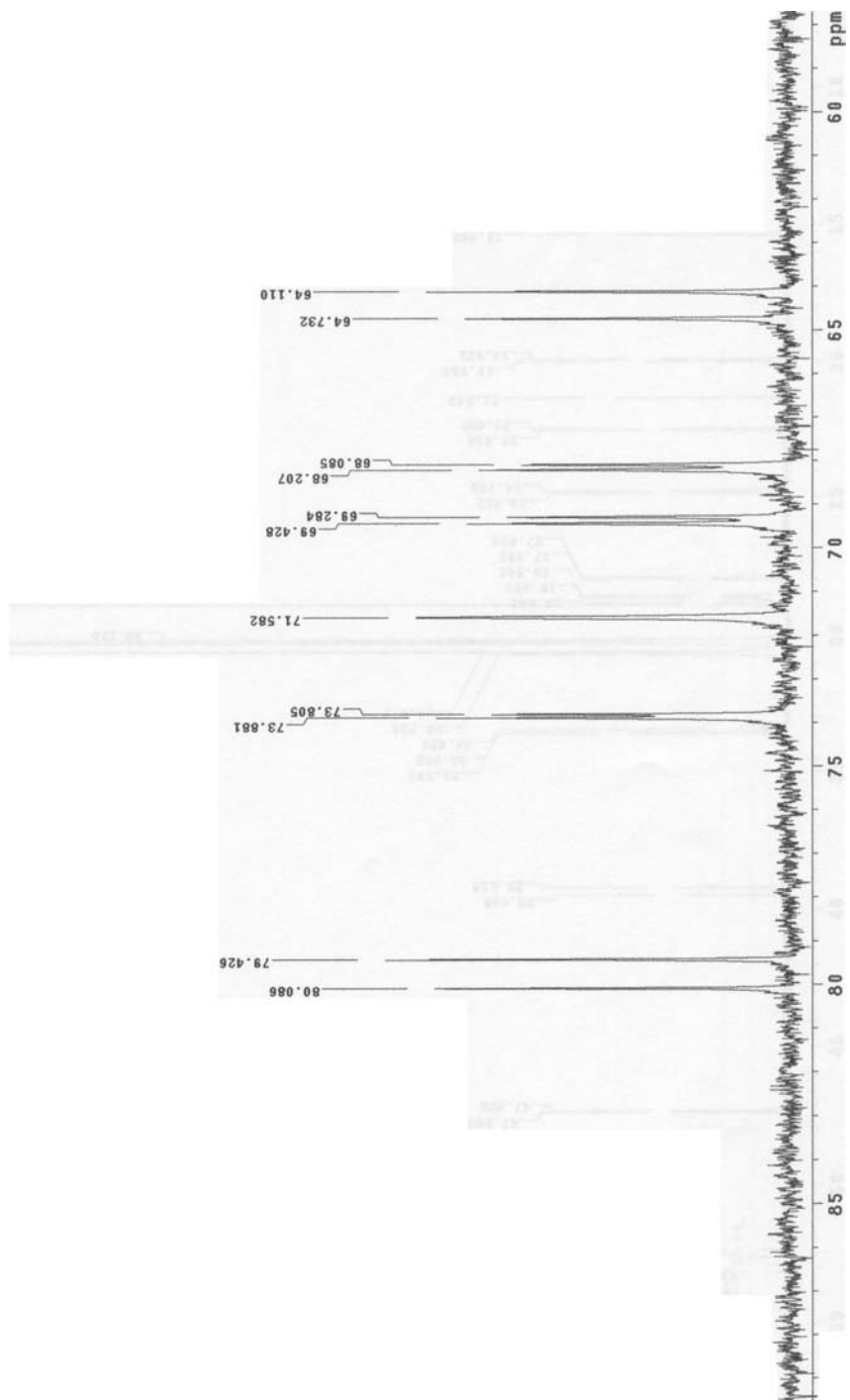
^{13}C -NMR

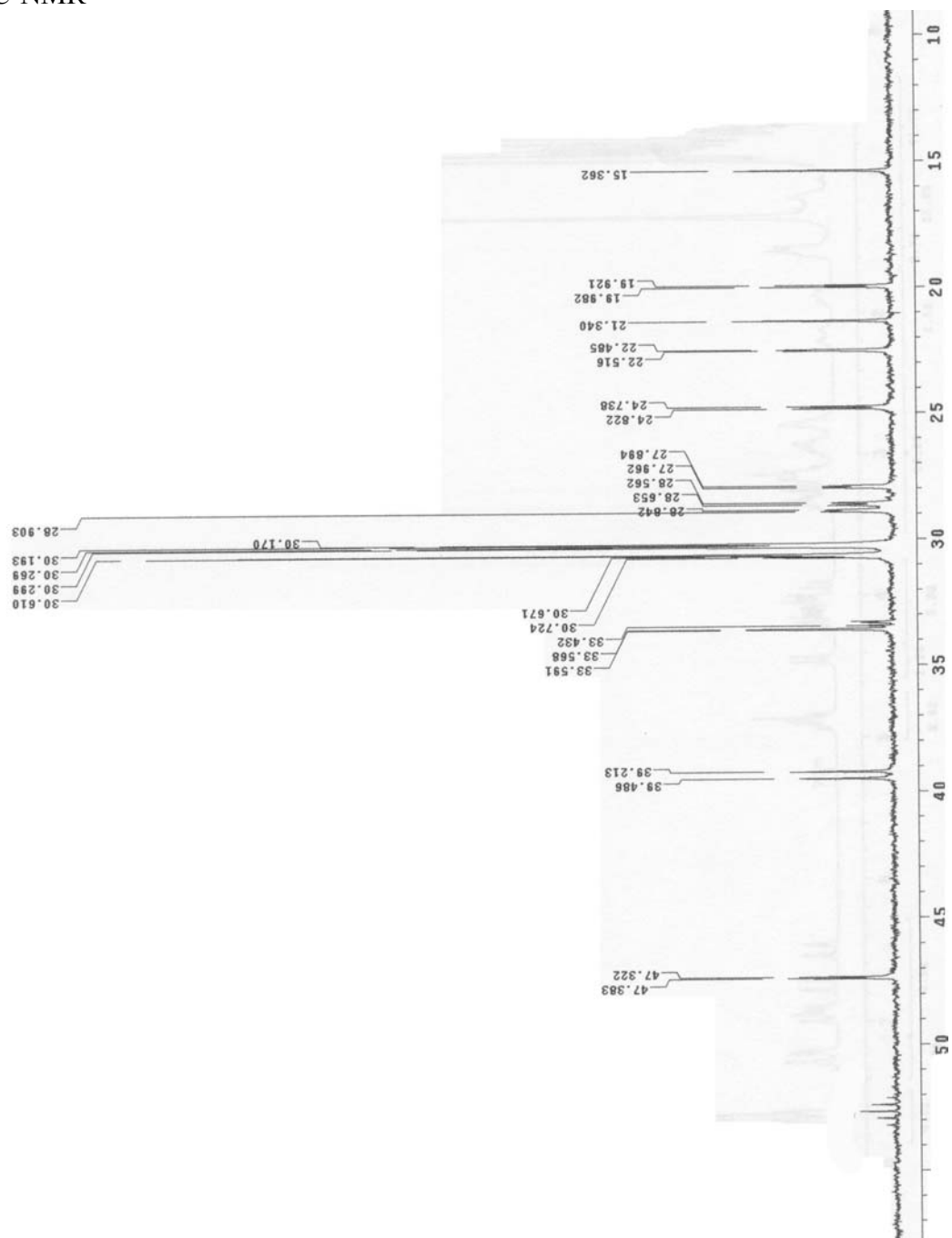
4-bromomethyl-methyl benzoate $^1\text{H-NMR}$ 

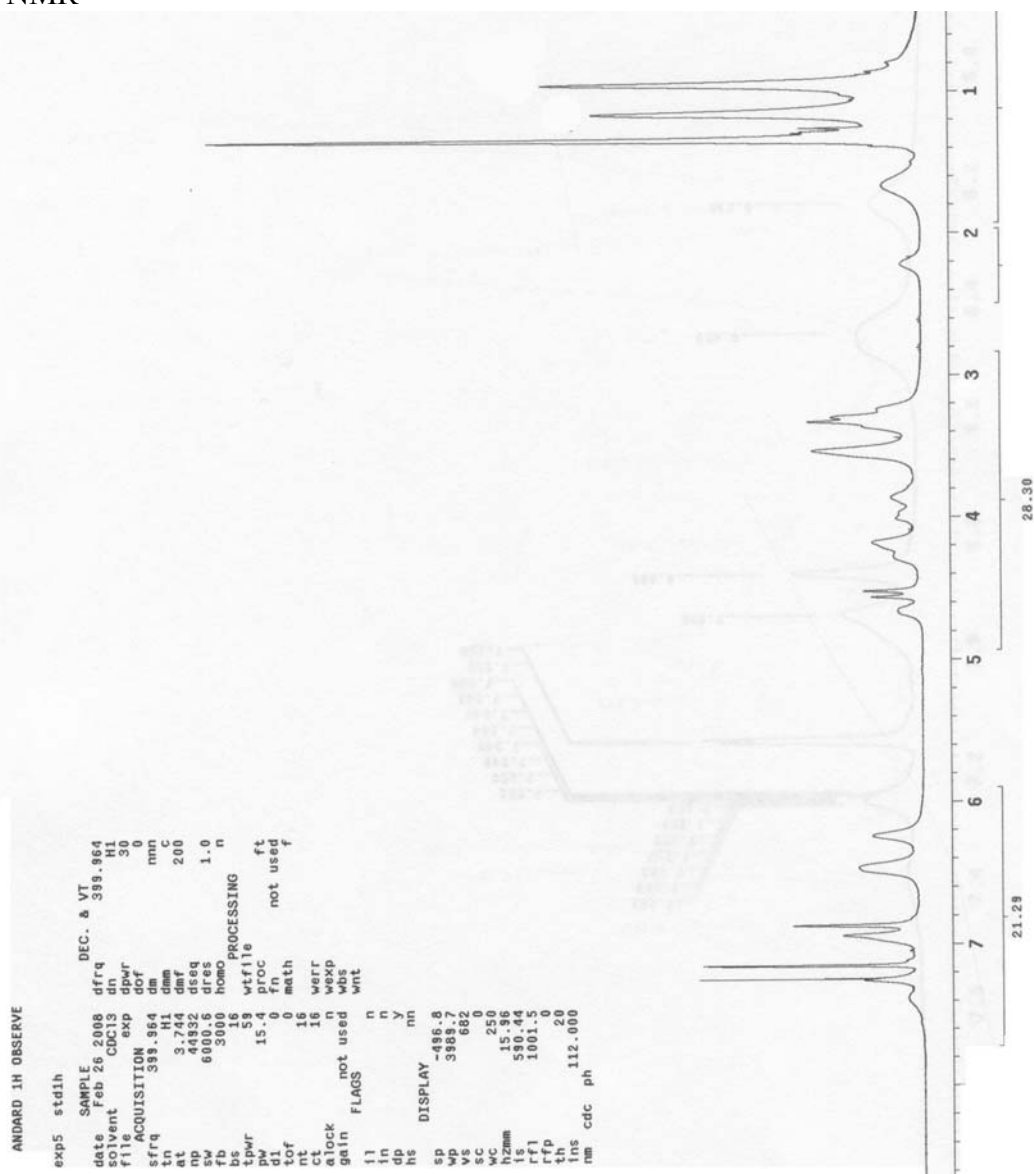
14 $^1\text{H-NMR}$ 

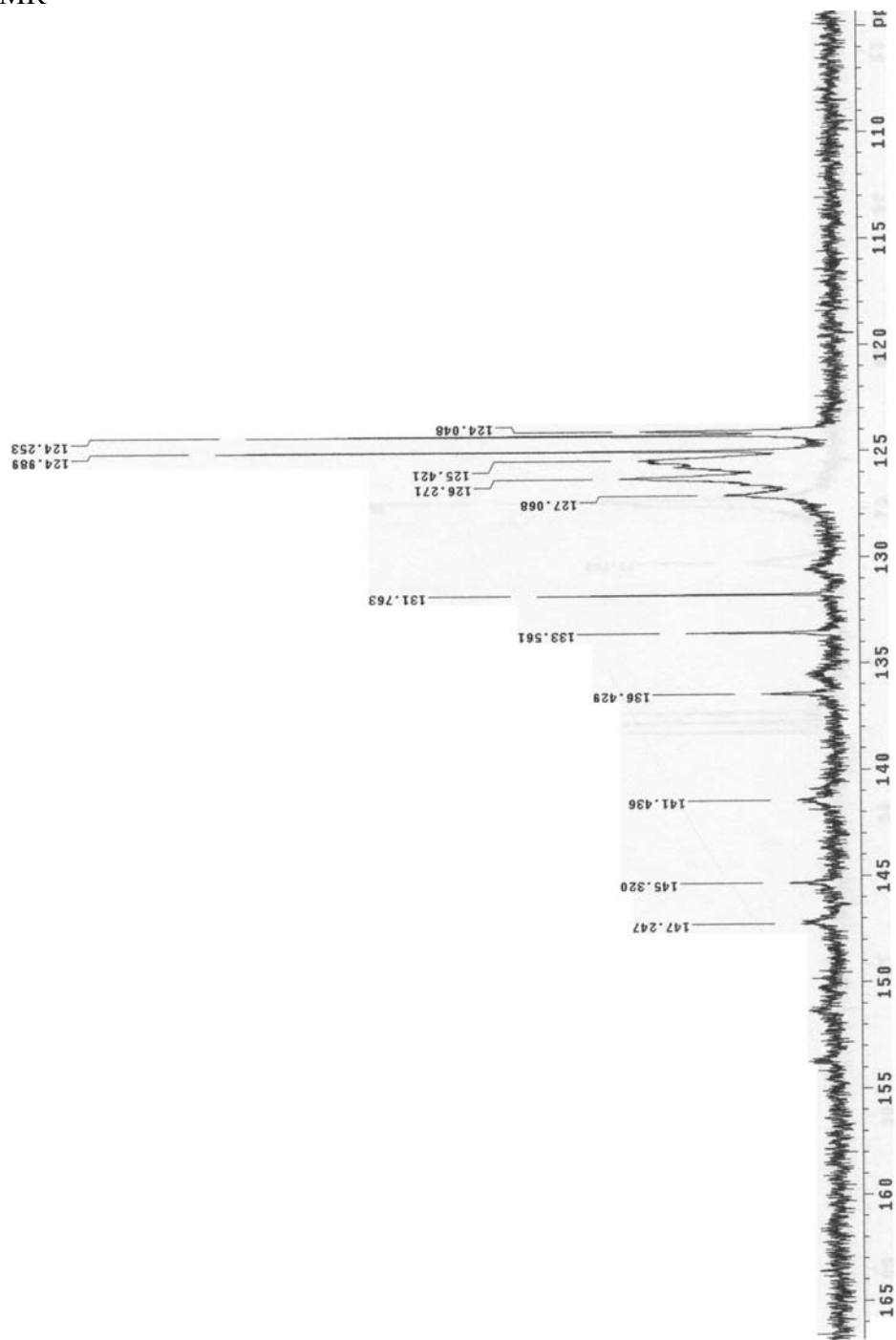
$^{15}\text{H-NMR}$ 

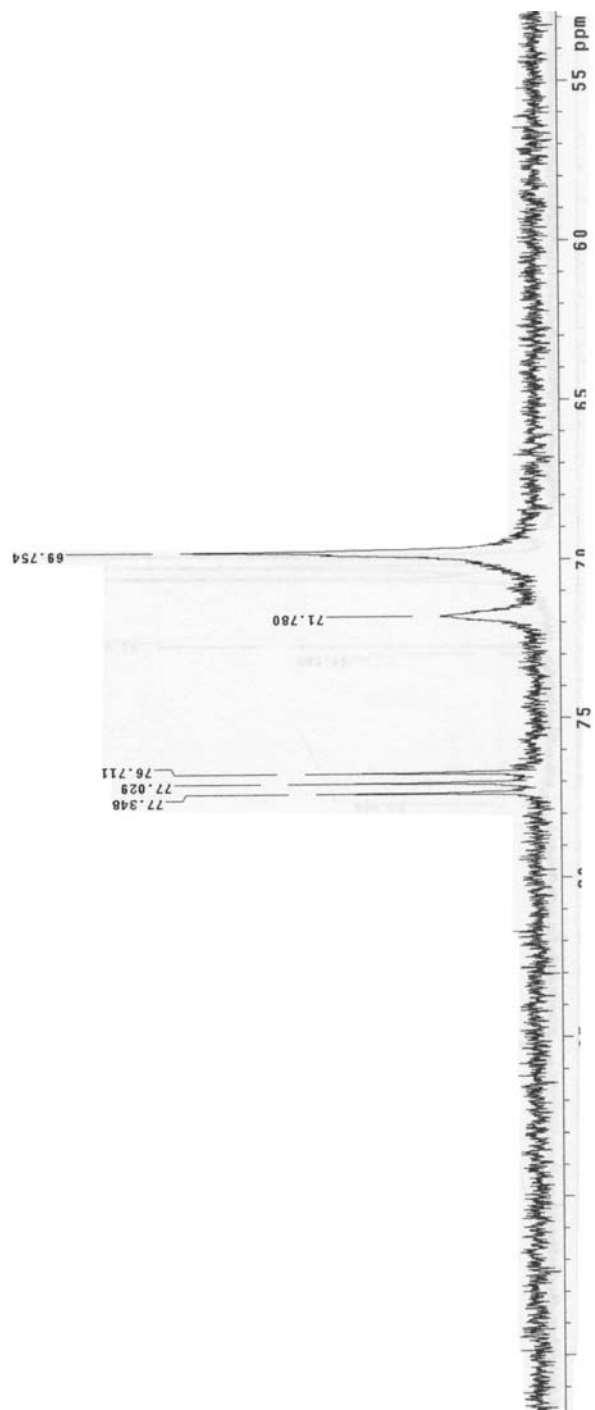
$^{15}\text{C-NMR}$ 

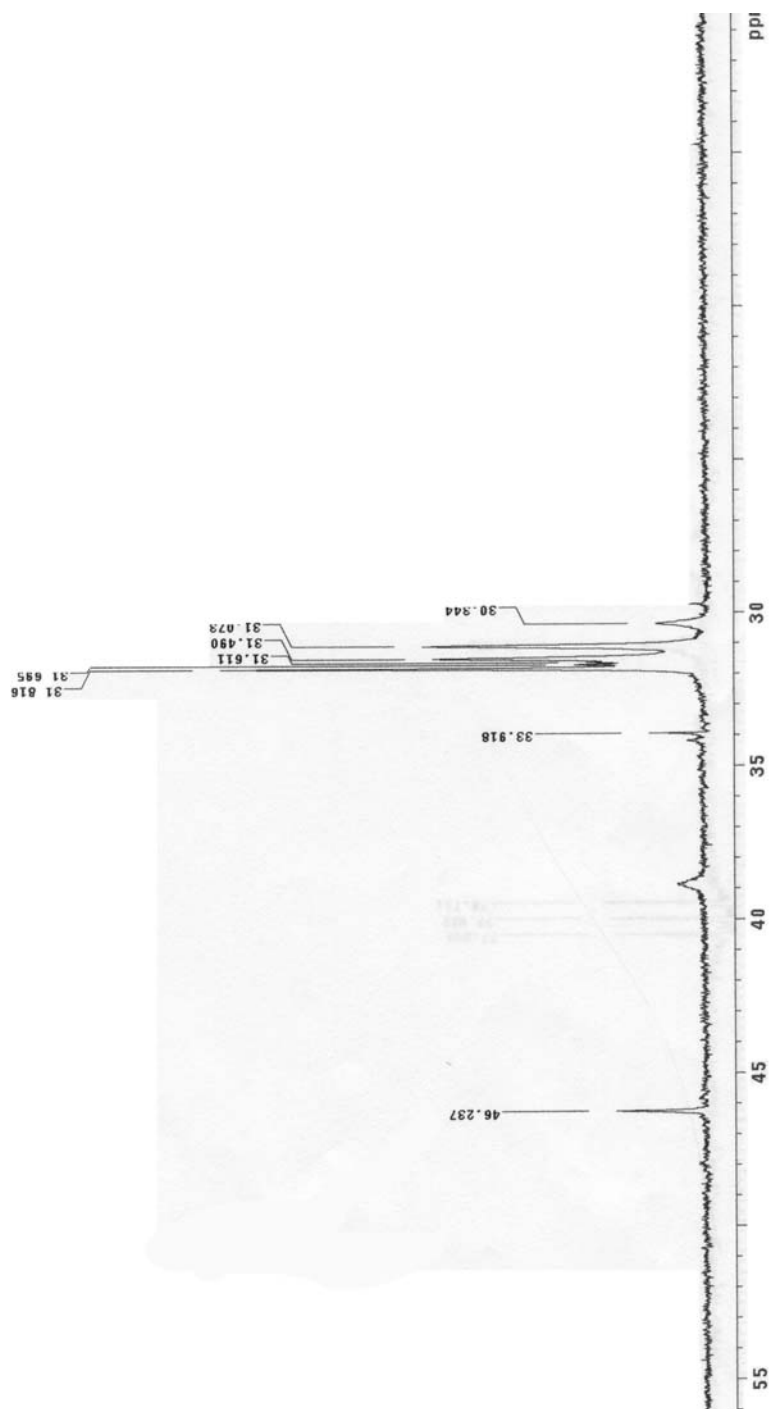
^{13}C -NMR

^{13}C -NMR

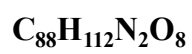
$^{16}\text{H-NMR}$ 

^{13}C -NMR

^{13}C -NMR

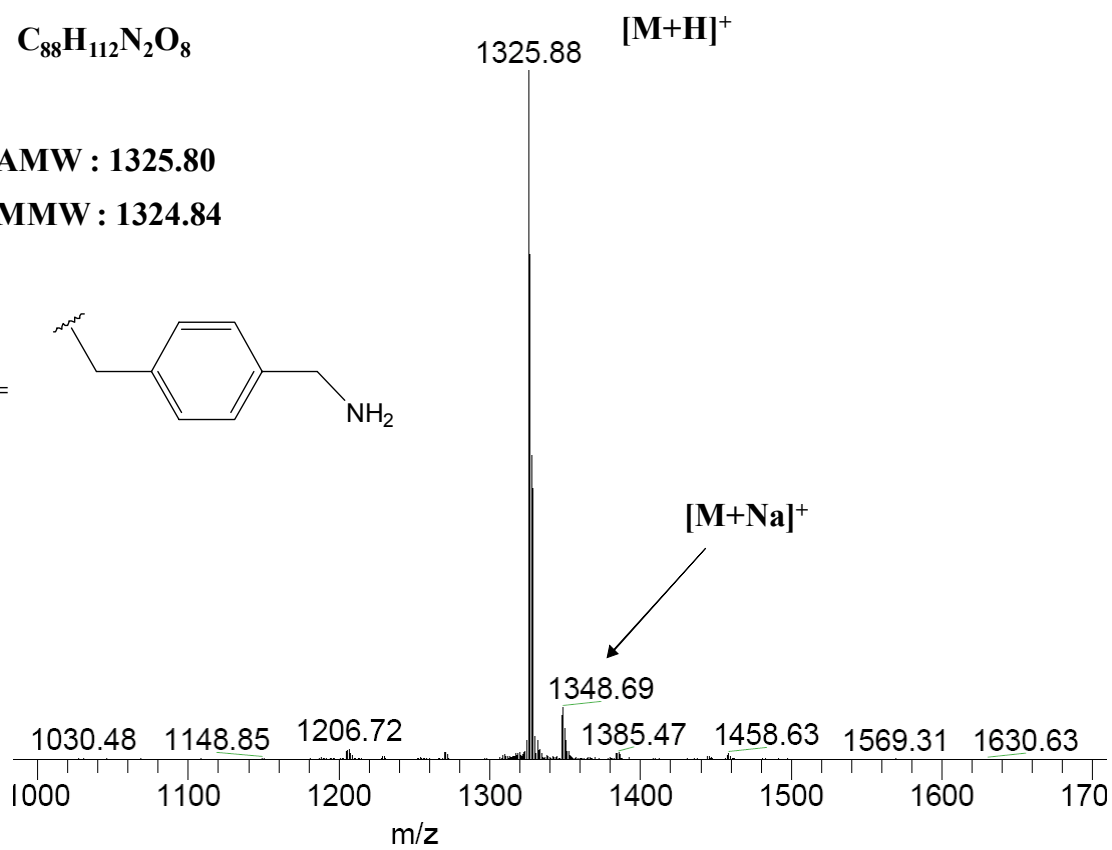
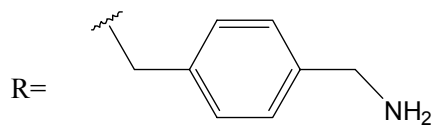
^{13}C -NMR

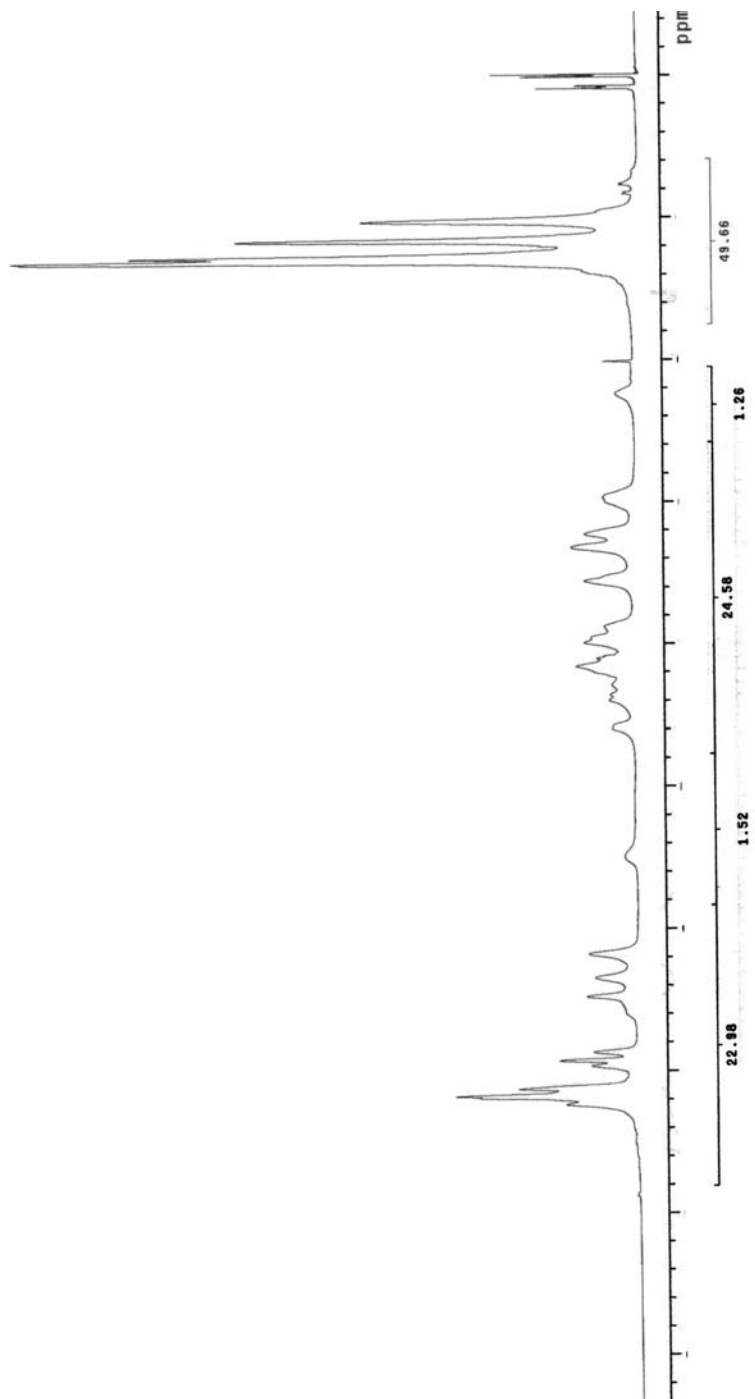
16 ESI-MS in PIM

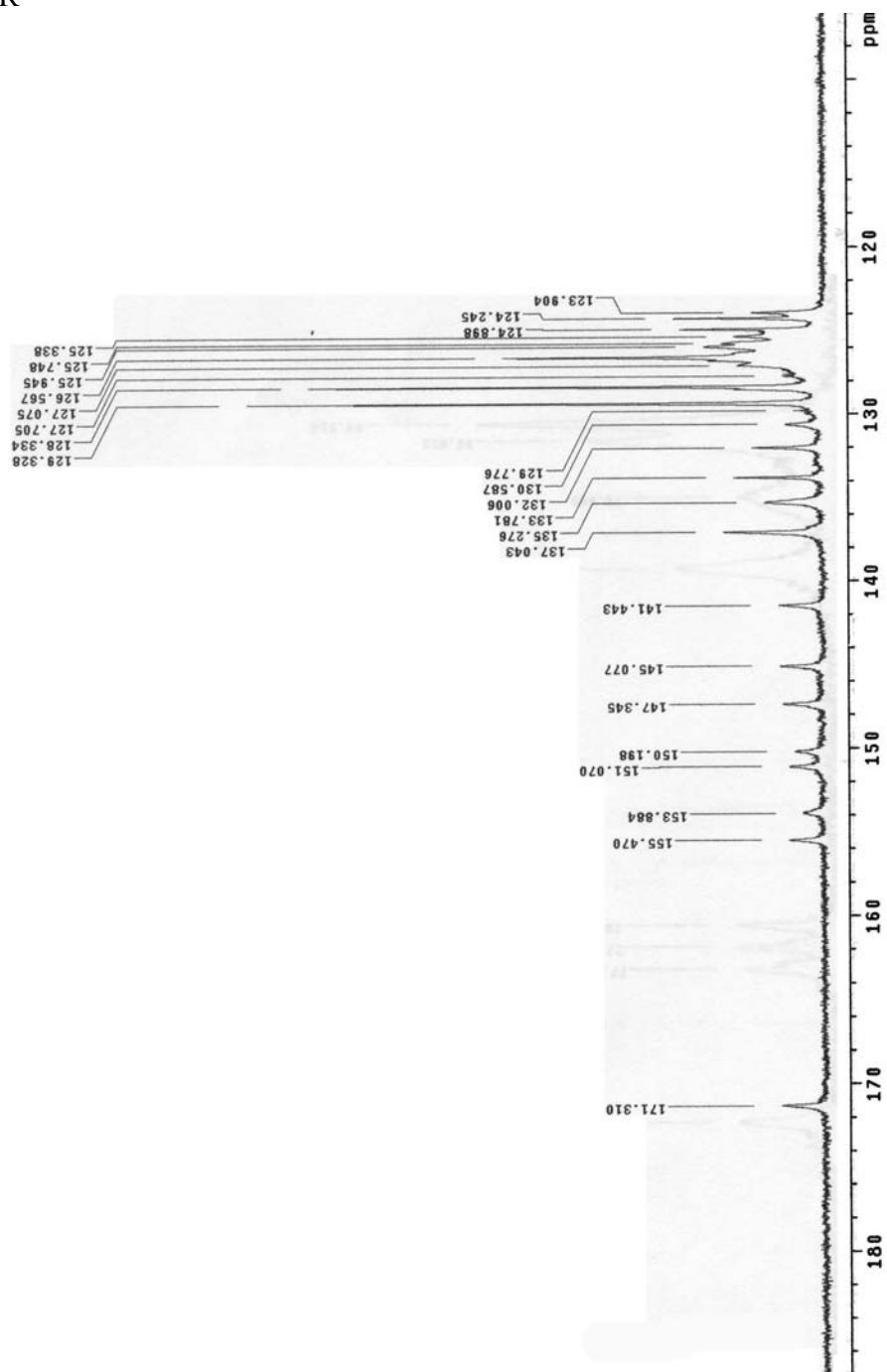


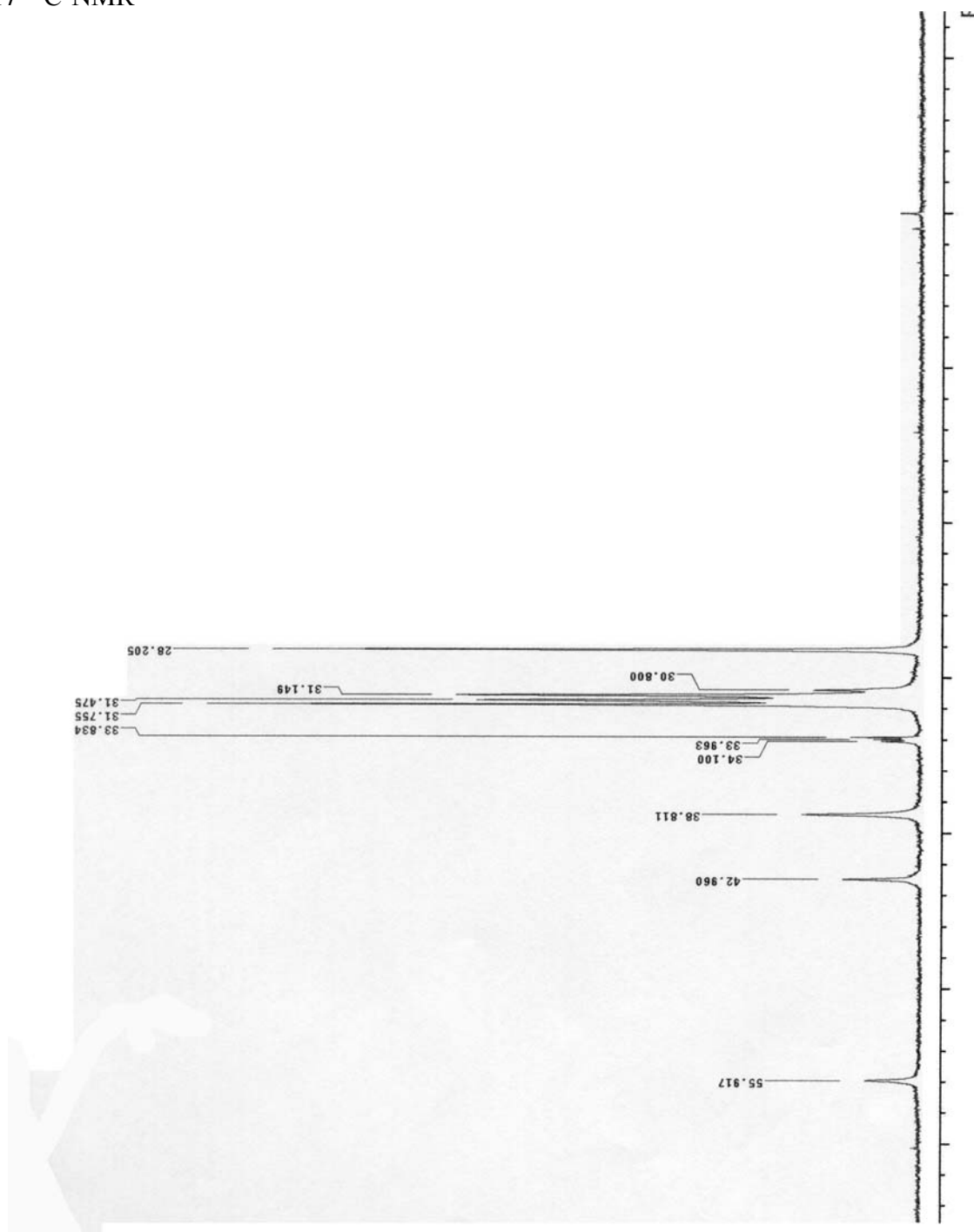
AMW : 1325.80

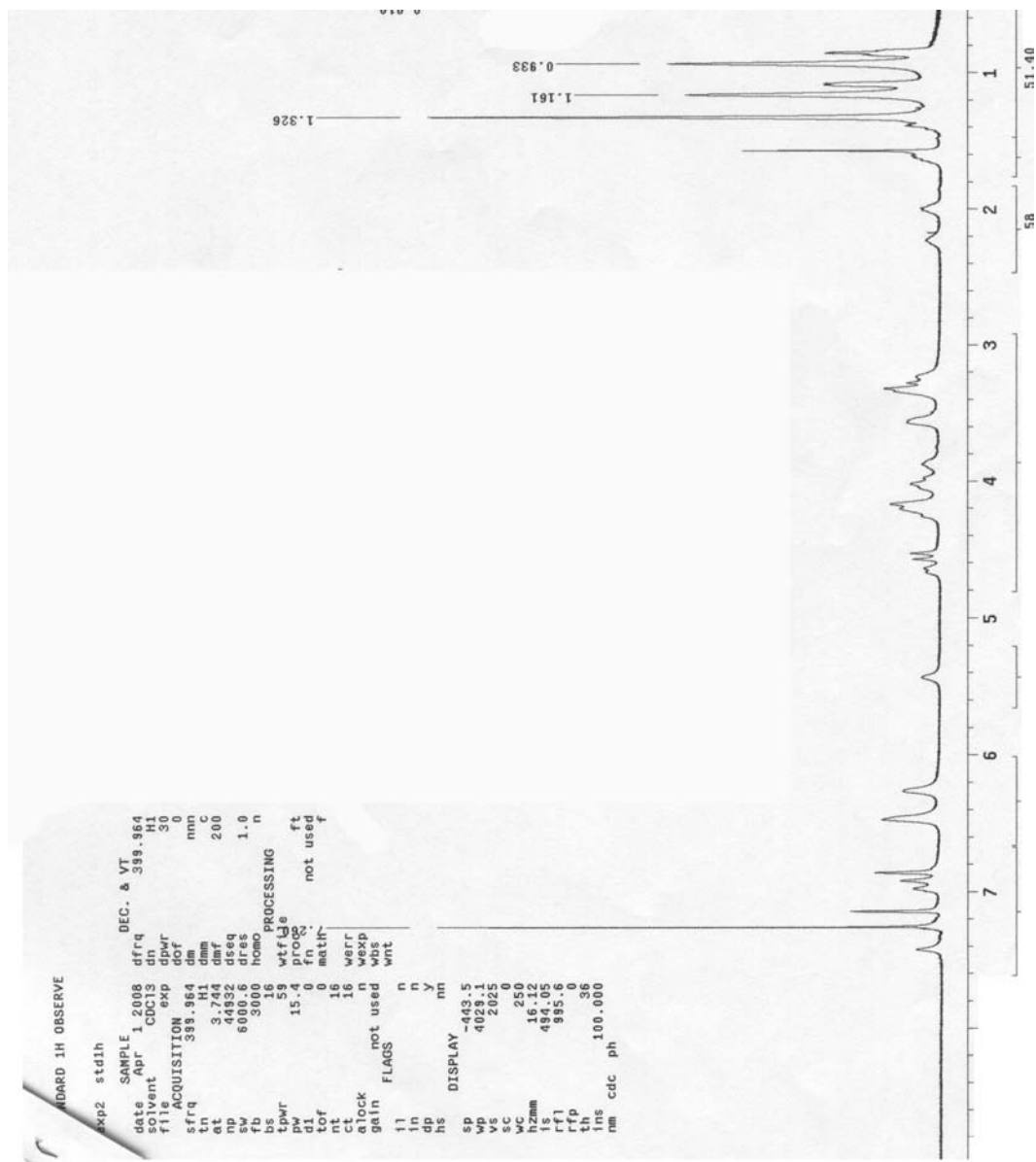
MMW : 1324.84

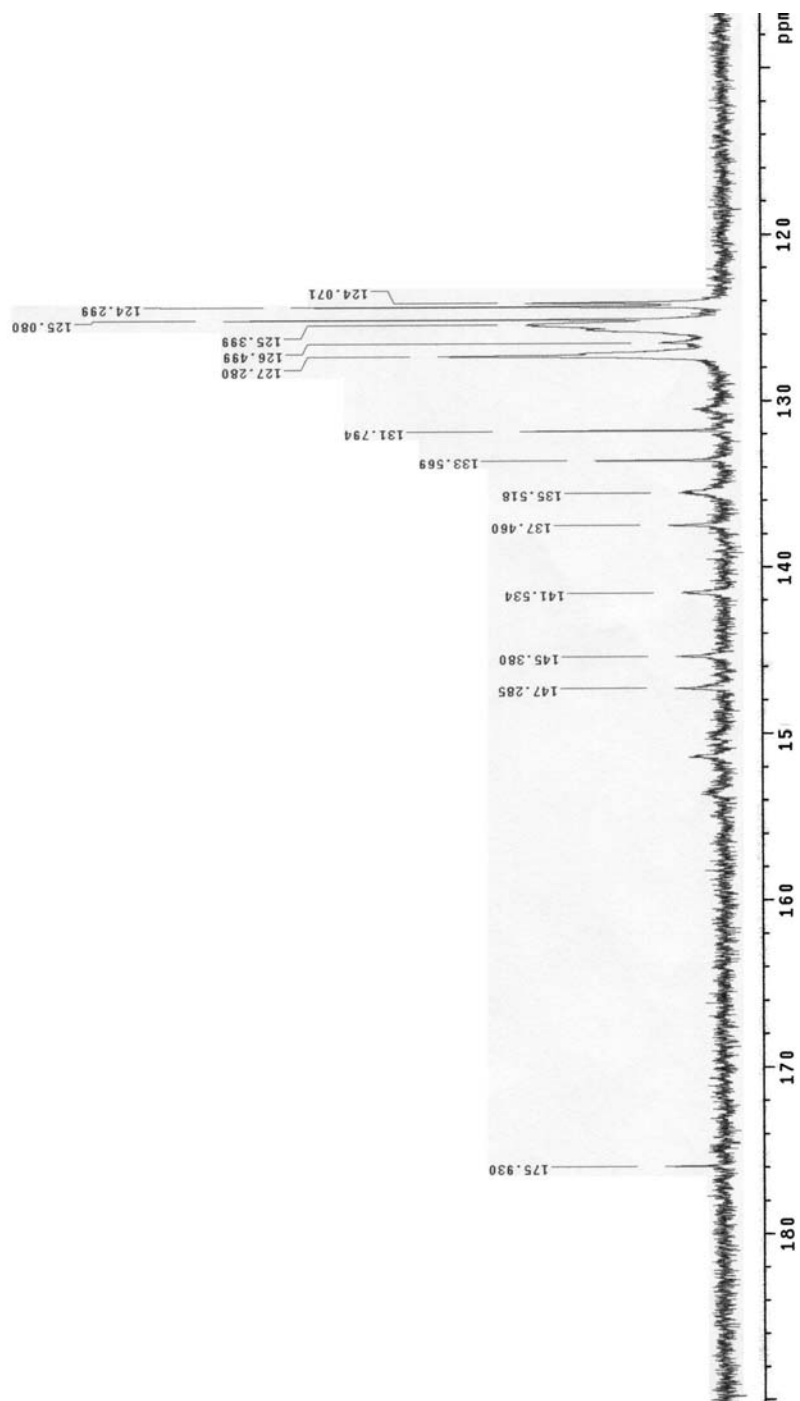


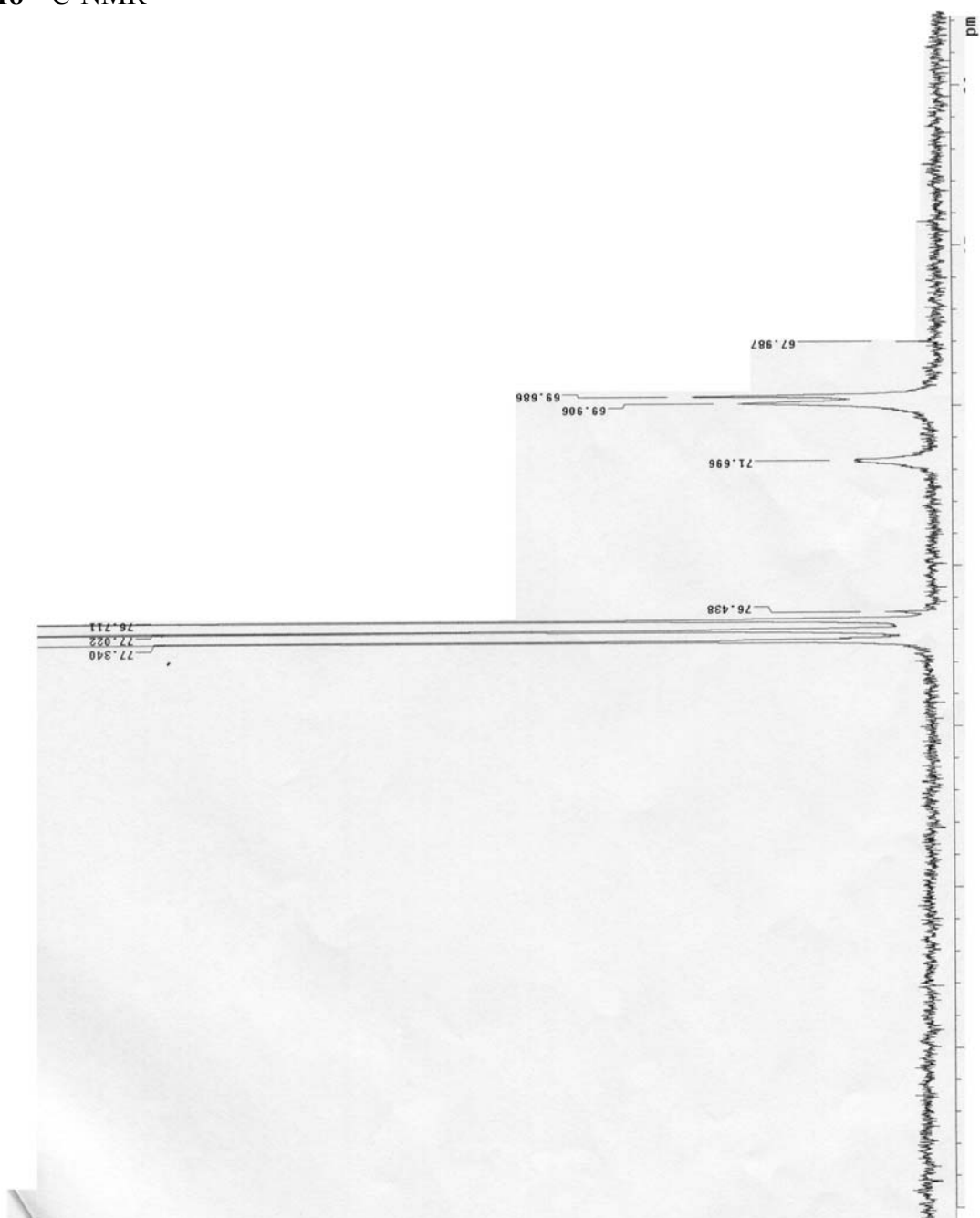
17 $^1\text{H-NMR}$ 

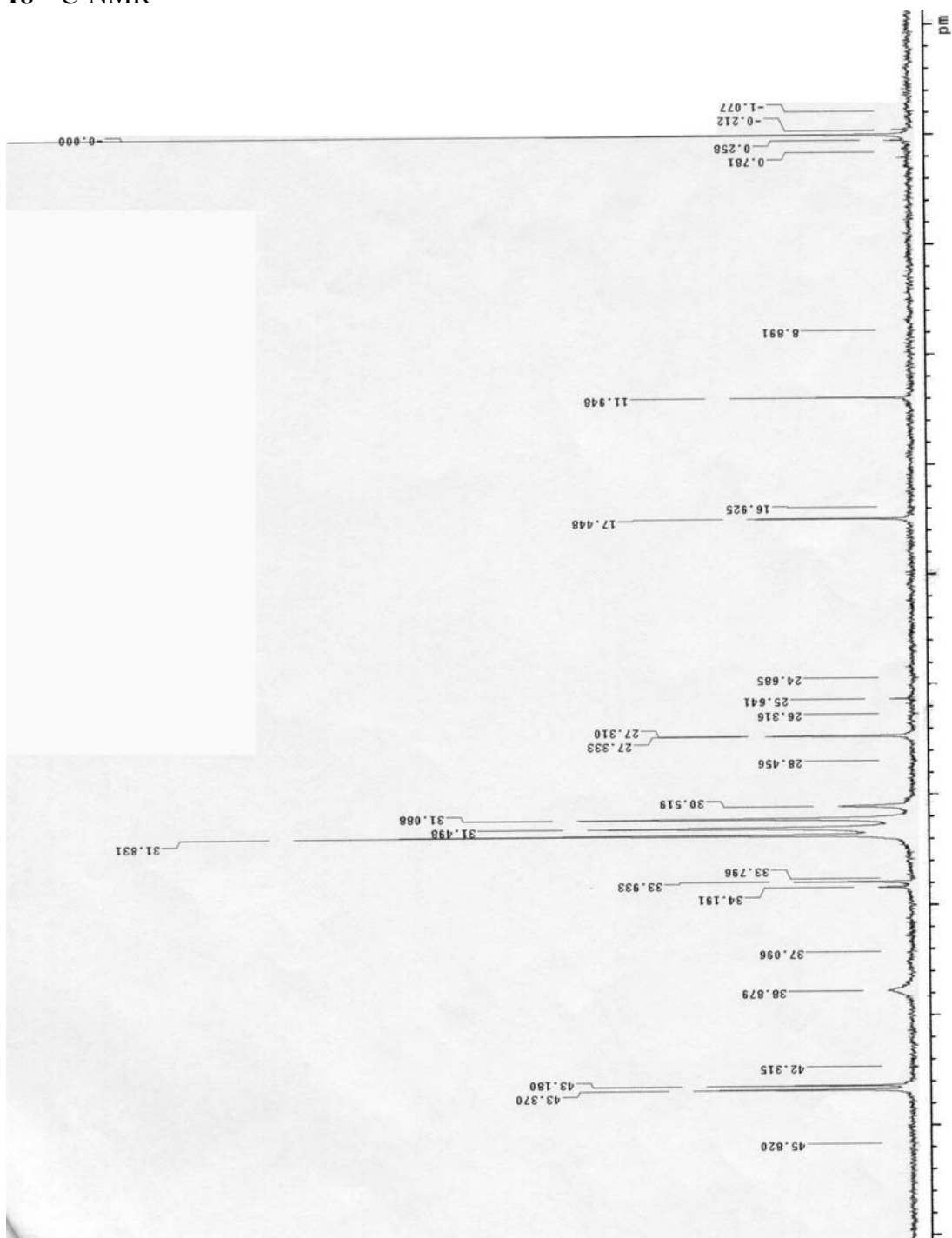
^{13}C -NMR

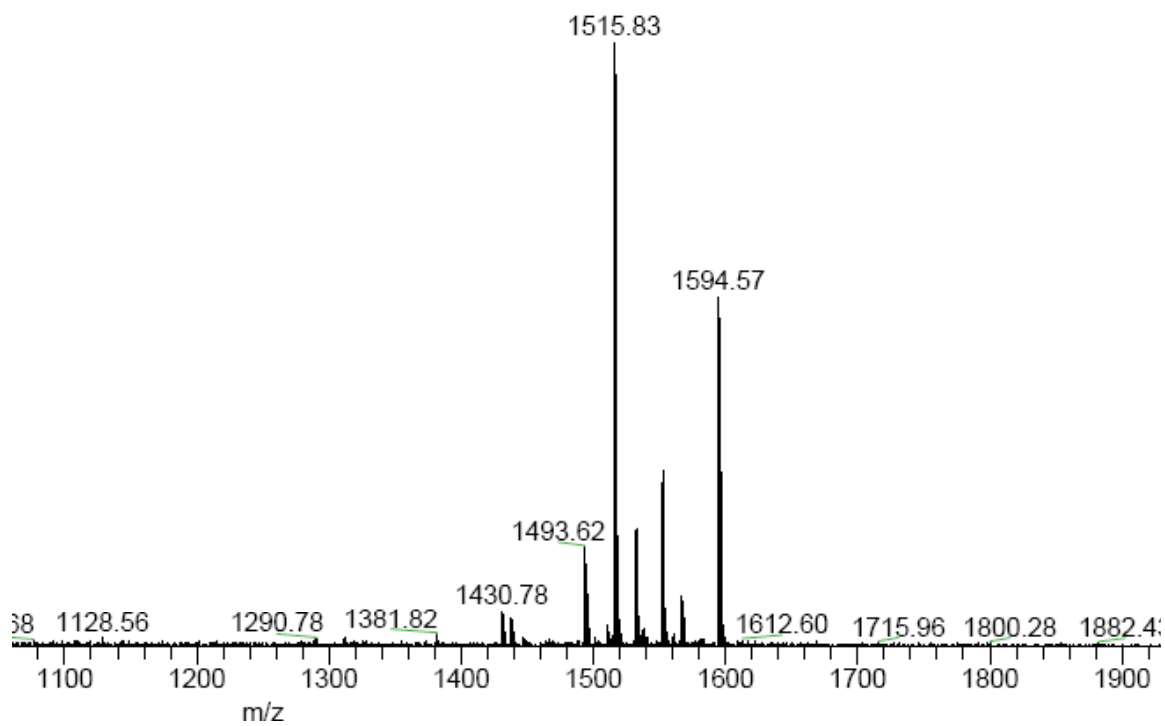
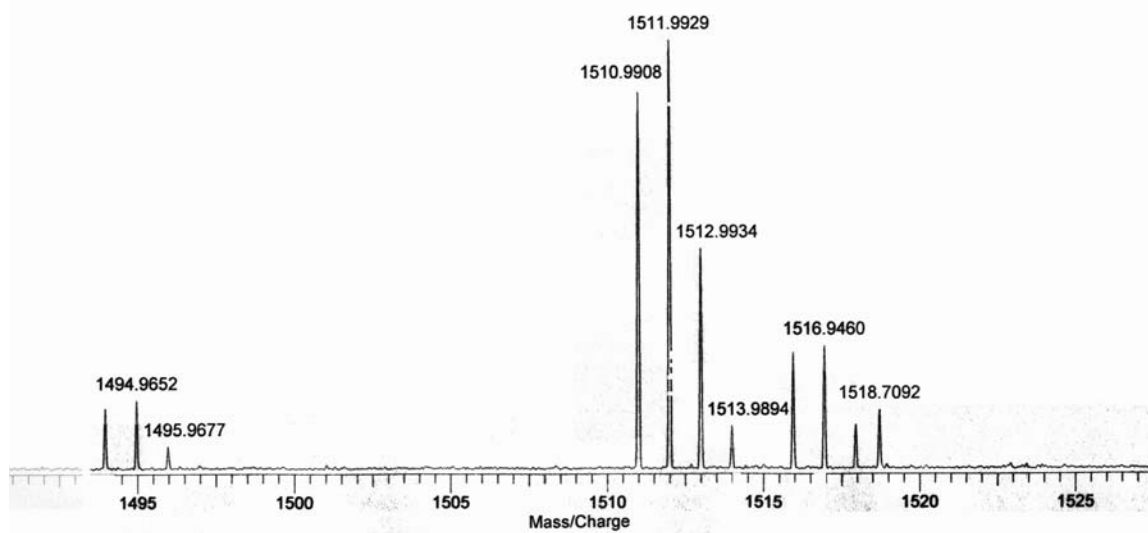
$^{13}\text{C-NMR}$ 

^{18}F -NMR

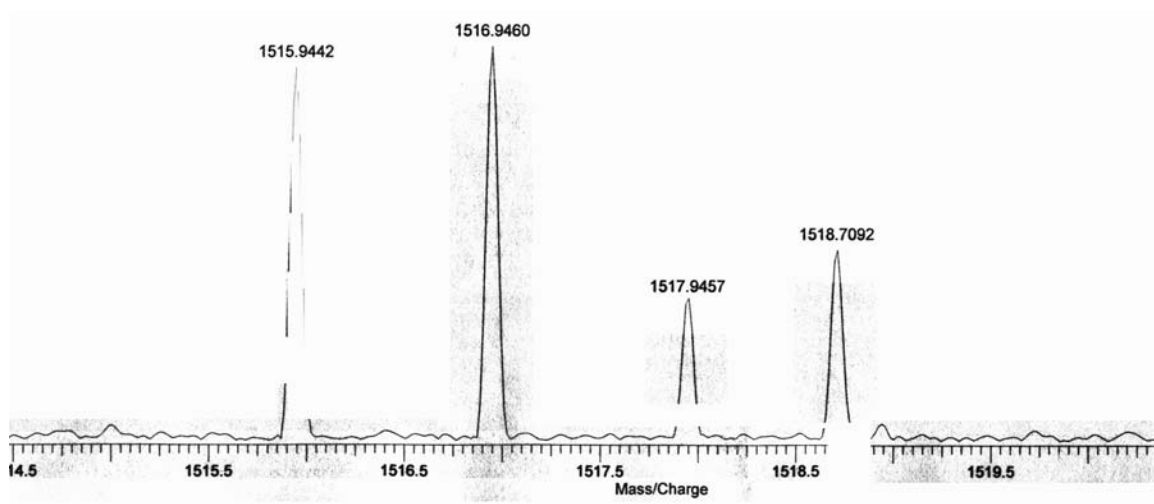
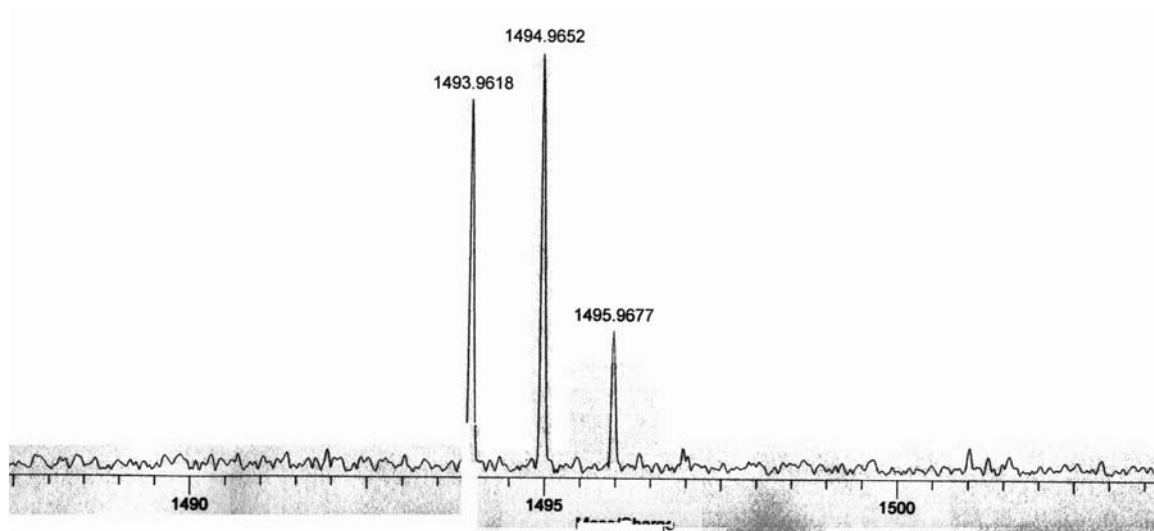
18 ^{13}C -NMR

^{13}C -NMR

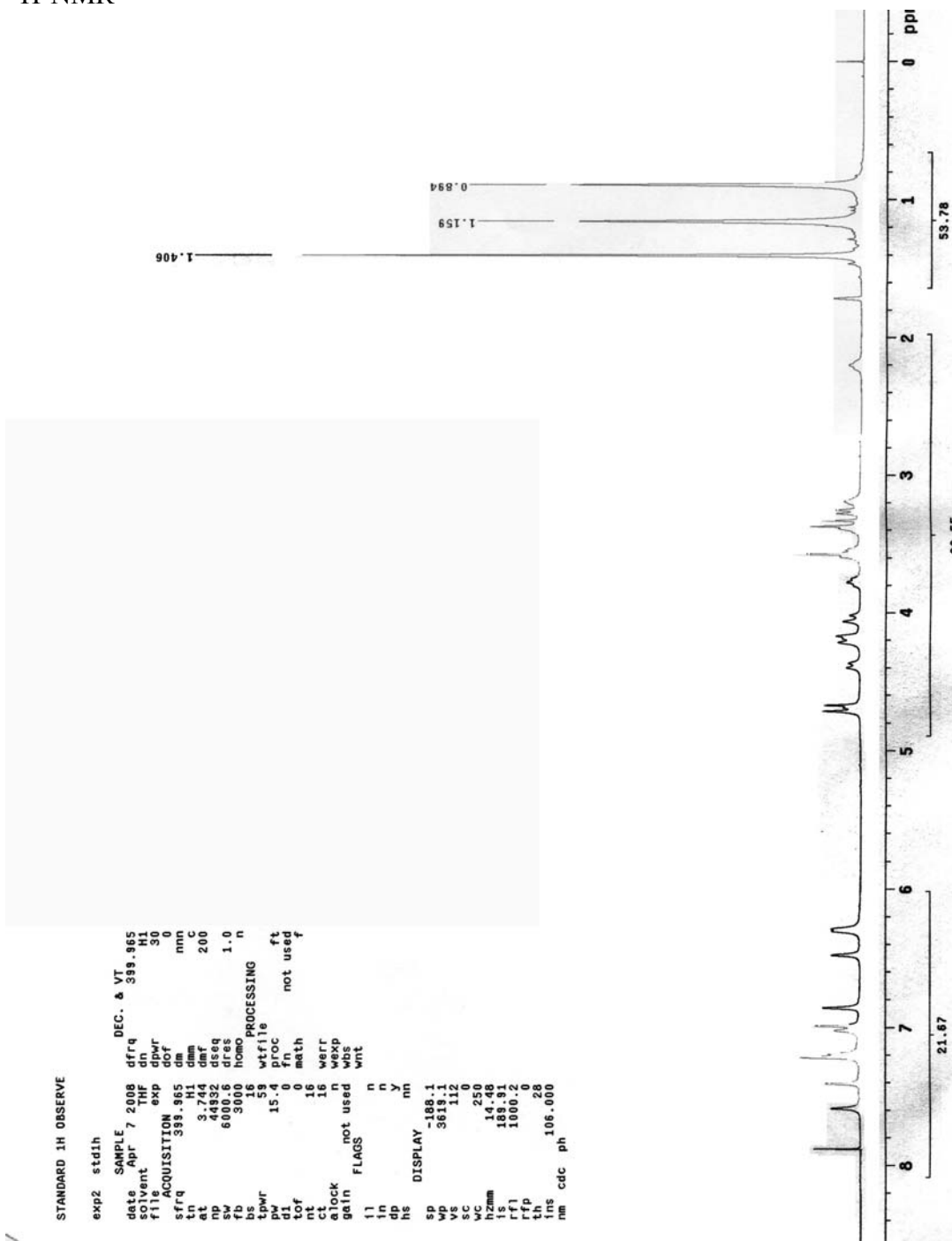
$^{13}\text{C-NMR}$ 

18 ESI-MS (PIM)**18 High-res MS**

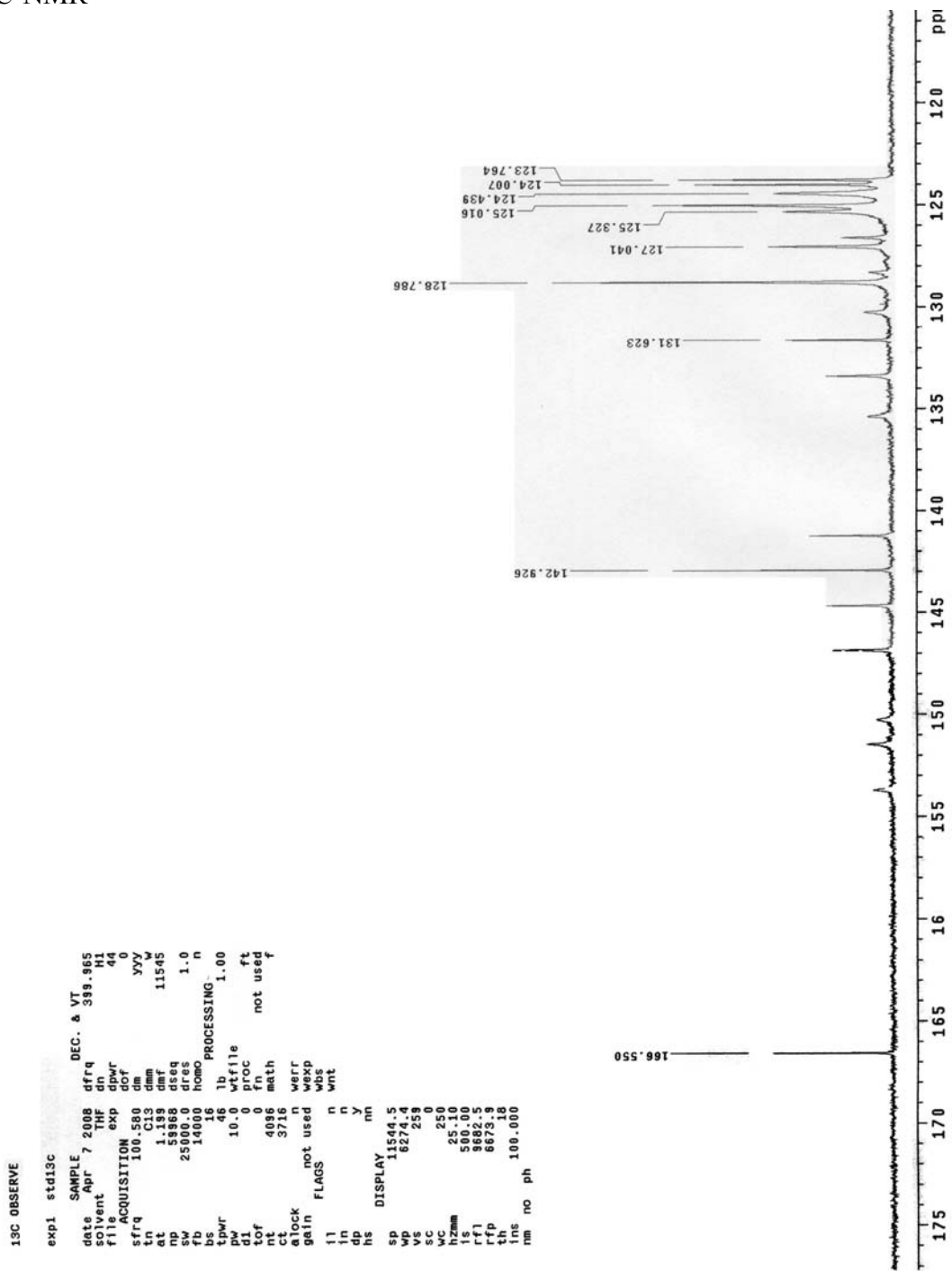
18 High-res MS

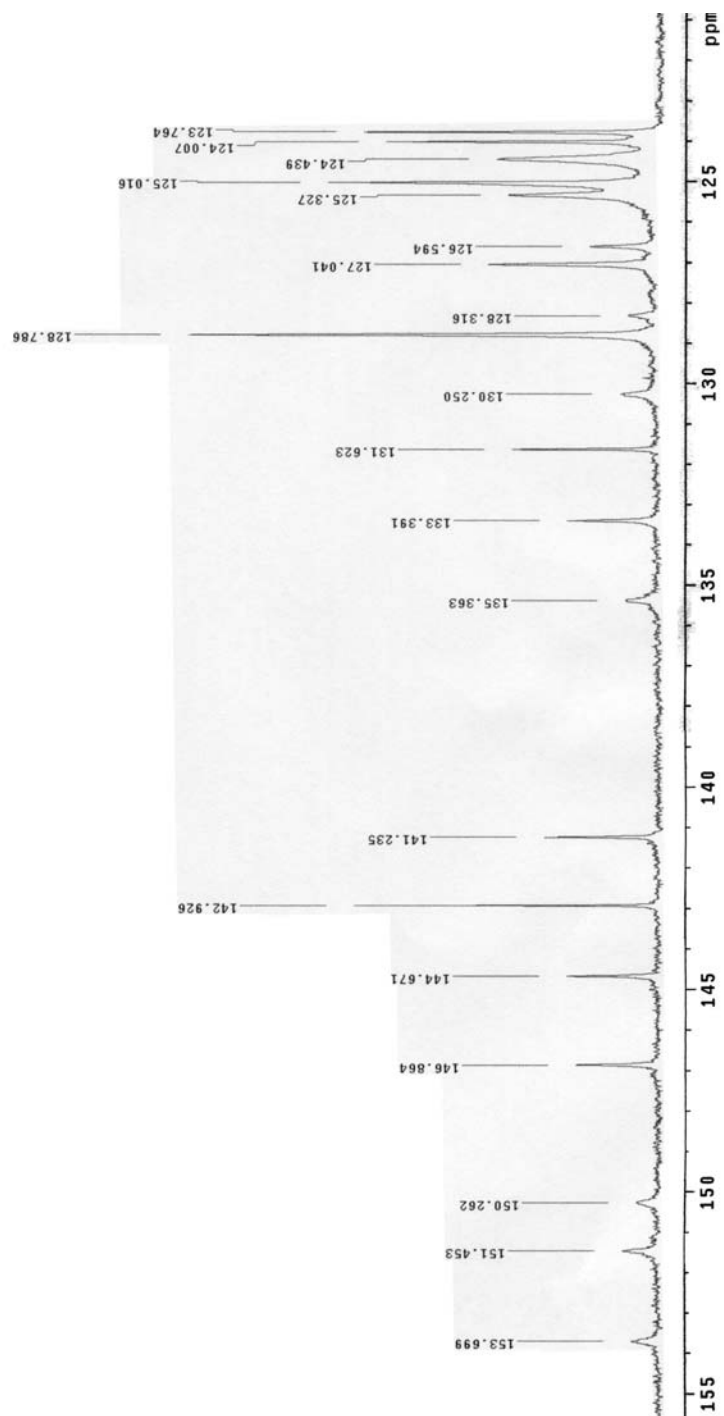


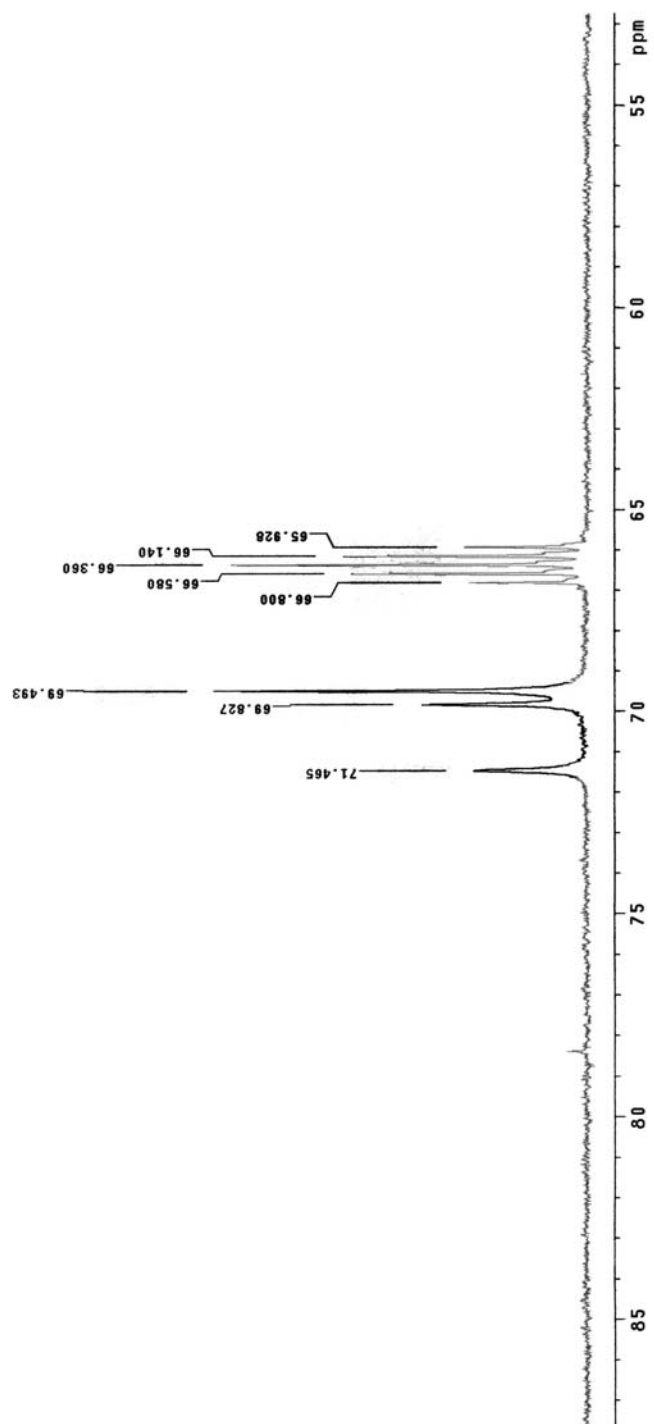
19 ¹H-NMR

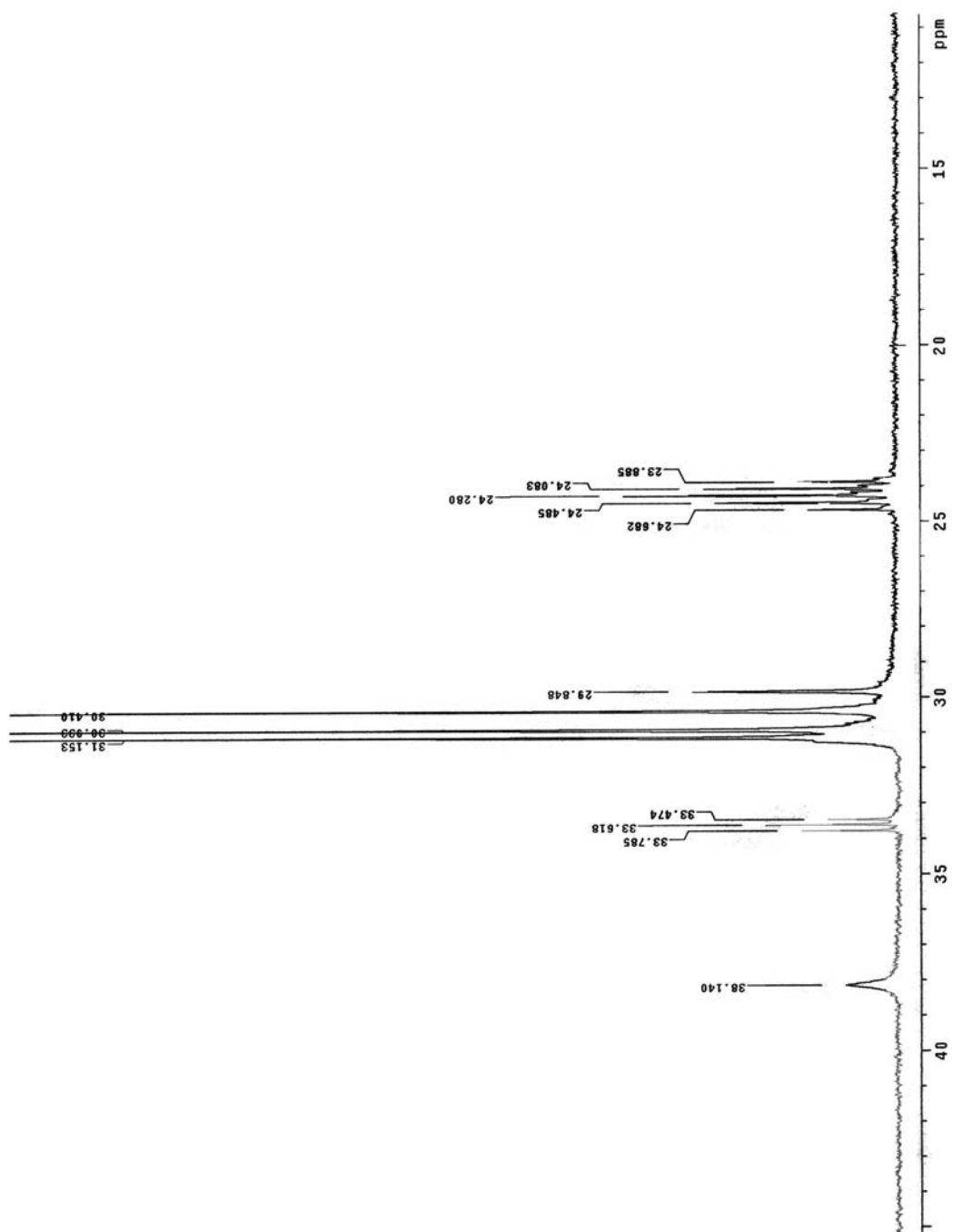


19 ¹³C-NMR

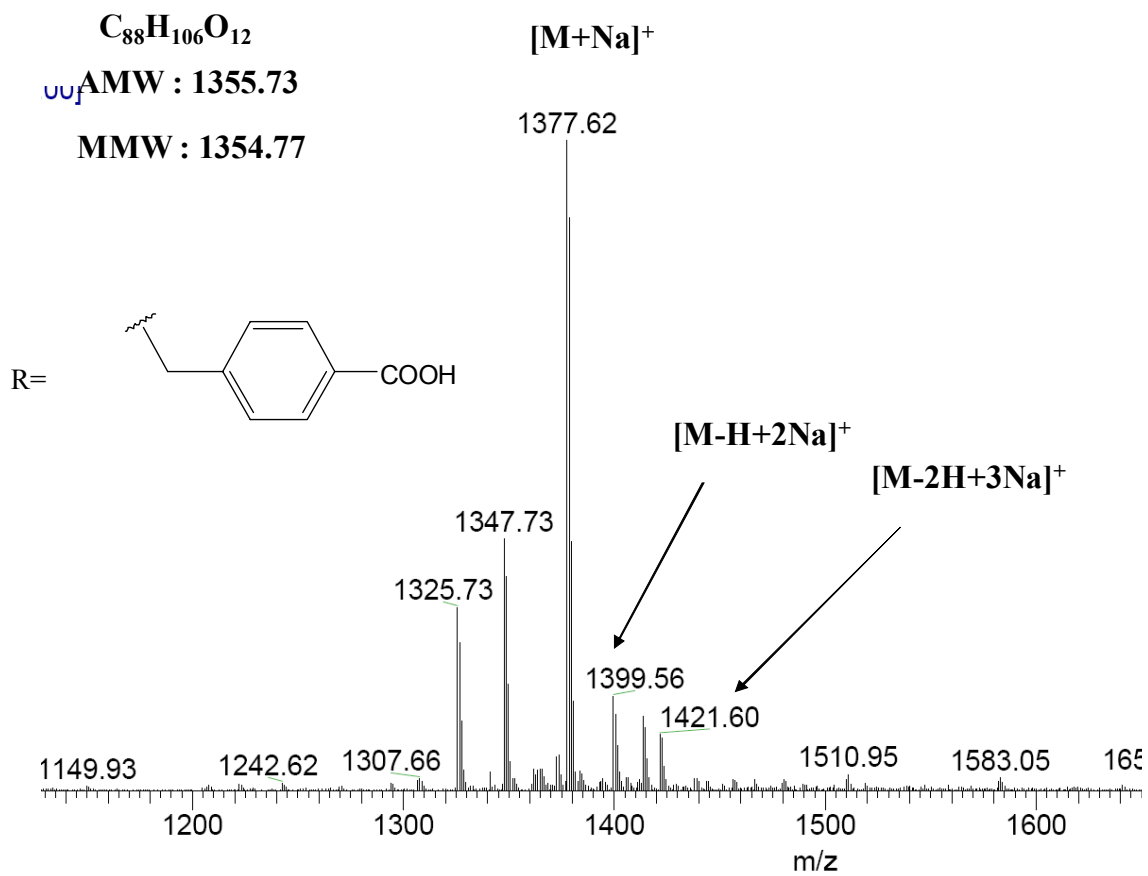


19 ^{13}C -NMR

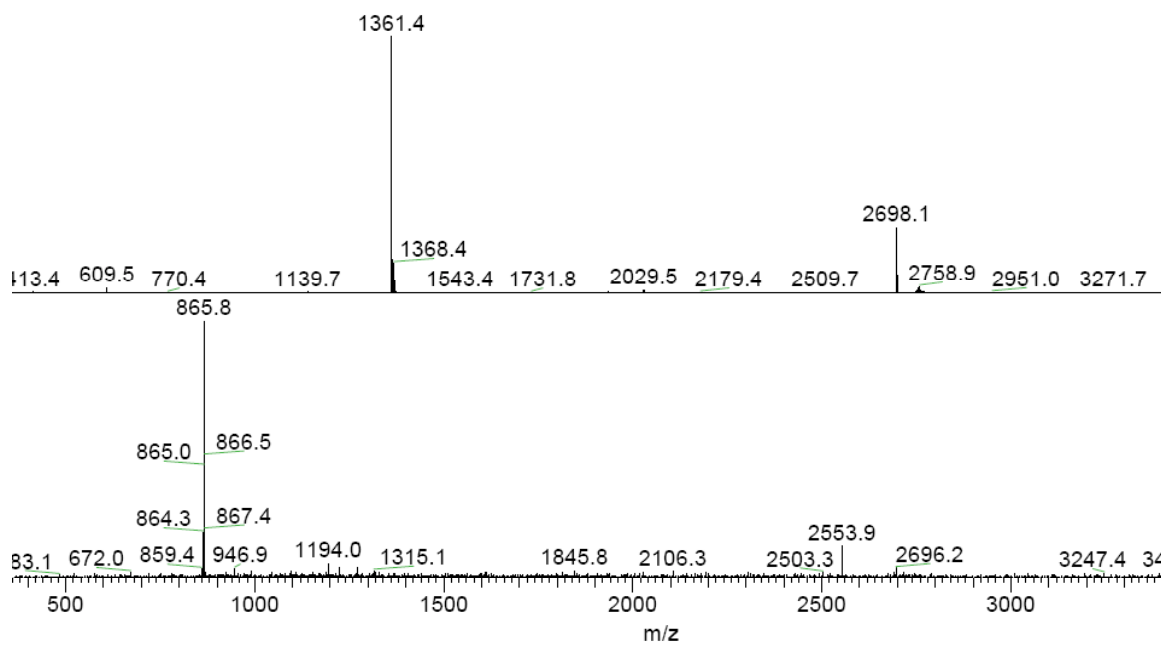
$^{13}\text{C-NMR}$ 

^{13}C -NMR

19 ESI-MS (PIM)



20 ESI-MS (PIM)



REFERENCES

1. Gutsche, C. D.; Dhawan, B.; Hyun No, K.; Muthukrishnan, R. *J. Am. Chem. Soc.* **1981**, *103*, 3782.
2. Gutsche, C. D.; Muthukrishnan, R.; No, K. H. *Tetrahedron Lett.* **1979**, 2213.
3. Otsuka, H.; Araki, K.; Shinkai, S. *Chem Express* **1993**, *8*, 479.
4. Otsuka, H.; Araki, K.; Sakaki, T.; Nakashima, K.; Shinkai, S. *Tetrahedron Lett.* **1993**, *34*, 7275.
5. Van Duynhoven, J. P. M.; Janssen, R. G.; Verboom, W.; Franken, S. M.; Casnati, A.; Pochini, A.; Ungaro, R.; de Mendoza, J.; Nieto, P. M.; Prados, P.; Reinhoudt, D. N. *J. Am. Chem. Soc.* **1994**, *116*, 5814.
6. Kanamathareddy, S.; Gutsche, C. D. *J. Org. Chem.* **1994**, *59*, 3871.
7. Kanamathareddy, S.; Gutsche, C. D. *J. Am. Chem. Soc.* **1993**, *115*, 6572.
8. Iwamoto, K.; Yanagi, A.; Arimura, T.; Matsuda, T.; Shinkai, S. *Chem. Lett.* **1990**, 1901.
9. Iwamoto, K.; Shimizu, H.; Araki, K.; Shinkai, S. *J. Am. Chem. Soc.* **1993**, *115*, 3997.
10. Otsuka, H.; Shinkai, S. *J. Am. Chem. Soc.* **1996**, *118*, 4271.
11. Kanamathareddy, S.; Gutsche, C. D. *J. Org. Chem.* **1992**, *57*, 3160.
12. Konrad, S.; Bolte, M.; Nather, C.; Luning, U. *Eur. J. Org. Chem.* **2006**, 4717.
13. Li, S.Y.; Zheng, Q. Y.; Chen, C.F.; Huang, Z. T. *Tetrahedron: Asymmetry* **2005**, *16*, 641.
14. Cacciapaglia, R.; Casnati, A.; Mandohi, L.; Ungaro, R. *J. Am. Chem. Soc.* **1992**, *114*, 10956.

15. Gonza, J. J.; Ferdani, R.; Albertini, E.; Blasco, J. M.; Arduini, A.; Pochini, A.; Prados, P.; de Mendoza, J. *Chem. Eur. J.* **2000**, *6*, 73.
16. Le Gac, S.; Marrot, J.; Reinaud, O.; Jabin, O. *Angew. Chem. Int. Ed.* **2006**, *45*, 3123.
17. Ikeda, A.; Udzu, H.; Zhong, Z.; Shinkai, S.; Sakamoto, S.; Yamaguchi, K. *J. Am. Chem. Soc.* **2001**, *123*, 3872.
18. Castellano, R. K.; Kim, B. H.; Rebek, J. J. *J. Am. Chem. Soc.* **1997**, *119*, 12671.
19. Castellano, R. K.; Nuckolls, C.; Rebek, J. J. *J. Am. Chem. Soc.* **1999**, *121*, 11156.
20. Block, M. A.; Kaiser, C.; Khan, A.; Hecht, S. "Discrete organic nanotubes based on a combination of covalent and non-covalent approaches" in *Functional Molecular Nanostructures*; Topics in Current Chemistry; Springer: Berlin/Heidelberg **2005**; 89-150. Bong, D. T.; Clark, T. D.; Granja, J. R.; Ghadiri, M. R. "Self-assembling organic nanotubes" *Angew. Chem. Int. Ed.* **2001**, *40*, 988-1011.
21. Organo, V.G.; Rudkevich, D. M. "Emerging host-guest chemistry of synthetic nanotubes" *Chem. Commun.* **2007**, 3891-3899.
22. Pasini, D.; Ricci, M.; "Macrocycles as Precursors for Organic Nanotubes" *Current Organic Synthesis*, **2007**, *4*, 59-80.
23. a) Lazar, A. N.; Dupont, N.; Navaza, A.; Coleman, A. W. "Helical Aquatubes of Calix[4]arene di-Methoxycarboxylic acids." *Chem. Commun.* **2006**, 1076-1078. b) Heaven, M. W.; Cave, G. W. V.; McKinlay, R. M.; Antesberger, J.; Dalgarno, S. J.; Thallapally, P. K.; Atwood, J. L. "Hydrogen-Bonded Hexamers Self-Assemble as Spherical and Tubular Superstructures on the Sub-Micron scale." *Angew. Chem. Int. Ed.* **2006**, *45*, 6221-6224. c) Organo, V.G.; Sgarlata, V.; Firouzbakht, F.; Rudkevich, D. M. "Long Synthetic Nanotubes from Calix[4]arenes." *Chem. Eur. J.* **2007**, *13*, 4014-4023. d) Sgarlata, V.; Organo, V. G.; Rudkevich, D. M. "A Procedure for Filling Calixarene Nanotubes." *Chem. Commun.* **2005**, 5630-5632.
24. Pantos, G. D.; Pengo, P.; Sanders, J. K. M. "Hydrogen-Bonded Helical Organic Nanotubes." *Angew. Chem. Int. Ed.* **2007**, *46*, 194-197.

25. Blanda, M. T.; Edwards, L.; Salazar, R.; Boswell, M. *Tetrahedron Lett.* **2006**, *47*, 7081.
26. Neri, P.; Pappalardo, S. *J. Org. Chem.* **1993**, *58*, 1048-1053.
27. *J Am Soc Mass Spectrom* **2005**, *16*, 553-564.
28. Kazushi, K.; Hashimoto, Y.; Sukegawa, M; Nohira, H; Saigo, K. *J. Am. Chem. Soc.* **1996**, *118*, 3441-3449.
35. Catanescu, O.C.; Chien, L.C. *Mol. Cryst. Liq. Cryst.*, **2004**, *411*, 1135-1144.
36. Ebbers, E. J.; Plum, B. J. M.; Ariaans, G. J. A.; Kaptein, B.; Broxterman, Q. B.; Bruggink, A.; Zwanenburg, B. *Tetrahedron Asymmetry* **1997**, *8*, 4047.
37. Gibson, H.W.; Pochan, J.M. *Journal of Physical Chemistry* **1973**, *6*, 837.
38. Boyd, B. J.; Krodkiewska, I.; Drummond, C. J.; Grieser, F. *Langmuir* **2002**, *18*, 597-601.
39. Clapper, J.D.; Sievens-Figueroa, L.; Guymon, C. A. "Photopolymerization in Polymer Templating." *Chem. Mater.* **2008**, *20*, 768-781.
40. Friberg, S. E.; Wohn, C. S.; Lockwood, F. E. "Polymerization in Non-aqueous Lyotropic Liquid Crystals with a Polymerizable Solvent." *Macromolecules* **1987**, *20*, 2057-2059.
41. Ajayaghosh, A.; Francis, R. "Narrow Polydispersed Reactive Polymers by a Photoinitiated Free Radical Polymerization Approach. Controlled Polymerization of Methyl Methacrylate." *Macromolecules (Communication to the Editor)* **1998**, *31*, 1436-1438.
42. Di Marco, V. B.; Bombi, G. G. "Electrospray mass spectrometry (ESI-MS) in the study of metal-ligand solution equilibria." *Mass Spec Rev.* **2006**, *25*, 347-379.
43. Nierengarten, H.; Leize, V.; Garcia, C.; Jeminet, G.; Van Dorsselaer, A. "Electrospray Ionisation Mass Spectrometry (ESI-MS): a powerful tool for the evaluation of chiral recognition in host-guest complexation." *Analisis* **2000**, *28*, 259-263.
44. Oshima, T.; Matsuda, F.; Fukushima, K.; Tamura, H.; Matsubayashi, G.;

Arakawa, R. "Selective cation binding of crown ether acetals in electrospray ionization mass spectrometry." *J. Chem. Soc., Perkin Trans.* **1998**, 2, 145-148.

VITA

Monty Hayes was born in New York, NY, on January 23, 1981, the son of Anne Hayes and John Gateley. He received the degree of Bachelor of Science in Chemistry at the Virginia Polytechnic and State University in May 2005. In January 2007, he entered the Graduate College of Texas State University-San Marcos.

Permanent Address: 39 Monroe Avenue

Staten Island, NY 10301

This thesis was typed by Monty Hayes.

